Rivers in the Silica and Carbon Cycles

A Quantitative Analysis for North America

Dissertation zur Erlangung des Doktorgrades der Naturwissenschaften im

Department Geowissenschaften der Universität Hamburg

Vorgelegt von

Ronny Lauerwald

aus

Mühlhausen

Hamburg, 2011

Als Dissertation angenommen vom Department Geowissenschaften der Universität Hamburg aufgrund der Gutachten von

Prof. Dr. Jens Hartmann

und

Prof. Dr. Stephan Kempe

Hamburg, den

(Datum der vorläufigen Bescheinigung)

Prof. Dr. Jürgen Oßenbrügge

(Leiter des Departments Geowissenschaften)

Table of contents

List of publications, submission, and manuscripts in preparation **vii**

1 Introduction **1**

1.1 Rivers in the silica and carbon cycles 1

1.2 Spatially explicit approaches - state of the art 3

1.2.1 Dissolved silica 5

1.2.2 Dissolved organic carbon 5

1.2.3 Dissolved inorganic carbon 6

1.3 Contributions of this thesis 7

2 Retention of dissolved silica within the fluvial system of the conterminous USA **9**

2.1 Introduction **9**

2.2 Methods and data **11**

2.2.1 Data processing 11

2.2.2 Estimation of DSi retention 14

2.3 Results **14**

2.3.1 Total DSi retention within the study area 14

2.3.2 DSi retention per catchment and potential factors 15

2.4 Discussion **20**

2.4.1 Comparison with literature values 20

2.4.2 Uncertainties due to methods 22

2.5 Conclusion **29**

3 Loss of dissolved organic carbon within the fluvial system of North America **31**

3.1 Introduction **31**

3.2 Methods and data 32

3.2.1 Data processing 32
3.2.2 Statistical analyses 34
3.3 Results 36
3.3.1 Set up of empirical DOC flux equations 36
3.3.2 Spatially explicit application of the regression equations 41
3.3.3 Budget based on estimated and calculated specific DOC fluxes 43
3.4 Discussion 44
3.4.1 Validity of empirical models 44
3.4.2 Implications for in-river losses of DOC 51
3.4.3 Uncertainties 52
3.5 Conclusion 56

4 Controls of spatial patterns in the carbonate system of North American rivers 58
4.1 Introduction 58
4.1.1 Identification of the research gap 58
4.1.2 The carbonate system 59
4.1.3 Objective of this study 63
4.2 Methods 64
4.2.1 Processing of hydrochemical data 64
4.2.2 Calculation of catchment properties 67
4.2.3 Statistical analyses 69
4.3 Results and discussion 70
4.3.1 Statistical and spatial distribution 70
4.3.2 Controls of the carbonate system of rivers 73
4.3.3 Effects of catchment size 82
4.3.4 General uncertainties 85
4.4 Conclusion 86

5 Concluding remarks 88

6 References 92

7 Acknowledgements 102

8 Appendix 103

A Maps of selected geo-spatial data sets used for analyses 103

B Properties of catchments used for the spatially explicit assessment of DSi retention 106

C Properties of catchments used for the spatially explicit assessment of in-river DOC loss 109

D Properties of catchments used for the spatially explicit assessment of the carbonate system of North American rivers 110

E List of important acronyms 115

F Curriculum vitae 116

G Individual contributions to the list of publications, submitted manuscripts, and manuscripts in preparation 117

List of publications, submission, and manuscripts in preparation

The presented thesis is based on three studies which have been submitted or are prepared for publication. Further, the candidate acted as co-author of several studies which are thematically related to this thesis and which contributed to its preparation. A list of publications, submission, and manuscripts in preparation the candidate contributed to is given below. Individual contributions to those publications and manuscripts are given in Appendix G.

Submission and manuscripts in preparation from the presented thesis

Lauerwald, R., Hartmann, J., Moosdorf, N., Dürr, H. H., and Kempe, S., in prep., Retention of dissolved silica within the fluvial systems of the conterminous USA. (section 2)

Lauerwald, R., Hartmann, J., Ludwig, W., Moosdorf, N., submitted, Loss of DOC within the fluvial system of North America. Submitted to Journal of Geophysical Research - Biogeosciences. (section 3)

Lauerwald, R., Hartmann, J., Moosdorf, and Kempe, S., in prep., Controls of spatial patterns in the carbonate system of North American rivers. (section 4)

Contributions as co-author

In revision

Moosdorf, N., Hartmann, J., **Lauerwald, R.**, Hagedorn, B. and Kempe, S., in revision. Bicarbonate fluxes and CO2 consumption by chemical weathering in North America. Submitted to Geochimica et Cosmochimica Acta.

Published

Moosdorf, N., Hartmann, J. and **Lauerwald, R.**, 2011. Compatibility of space and time for modeling fluvial HCO3 - fluxes - A comparison. Applied Geochemistry, 26 (Suppl.): S295-S297. [Extended abstract]

Moosdorf, N., Hartmann, J. and **Lauerwald, R.**, 2011. Changes in dissolved silica mobilization into river systems draining North America until the period 2081-2100. Journal of Geochemical Exploration, 110(1): 31-39.

Jansen, N., Hartmann, J., **Lauerwald, R.**, Dürr, H.H., Kempe, S., Loos, S. and Middelkoop, H., 2010. Dissolved silica mobilization in the conterminous USA. Chemical Geology, 270 (1-4): 90-109.

1 Introduction

1.1 Rivers in the silica and carbon cycles

Biogeochemical cycling of carbon is relevant as carbon is a key element for life and of specific importance in the earth's climate system. Atmospheric CO_2 is an important green house gas which exerts a major control of the energy budget of earth's atmosphere (cf. IPCC, 2007). Over geologic time scales, silicate rock weathering and carbonate precipitation are the main sink for atmospheric CO_2 (cf. e.g. Garrels and Mackenzie, 1971; Holland, 1978; Berner, 1992).

The weathering of silicate rocks releases dissolved silica (DSi), an important nutrient, specifically in aquatic environments. Diatoms, for which DSi is a crucial nutrient, play a significant role in marine ecosystems and the marine carbon pump, i.e. the export of carbon from surface waters to the deep sea (Ragueneau et al., 2006). Thus, there is a twofold link between the carbon and the silica cycle.

Rivers are the main transport routes in the land-ocean matter transfer (e.g. Kempe, 1979; Meybeck, 1993; Treguer et al., 1995; Cole et al., 2007; Laruelle et al., 2009). Moreover, rivers are ecosystems in which biogeochemical transformation and retention of nutrients like carbon (Fig. 1) and silica occurs (e.g. Kempe, 1982; Cole et al., 2007; Battin et al., 2008; Battin et al., 2009; Laruelle et al., 2009; Aufdenkampe et al., 2011). Carbon enters the fluvial system in particulate and dissolved form, as organic and inorganic carbon. Of specific importance is the terrestrial export of dissolved inorganic carbon (DIC) to streams and rivers. DIC stems from dissolved CO_2, mainly from soil respiration, and the dissolution of carbonate minerals (e.g. Kempe, 1982; Telmer and Veizer, 1999; Cole et al., 2007). Dissolved CO_2 may act as weathering agent in chemical weathering processes and is then transformed to carbonate alkalinity (e.g. Garrels and Mackenzie, 1971). Generally, the part of DIC which is present as bicarbonate and carbonate ions counterbalanced by base cations is termed carbonate alkalinity (e.g. Stumm and Morgan, 1981; Drever, 1997). The other part of the DIC, the free dissolved CO_2, is of specific importance with regard to in-river biogeochemical processes. Soil- and groundwater directly entering streams and rivers usually show increased concentrations of free dissolved CO_2, referred to as partial pressures of CO_2 (PCO_2), which are often substantially higher than the atmospheric PCO_2 (cf. e.g. Brook et al., 1983; Finlay, 2003; Johnson et al., 2008; Macpherson, 2009).

Dissolved organic carbon (DOC) is mainly leached from upper, organic rich soil horizons (cf. e.g. Mulholland, 1997; Guéguen et al., 2006). Particulate organic carbon (POC) as well as particulate inorganic carbon (PIC) mainly stem from physical soil erosion (e.g. Meybeck, 1993; Beusen et al., 2005; Scott et al., 2006; Kim et al., 2007). The terrestrial inputs of organic carbon, and specifically the DOC (cf. Worrall et al., 2007; Battin et al., 2008), feed the in-river respiration, which increases the PCO_2. On average, in-river respiration exceeds in-river production (cf. Wetzel, 2001; Battin et al., 2008). Rivers are thus mainly net-heterotrophic systems, which are on average CO_2 supersaturated with respect to the ambient air, and which are thus a net source of CO_2 to the atmosphere (e.g. Kempe, 1982; Cole et al., 2007; Battin et al., 2008; Battin et al., 2009; Aufdenkampe et al., 2011).

DSi, which ultimately originates from the dissolution of silicate minerals, enters the rivers via soil water and groundwater (cf. e.g. Derry et al., 2005). Within the river systems, DSi can be subject to biotic uptake, mainly by riverine diatoms, and thereby be transformed to amorphous, biogenic silica (BSi). While dissolved matter moves with the flowing water, particulate matter, like POC, PIC, and BSi, might settle down where flowing velocity becomes low, i.e. specifically in riverine lakes and behind dams. These parts of the fluvial systems can be important sinks for carbon and silica (cf. e.g. Einsele et al., 2001; Vörösmarty et al., 2003; Beusen et al., 2005; Syvitski et al., 2005; Humborg et al., 2006; Triplett et al., 2008).

The fluvial exports of carbon and silica to the coasts are well known, as they can easily be assessed from observed data from the rivers mouths. Reported fluvial DSi exports range from 366 to 415 Mt SiO_2 a^{-1} at global scale (Meybeck, 1979; Treguer et al., 1995; Turner et al., 2003; Beusen et al., 2009; Dürr et al., 2011). The fluvial exports of carbon amount to 700 to 900 Mt C a^{-1} (Meybeck, 1993; Ludwig et al., 1996a; Cole et al., 2007). Of that carbon, about 45% is exported as DIC, 29% as DOC, and 26% as POC (Ludwig et al., 1996a). Fluvial exports of PIC are neglected in this estimate.

Due to retention, respiration, and outgassing, the terrestrial export of carbon and silica to the fluvial system should be higher than the fluvial export to the coasts. The amount of terrestrial carbon exported to streams and rivers would be of interest with regard to carbon-budgets of terrestrial ecosystems (cf. Jones and Mulholland, 1998a; Cole and Caraco, 2001; Billett et al., 2004; Jenerette and Lal, 2005; Jonsson et al., 2007; Battin et al., 2009; Aufdenkampe et al., 2011). However, the assessment of the terrestrial matter inputs to the fluvial system as well as retention within and CO_2

degassing from the fluvial system are more difficult to quantify than fluvial matter exports to the coastal zone.

At the global scale, estimates of the burial of carbon in sediments of continental waters range from 200 to 600 Mt C a^{-1} (Cole et al., 2007; Battin et al., 2009). The CO_2 evasion from continental waters to the atmosphere is estimated to amount to 750 to 1,400 Mt C a^{-1} globally (Cole et al., 2007; Battin et al., 2009; Aufdenkampe et al., 2011). Streams and rivers contribute about half of this CO_2 (Aufdenkampe et al., 2011). These estimates are based on literature reviews and do not account for the spatial variability of the related biogeochemical processes and matter fluxes. A spatially explicit assessment of carbon sinks and CO_2 evasion could improve our understanding of the role of rivers in the carbon cycle.

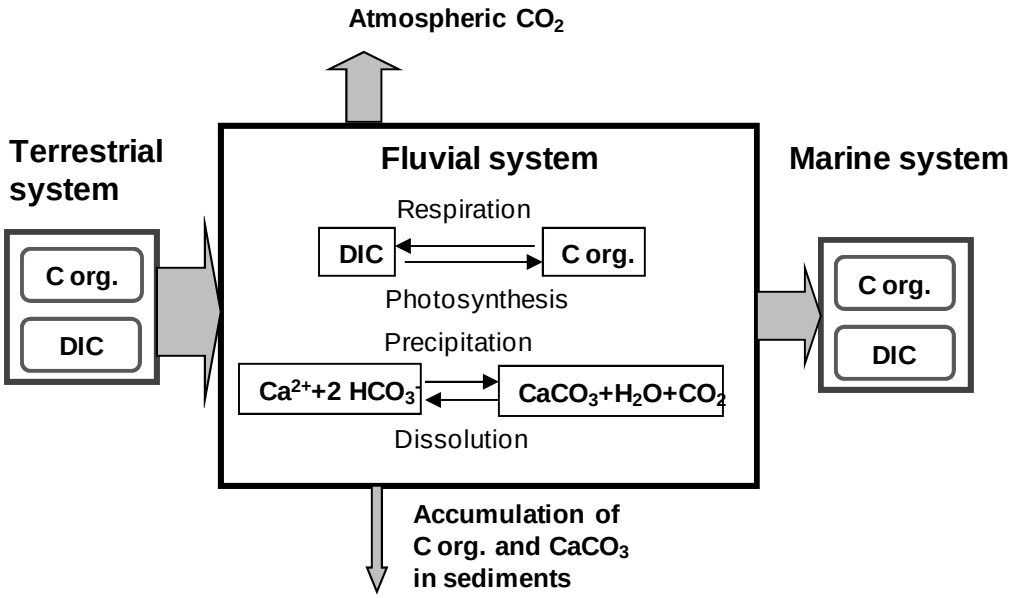

Fig. 1: Rivers in the carbon cycle – scheme.

A growing interest in DSi retention within the fluvial system arose specifically with regard to an anthropogenically increased DSi retention due to damming and eutrophication, and the thus reduced DSi exports to coastal zones (e.g. Schelske and Stoermer, 1971; Johnson and Eisenreich, 1979; Shapiro and Swain, 1983; Conley et al., 1993; Humborg et al., 1997; Friedl et al., 2004; Humborg et al., 2006; Humborg et al., 2008; Triplett et al., 2008). Reduced DSi exports, specifically when in combination with increased P and N loads, can cause an unfavorable shift in algae species composition of coastal ecosystems and in regional seas (e.g. Officer and Ryther, 1980; Danielsson et

al., 2008). A regional to global scale assessment of DSi retention, which accounts for the spatial variability in in-river processes and which identifies the controls of DSi retention, could provide a basic foundation for an evaluation of anthropogenic perturbations of the fluvial DSi exports and the potential risks for coastal ecosystems.

1.2 Spatially explicit approaches - state of the art

Biogeochemical processes and fluvial matter fluxes show substantial spatial variations at regional to global scales. The assessment of the spatial variability and the identification of highly active areas are important to improve our knowledge of the role of rivers in biogeochemical cycling. In this respect, spatially explicit assessment techniques have been proved to be appropriate tools (e.g. Ludwig et al., 1996b; Harrison et al., 2005a; Beusen et al., 2009; Hartmann, 2009; Hartmann et al., 2010a; Jansen et al., 2010). These techniques are based on functions predicting fluvial matter fluxes based on the physiographic properties of river catchments. Once trained on representative data from monitored river systems, they can be applied to obtain area-covering, and thus representative, estimates of fluvial matter transport, including non-monitored river systems. Specifically estimates of a high spatial resolution (about 1 km) were shown to be appropriate to account for highly active areas (Hartmann, 2009; Hartmann et al., 2009; Hartmann et al., 2010a; Moosdorf et al., 2011a; Moosdorf et al., 2011c) (example in Fig. 2).

The following subsections give an overview of existing spatially explicit studies assessing fluvial fluxes of DSi, DOC, or DIC, exposing existing research gaps, specifically with regard to in-river processes affecting the fluvial carbon and silica transport.

1.2.1 Dissolved silica

At the global scale, two spatially explicit studies exist which assessed natural fluvial DSi exports to the coastal zones (Beusen et al., 2009; Dürr et al., 2011). At the regional to continental scale, spatially explicit estimates of DSi mobilization from terrestrial system to the fluvial system exist for Japan and North America (Hartmann et al., 2010a; Jansen et al., 2010; Moosdorf et al., 2011a) (cf. Fig. 2). Up to now, however, no regional to global scale study exists, which quantifies DSi retention on an empirical basis.

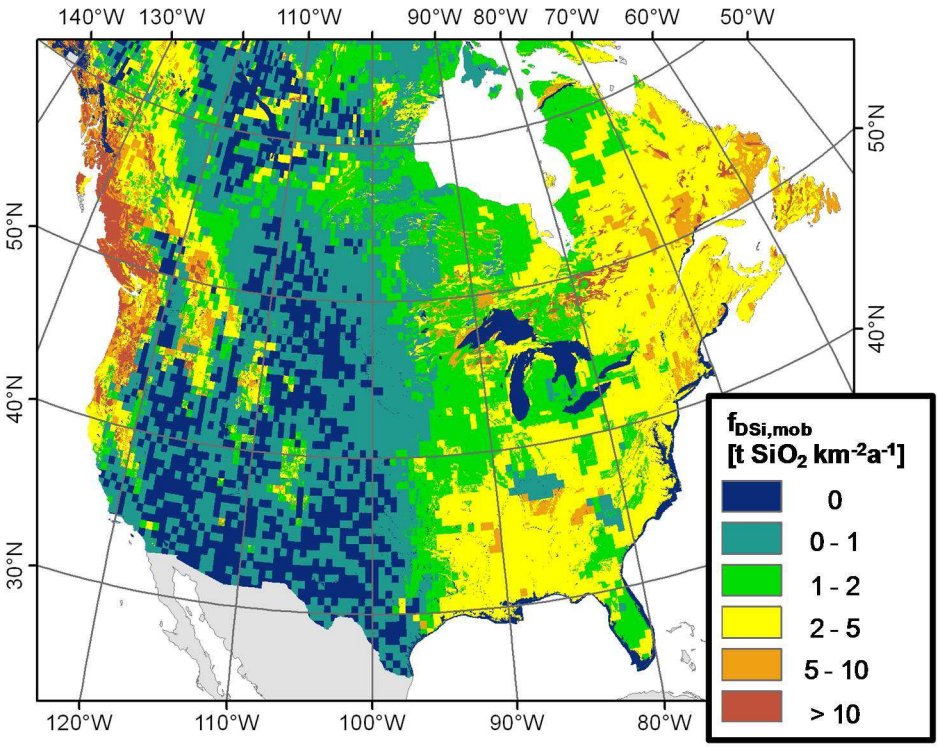

Fig. 2: Spatially explicit estimates of DSi mobilization ($f_{DSi,mob}$) into the fluvial system of North America (after Moosdorf et al., 2011a).

The studies by Beusen et al. (2009) and Dürr et al. (2011) gave first-order estimates of DSi retention. Note that both studies were based on hydrochemical data taken from the mouths of large rivers and representing natural DSi exports (after a compilation by Meybeck and Ragu, 1995), i.e. avoiding anthropogenically increased DSi retention. Beusen et al. (2009) gave first-order estimates of DSi retention within large reservoirs, assuming DSi retention to equal the retention of suspended sediments (after Vörösmarty et al., 2003) or dissolved inorganic phosphorous (after Harrison et al., 2005a). At the global scale, they estimated a total DSi retention in large reservoirs of 68-73 Mt SiO_2 a^{-1}, i.e. 18-19% of the natural fluvial DSi export.

Dürr et al. (2011) gave a first-order estimate of DSi retention in lakes, reservoirs, and floodplains, assuming a DSi retention of 20±10 g SiO_2 $m^{-2}a^{-1}$ for lakes and reservoirs (after averages given by Campy and Meybeck, 1995), and 3±1.5 g SiO_2 $m^{-2}a^{-1}$ in riparian wetlands. They estimated a retention of 69±35 Mt SiO_2 a^{-1} in natural lakes and wetlands (giving a retention rate of 16±8%) and 26.4±13.2 Mt SiO_2 a^{-1} within reservoirs (giving a retention rate of 6±3%). Note that specifically the estimates of DSi retention within reservoirs differ substantially between the studies of Beusen et al.

(2009) and Dürr et al. (2011), underscoring the need for an empirically validated assessment of DSi retention within the fluvial system at these spatial scales.

1.2.2 Dissolved organic carbon

At the global scale, two spatially explicit approaches exist which assessed fluvial exports of DOC to the coasts (e.g. Ludwig et al., 1996b; Harrison et al., 2005a). These studies were based on hydrochemical data from the mouths of large rivers. However, the catchment properties applied as predictors were related to the DOC mobilization from terrestrial systems. In-river losses were not taken into account by these studies and fluvially transported DOC was thus implicitly assumed to behave conservative. However, it can be expected that the terrestrial DOC export to the fluvial system is substantially higher than the fluvial export of DOC to the coasts.

An interesting attempt to assess in-river DOC respiration and subsequent CO_2 evasion in its spatial variability at regional scale was done by Worrall et al. (2007). Their estimates of in-river DOC loss were based on the biogenic oxygen demand measured at the rivers' mouths, which gave the degradability of the transported DOC at these points. However, as it can be expected that DOC becomes more refractory during fluvial transport and ongoing decomposition, these measurements are not representative for the in-river respiration of the whole fluvial system and are rather conservative estimates of the actual in-river DOC loss (Worrall et al., 2007).

At regional to global scales, studies are missing which quantify in-river DOC losses spatially explicitly on an empirical basis by comparing upstream and downstream DOC fluxes. Such an assessment could provide valuable constraints for earth system models taking into account the role of rivers in the global carbon cycle.

1.2.3 Dissolved inorganic carbon

Existing spatially explicit approaches to assess fluvial DIC fluxes concentrated on carbonate alkalinity, in a simplifying manner sometimes referred to as bicarbonate fluxes. Specifically, the proportion of carbonate alkalinity stemming from the dissolved CO_2 was focused, which can be regarded as being sequestered in the process of chemical weathering (Amiotte-Suchet and Probst, 1993; Amiotte-Suchet and Probst, 1995; Ludwig et al., 1998; Gaillardet et al., 1999; Amiotte-Suchet et al., 2003; Hartmann et al., 2009; Moosdorf et al., 2011c). Up to now, spatially explicit approaches focusing on the PCO_2 and the CO_2 evasion from rivers do not exist at continental to global scales.

At the regional scale, the spatial patterns of PCO_2 in river systems were described for the conterminous USA (Jones et al., 2003). However, studies analyzing potential controls of the spatial variability of the PCO_2 of rivers are missing. Such an analysis would be required to provide an empirical basis for the spatially explicit assessment of CO_2 evasion from river systems. Similarly, studies revealing spatial patterns in river water pH, which is closely related to the carbonate system of rivers, and potential predictors for its spatial variability, could be a worthwhile basis for regional scale ecological studies, e.g. addressing surface water acidification.

1.3 Contributions of this thesis

The objective of this thesis is to fill the gap left open by existing studies at regional to global scales: the spatially explicit assessment of in-river processes affecting the silica and carbon cycles. The study area is continental North America, more specifically the conterminous USA and southern parts of Canada, covering climatic zones from the boreal zone to the sub-tropics, and from arid to perhumid regions. The thesis is subdivided into three parts, each representing an individual study focusing specific in-river processes.

In the first part of the thesis, an attempt is made to quantify DSi retention within the fluvial system of the conterminous USA (section 2). It is hypothesized that DSi retention can be calculated in a spatially explicit budget approach applying spatially explicit estimates of terrestrial DSi mobilization into streams and rivers (Moosdorf et al., 2011a; Fig. 2) and fluvial DSi fluxes calculated from hydrochemical monitoring data. The calculated estimates of DSi retention are analyzed with regard to potential controlling factors.

In the second part of the thesis, an attempt is made to quantify the DOC loss within the fluvial system of North America (section 3). It is hypothesized that the in-river loss of DOC can be quantified in a budget approach using two spatially explicit estimates of fluvial DOC fluxes; one representing fluvial DOC fluxes from smaller catchments, the other one representing DOC fluxes from larger catchments. It is expected that the fluvial DOC fluxes from the smaller catchments are higher due to a lower in-river DOC loss compared to the larger catchments, assuming that the length of rivers and thus the travel time of the dissolved loads increases with catchment size. An additional research question refers to the predictors applied in the spatially explicit estimation: How do the effects of the predictors differ between the estimation equation for the smaller and that for the larger catchments?

The third part of the thesis is concerned with the carbonate system of North American rivers. The main research questions are: What are the spatial patterns of PCO_2, alkalinity, and pH of North American rivers? What are the controls behind these spatial patterns? Is it possible to predict mean PCO_2, alkalinity, and pH based on catchment properties? Specifically the last question is of importance with regard to the feasibility of a spatially explicit estimation of CO_2 evasion from rivers, and will be discussed in this respect. Note that not the fluvial fluxes of carbonate alkalinity are focused (cf. Moosdorf et al., 2011c) here, but the mean chemical properties of river water.

The candidate contributed to different studies as co-author (Jansen et al., 2010; Moosdorf et al., 2011a; Moosdorf et al., 2011b; Moosdorf et al., 2011c, Details are given in Appendix G), which are thematically closely related to this thesis. These studies provided important preparatory work to develop the methodological framework of this thesis.

2 Retention of dissolved silica within the fluvial system of the conterminous USA

2.1 Introduction

Dissolved silica (DSi) is an important nutrient in terrestrial and aquatic ecosystems (e.g. Conley et al., 1993; 2002). Its primary source is the weathering of silicate minerals (e.g. Bluth and Kump, 1994; Derry et al., 2005). The land-ocean transfer of DSi through rivers is an important part of the global silica cycle. For many coastal areas, the fluvial export of silica is the main source of this nutrient (e.g. Meybeck et al., 2007).

Rivers are not just conduits between the terrestrial and the marine system. Moreover, part of the terrestrial DSi is retained within the fluvial system due to biotic uptake, mainly by diatoms, and net-losses of biogenic, amorphous silica (BSi) to sediments. Of the total bioavailable silica (DSi+BSi) exported to the coasts, about 15-16% are contributed by BSi, mainly in the form of living diatoms (derived by Conley, 1997 from ten large world rivers sampled at the rivers' mouths). However, existing data on riverine BSi are not sufficient for an extensive statistical analysis addressing whole river systems including upstream reaches and smaller rivers.

Eutrophication and construction of dams and locks can lead to an increase in DSi retention and a subsequent decrease in DSi export (e.g. Van Bennekom and Salomons, 1981; Conley et al., 1993; Friedl et al., 2004; Humborg et al., 2008) with potentially severe consequences for coastal ecosystems (e.g. Danielsson et al., 2008). For the Baltic Sea, for instance, Humborg et al. (2008) estimated a decrease in fluvial DSi inputs of 30-40% over the last hundred years.

Recently, the global silica cycle and its anthropogenic perturbation were assessed in a box model approach (Laruelle et al., 2009). However, long-term fluvial fluxes of DSi vary substantially among different rivers, with consequences for the receiving coastal zones (e.g. Beusen et al., 2009; Dürr et al., 2011). It is thus necessary to analyze DSi mobilization, DSi retention, and fluvial DSi export in their spatial variability.

The spatial variability of total fluvial DSi exports to the coasts were assessed at global scale in different studies based on hydrochemical data from the mouths of large rivers (Beusen et al., 2009; Dürr et al., 2011). In these studies, the DSi mobilization from the terrestrial system into the rivers was

not assessed directly. The studies by Dürr et al. (2011) and Beusen et al. (2009) were based on river chemistry data representing rather pristine states, i.e. effects of anthropogenically enhanced DSi retention were avoided.

Spatial patterns and first order controls of terrestrial DSi exports to fluvial systems were more directly investigated at regional to continental scale for North America and Japan (Hartmann et al., 2010a; Jansen et al., 2010; Moosdorf et al., 2011a). Based on spatially explicit estimates of DSi mobilization these studies showed the significance of highly active areas.

DSi retention was mainly assessed for individual lakes and reservoirs using direct mass balances (eg. Schelske, 1985; Garnier et al., 1999; Hofmann et al., 2002; Triplett et al., 2008; Cook et al., 2010). Fluvial DSi fluxes distinguishing DSi mobilization and DSi retention were assessed for a small number of rivers applying a deterministic model (Riverstrahler model; for the Seine River by Sferratore et al., 2005; the Luleälven and Kalixälven Rivers by Sferratore et al., 2008; for the Red River (Vietnam/China) by Le Thi Phuong et al., 2010). At the regional scale, Humborg et al. (2008) investigated statistic relations between DSi yields from river basins tributary to the Baltic Sea and catchment characteristics which can be related to DSi retention; however not accounting for the spatial variability of DSi mobilization from the terrestrial system. These studies suggest a strong negative influence of lakes and reservoirs on fluvial DSi exports to the coastal zones.

Concerning DSi retention at the global scale, a box model (Laruelle et al., 2009) and two first order estimates exist (Beusen et al., 2009; Dürr et al., 2011). In their box model, Laruelle et al. (2009) estimated that 21% less DSi is exported by rivers to coasts (373 Mt SiO_2 a^{-1}) as it is mobilized from the terrestrial system into the fluvial system (469 Mt SiO_2 a^{-1}).

Beusen et al. (2009) gave a first-order estimate of DSi retention within large reservoirs. For this they assumed DSi retention rates to equal that of dissolve inorganic phosphorous after Harrison et al. (2005b) (18% at global scale) or that of sediments after Vörösmarty et al. (2003) (19% at global scale).

Dürr et al. (2011) estimated a natural DSi retention within lakes and wetlands of 16±8% and a anthropogenically induced DSi retention within reservoirs of 6±3%. For this first-order estimate, they assumed an annual retention of 20±10 g SiO_2 per m^2 of lake area (Campy and Meybeck, 1995) as representative for all natural lakes and reservoirs; for wetlands the silica retention per area was assumed to be 15% of that in lakes (Dürr et al., 2011).

There is still a need for regional to continental scale studies empirically analyzing DSi retention, explicitly taking into account the spatial variability of DSi mobilization from the terrestrial system. Up to now, it is however unknown if available data are suitable for such analyses. The here presented study explores the possibility of empirically analyzing DSi retention within the fluvial system of the conterminous USA. For this, spatially explicit estimates of DSi mobilization are taken from the study by Moosdorf et al. (2011a), which is based on the empirical function described by Jansen et al. (2010). It is hypothesized that for larger catchments and catchments with higher lake area proportions, an estimate of silica retention can be calculated as the difference between these spatially explicit estimates of DSi mobilization and fluvial DSi fluxes calculated from hydrochemical monitoring data. The estimated DSi retention is checked for statistical relations to potential controlling factors suggested in the literature, i.e. areal proportions of lakes and reservoirs, and water quality parameters as concentrations of N, P, and suspended matter.

2.2 Methods and data

2.2.1 Data processing

Hydrochemical data (USGS; Alexander et al., 1997) from 624 sampling locations (cf. Fig. 3) and long-term average annual runoff from the UNH/GRDC data set (Fekete et al., 2002) were used to calculate fluvial DSi fluxes. Sampling locations were selected following four criteria:

1) DSi concentrations and instantaneous discharge measurements were available for at least twelve consecutive months,
2) the sampling location could be positioned on the stream network represented by the Digital Elevation Model (DEM) used (Hydrosheds DEM by Lehner et al., 2008, 15" resolution),
3) the computed catchments were consistent with USGS meta data (20% maximum deviation between reported and computed catchment areas) and satellite imagery (visual check), and
4) the runoff data set gave a long-term average annual runoff of more than 0 mm a^{-1}.

For the Mississippi River, only sampling locations upstream of the diversion at the Old River outflow channel (cf. Goolsby et al., 1999) were considered, because diversions are not depicted in the stream

network derived from a digital elevation model (DEM). Artificial waterways and streams and rivers directly influenced by water diversion were omitted for the same reason.

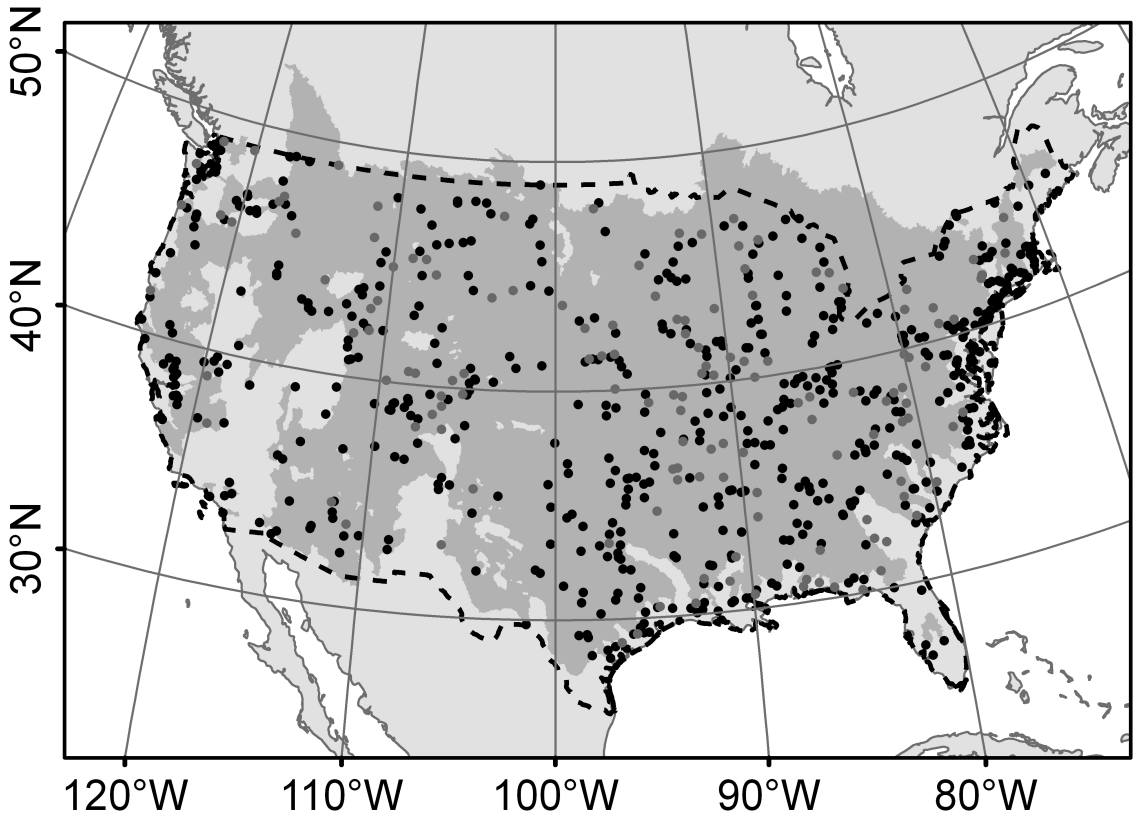

Fig. 3: USGS sampling locations used in the analyses. The dark grey area represents the monitored area addressed by this study. The dashed line encircles the conterminous USA. The grey points represent the sampling locations used by Jansen et al. (2010).

As many non-overlapping series of twelve consecutive monthly measurements as possible were identified from the time series of each sampling location (on average 3.3 twelve-month-series per station). The averages of DSi concentrations were then weighted by the instantaneous discharge measurements. Based on the computed catchment boundaries and geodata (Table 1), catchment properties were calculated. For all geodata processing, the software ArcGIS 9.3 (ESRI^{TM}) was used.

Table 1: Geodata used for deriving catchment properties.

Parameter	Source	Resolution
Lithology	Lithological map of North America v1.0 (Jansen et al., 2010)	Based on geologic maps 1:1,000,000 to 1:5,000,000
Land cover	GlobCover (Arino et al., 2007), reclassified after Jansen et al. (2010)	10''
Lakes	SRTM water body data set (NASA/NGA, 2003)	Based on SRTM DEM with 3'' resolution
Runoff	UNH/GRDC runoff (Fekete et al., 2002)	30'
Climate	WorldClim (Hijmans et al., 2005)	30''
DEM derived flow directions	Hydrosheds (Lehner et al., 2008)	15''
DSi mobilization into streams	Moosdorf et al. (2011)	1.4 km²
Population density (1990)	Gridded population of the world v3 (CIESIN, 2005)	2.5'

Long-term averages of annual runoff were derived from the UNH/GRDC runoff composites (Fekete et al., 2002), a spatial raster data set with 0.5° resolution. To assure runoff values are available for the whole terrestrial area considered, the runoff rasters were extended by one raster cell, each new cell assigned the average runoff of the adjacent cells. Note that UNH/GRDC runoff is based on discharge gauging data covering time series comprising at least twelve years in the time span 1960 to 1990; the exact time spans covered by the time series differ (Fekete et al., 2002). However, it is assumed that the runoff data are representative long-term averages for that period. River chemistry data refer to samples taken between 1967 and 2007.

Land cover information was derived from the GlobCover data set (Arino et al., 2007) that is based on remote sensing data (MERIS) between 2004 and 2006. Lake area was taken from the SRTM Water Body data set (NASA/NGA, 2003). This data set represents all standing water bodies of a size of at least 0.1 km^2 (at least 600 m length and 183 m width) in February 2000, as they were derived from remote sensing data (Landsat TM5, SRTM derivatives) (NASA/NGA, 2003). This includes natural lakes as well as reservoirs and larger ponds. It is assumed that this state of water body distribution is fairly representative for the time since the 70's, as most dams have been created during the 1950's and 1960's (e.g. for the Mississippi/Atchafalya River Basin cf. Goolsby et al., 1999).

2.2.2 Estimation of DSi retention

Silica retention (Eq. 1) was calculated from the specific fluvial fluxes of DSi ($f_{DSi,calc}$), which were derived from USGS hydrochemical data and UNH/GRDC runoff data, and the spatially explicit estimates of DSi mobilization from Moosdorf et al. (2011a) ($f_{DSi,mob}$).

Eq. 1

$$r_{DSi} = \frac{(f_{DSi,mob} - f_{DSi,calc})}{f_{DSi,mob}}$$

$f_{DSi,calc}$ long-term annual fluvial flux of DSi calculated from USGS hydrochemical data [t SiO_2 $km^{-2}a^{-1}$]

$f_{DSi,mob}$ estimated long-term annual DSi mobilization from the terrestrial system into the fluvial system [t SiO_2 $km^{-2}a^{-1}$]

Total DSi retention within the study area was calculated from the average specific DSi mobilization within the entire monitored area and an area-weighted average $f_{DSi,calc}$ from a subset of 161 catchments that cover the entire monitored area without overlaps ('non-overlapping catchments').

DSi retention rates calculated for each individual catchment were analyzed for statistical correlations (Pearson correlations) with catchment properties and hydrochemical characteristics that might show a potential influence on DSi retention. Of the 624 river catchments analyzed here, 140 had previously been used by Jansen et al. (2010) to fit the empirical DSi mobilization equation, assuming the DSi retention within these 'training catchments' is negligible. For the statistical analyses, 'training catchments' and 'non-training catchments' (n=484) were thus considered separately.

2.3 Results

2.3.1 Total DSi retention within the study area

The empirical mobilization equation, derived by Jansen et al. (2010) and applied spatially explicity to North America by Moosdorf et al. (2011), gives an average DSi mobilization of 1.65 t SiO_2 km^{-2} a^{-1} and a total DSi mobilization of 13.1 Mt SiO_2 a^{-1} for the conterminous USA. Within the monitored area considered here (cf. Fig. 3), the estimated DSi mobilization amounts to 10.9 Mt SiO_2 a^{-1}. For the catchments representing this area without overlaps ('non-overlapping catchments', n=161), a fluvial DSi flux of 9.4 Mt SiO_2 a^{-1} was calculated. Considering both values as representative for this area, a total retention of 1.4 Mt SiO_2 a^{-1} or 13 % was estimated.

2.3.2 DSi retention per catchment and potential factors

The DSi retention estimated for individual catchments is more uncertain and partly takes negative values. The spatial distribution of estimated DSi retention per catchment is characterized by a regional clustering with negative retention estimates dominating the western part of the study area and positive retention estimates in the eastern part (Fig. 4). Some examples of estimated DSi retention are given in Table 2, comprising the three largest of the basins considered here (Mississippi R., Colorado R., and St. Lawrence R.) and two more catchments within the St. Lawrence River Basin partly covering the Great Lakes (St. Mary's River and Detroit River).

The DSi retention estimated per catchment is on average negative for the training catchments as well as the non-training catchments, with a very similar mean of -7.6% and -7.5%, respectively. The estimated DSi retention shows a strong negative correlation with DSi concentration, for both the training and the non-training catchments (Table 3, Fig. 6a,b). For the training catchments, for which $f_{DSi,mob}$ is an estimate of the specific fluvial DSi flux assuming minimal DSi retention, this correlation is likely due to the fact, that the mobilization equation tends to underestimate specific fluxes with high DSi concentrations and overestimate specific DSi fluxes with low DSi concentrations (Jansen et al., 2010). However, the negative correlation between DSi concentration and estimated DSi retention was found here to be of a similar intensity within the non-training catchments (Table 3, Fig. 6a,b). Note that the statistical distribution of mean DSi concentrations per catchment is similar for both subsets of catchments (cf. Table B.1 in Appendix). The strong negative correlation between DSi concentration and DSi retention estimates are further visible in the similar spatial patterns of high DSi concentrations and negative DSi retention estimates (Fig. 4, Fig. 5). As the same runoff data were used for the calculation of $f_{DSi,calc}$ and the estimation of $f_{DSi,mob}$, there is no significant correlation between DSi retention estimates and runoff (cf. Table 3).

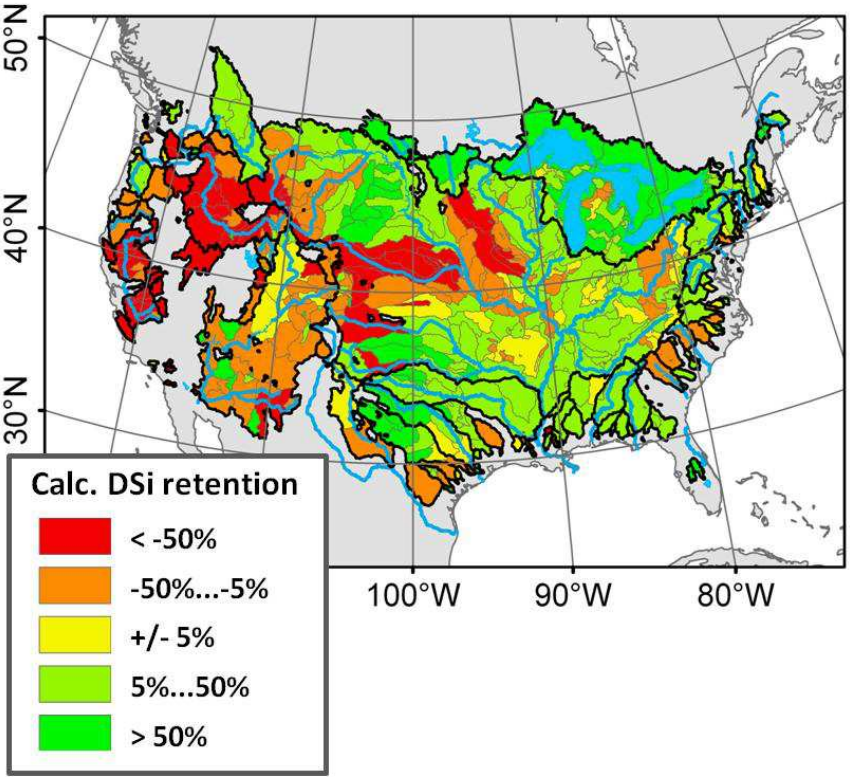

Fig. 4: Estimated DSi retention, calculated for each catchment (Eq. 1).

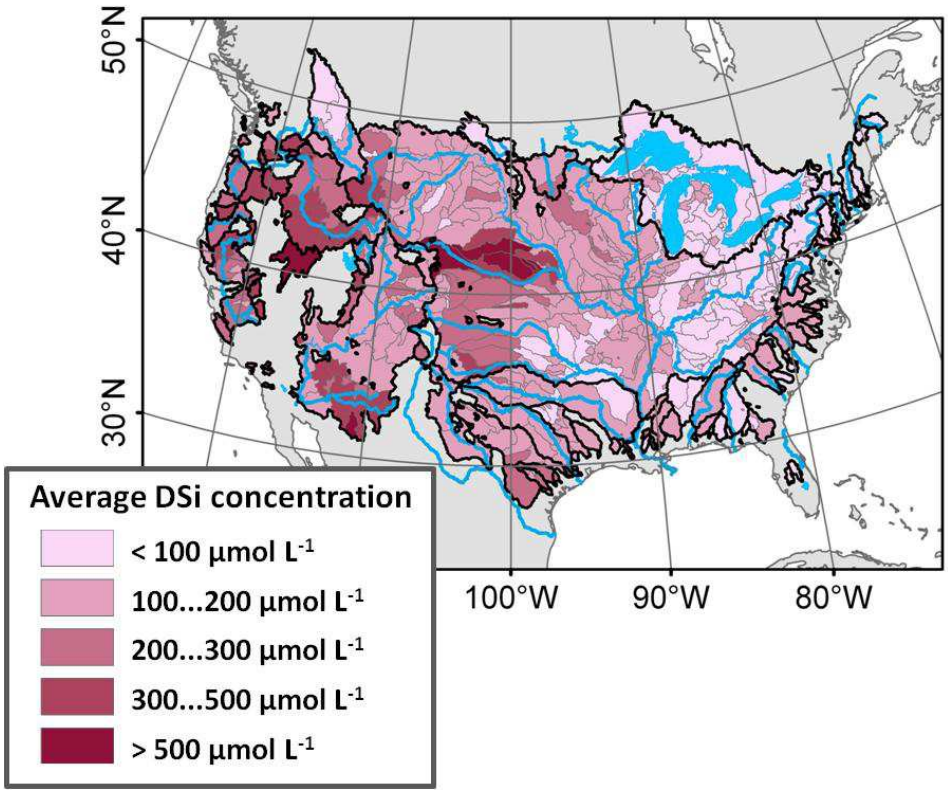

Fig. 5: Mean DSi concentrations derived from hydrochemical monitoring data. Averages are weighted by instantaneous discharge.

Table 2: Examples for estimated DSi retention, relative and in g SiO_2 m² lake area a^{-1}.

Sampling location	Twelve-month-series	Catchment area [km²]	Lake area prop.	DSi retention relative	DSi retention [g SiO_2 m^{-2} a^{-1}] [a]
Mississippi at Vicksburg	3	2,914,988	0.9%	13%	18.8
Colorado above Morelos Dam near Andrade	10	615,827	0.3%	-28%	-21.0
St. Mary's River	2	209,316	43.9%	67%	3.3
Detroit River	1	592,720	37.1%	81%	3.5
St. Lawrence River at Cornwall	1	771,620	34.7%	91%	4.3

[a]Refers to lake area within each catchment.

Because it was expected that biotic uptake and retention of DSi increase with catchment size and areal proportion of lakes, these parameters were expected to show significant correlations to estimated DSi retention. However, these parameters were not found to be statistically related to the estimated DSi retention per catchment (cf. Table 3, Fig. 6c,d,e,f). For the Great Lakes (cf. St. Lawrence R., Detroit R., St. Mary's R. in Table 2), the lake effects became indeed clearly visible. However, for most of the catchments considered in this study, areal proportions of lakes are rather low (90^{th} percentile = 2%). Thus, the set of river catchments analyzed here is probably less suitable to analyze correlations between lake area proportions and DSi fluxes as e.g. the river catchments draining to the Baltic Sea studied by Humborg et al. (2008).

For the non-training catchments, there are no significant correlations to hydrochemical properties of potential interest, i.e. nutrient concentrations, water temperature, and suspended matter concentrations, with the exception of total phosphorous concentration (TP) (cf. Table 3). However, the weak correlation between TP and estimated DSi retention depends on few very high values. If TP concentrations higher than 80 µmol L^{-1} are discarded the correlation becomes insignificant (3 cases omitted, r=-0.024, p=0.604).

For the non-training catchments, there is a low but significant correlation between estimates of DSi retention and mean annual air temperature (r=0.199, p=0.000, Fig. 6h). However, this correlation is due to catchments with high DSi concentrations and highly negative DSi retention estimates, which to a larger proportion show lower mean air temperatures (cf. Fig. 6h). If catchments with DSi concentrations higher than 200 µmol L^{-1}, i.e. about the upper quartile of all catchments (188 µmol L^{-1}),

are discarded from the analysis, the correlation becomes insignificant (n=371, r=0.091, p=0.080). With regard to DSi retention within the fluvial system, land cover could be interesting as potential factor controlling water quality and thus indirectly controlling diatom growth and sedimentation. Indeed, there are statistically significant but low correlations between land cover and estimated DSi retention. However, because no correlations with potential water quality parameters were found, the indirect effects from land cover on DSi retention cannot be identified sufficiently in this study.

Table 3: Correlation matrix: estimated DSi retention per catchment vs. catchment characteristics and water quality parameters for all catchments and different subsets of catchments.[a]

	DSi retention (r_{DSi})							
Set of catchments (c.)	**All c.**		**Training c.**		**Non-training c.**		**Non-overl. c.**	
Parameter	**N**	**r**	**N**	**r**	**N**	**r**	**N**	**r**
Catchment size [m²]	624	*0.02*	140	*-0.16*	484	*0.02*	161	*0.06*
$\log_{10}$(Catch. size [m²])	624	*-0.07*	140	*-0.10*	484	*-0.07*	161	*-0.02*
q [mm a^{-1}]	624	*0.06*	140	*0.14*	484	*0.04*	161	*0.07*
DSi conc. [µmol L^{-1}]	624	**-0.68**	140	**-0.70**	484	**-0.68**	161	**-0.64**
$f_{DSi,calc}$ [t SiO_2 $km^{-2}a^{-1}$]	624	**-0.27**	140	*-0.13*	484	**-0.30**	161	**-0.22**
$f_{DSi,mob}$ [t SiO_2 $km^{-2}a^{-1}$]	624	**0.08**	140	*0.13*	484	*0.07*	161	*0.13*
Air temperature [°C]	624	**0.15**	140	*-0.03*	484	**0.20**	161	*0.13*
Population density (1990) [persons km^{-2}]	624	*0.06*	140	*0.09*	484	*0.07*	161	*0.01*
Agricultural lands [1]	624	*0.01*	140	**-0.22**	484	*0.07*	161	*0.03*
Broadleaved forest [1]	624	**0.19**	140	*0.16*	484	**0.20**	161	*0.11*
Coniferous forest [1]	624	**-0.14**	140	*0.16*	484	**-0.22**	161	*-0.03*
Shrublands [1]	624	**-0.15**	140	*-0.06*	484	**-0.16**	161	**-0.25**
Grasslands [1]	624	*0.01*	140	**-0.28**	484	**0.09**	161	*0.08*
Artificial areas [1]	624	**0.09**	140	*0.12*	484	**0.10**	161	*0.06*
Lake area proportion [1]	624	*0.04*	140	*0.05*	484	*0.04*	161	*0.13*
Water temperature [°C]	613	*0.05*	138	*-0.07*	475	*0.07*	159	*-0.02*
SPM conc. [mg L^{-1}]	496	*-0.03*	115	**-0.24**	381	*0.04*	131	**-0.28**
pH	614	*-0.03*	138	*-0.14*	476	*-0.01*	159	*0.02*
NO_2^- ,NO_3^- conc. [µmol L^{-1}]	603	**-0.10**	136	**-0.19**	467	*-0.08*	157	*-0.04*
TP conc. [µmol L^{-1}]	600	*-0.06*	135	*-0.01*	465	**-0.10**	157	**-0.32**

[a]Correlations which are significant to the p=0.05 level are highlighted in bold letters.

q runoff
SPM suspended matter
TP total phosphorous

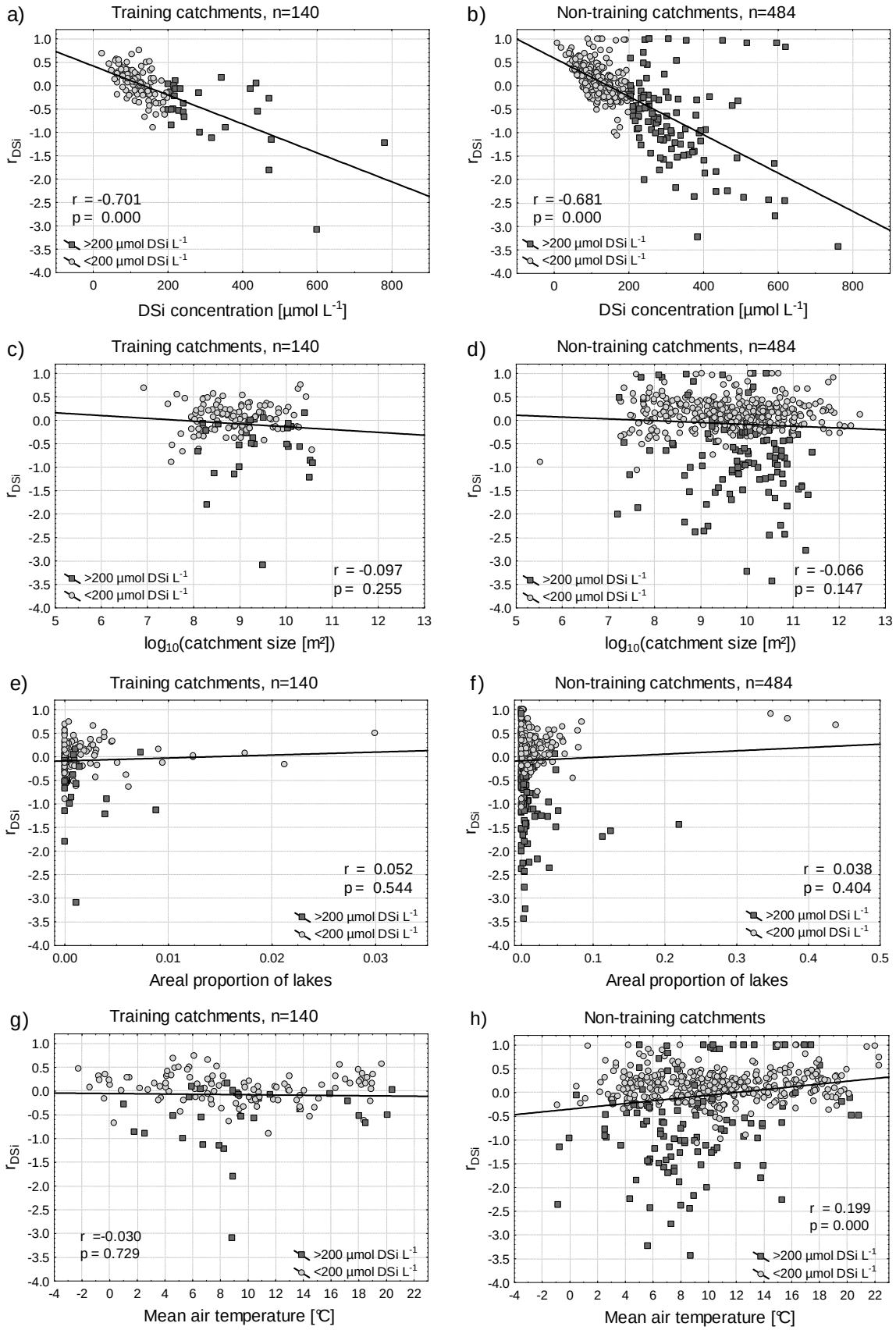

Fig. 6: Scatter-plots of estimated DSi retention r_{DSi} (Eq. 1) vs. catchment properties and hydrochemical properties. Cases with mean DSi concentrations higher than 200 µmol L^{-1}, corresponding to about the upper quartile of 188 µmol L^{-1}, are plotted as dark squares.

2.4 Discussion

2.4.1 Comparison with literature values

The total DSi retention of 13% estimated for the monitored area is lower than the 21-22% expected by Beusen et al. (2009) for the entire North American continent. In the following, this difference is discussed with regard to the different methodological approaches.

As Beusen et al. (2009) focused on anthropogenically induced DSi retention in large reservoirs (dams of at least 15 m height), they did not account for unperturbed DSi retention and DSi retention within natural lakes and smaller reservoirs. Further, for the northern, less densely populated parts of North America not included in this study, fluvial systems can be expected to be less perturbed by human activity. Thus, the DSi retention within the conterminous USA should be higher than given for the total continent.

In this respect, it is important to note that Moosdorf et al. (2011) give a DSi mobilization estimate for entire North America that is 22% lower than that given by Beusen et al. (2009) and even 6% lower than the fluvial DSi export estimated by Dürr et al. (2009) (cf. Dürr et al., 2011; Moosdorf et al., 2011a). The lower DSi mobilization used here is a probable reason for the comparatively low calculated DSi retention. For the area represented by the training catchments, the spatially explicit estimation by Moosdorf et al. (2011) gives a total DSi flux of 0.89 Mt SiO_2 a^{-1}, while the total flux of DSi calculated from hydrochemical monitoring data amounts to 0.97 Mt SiO_2 a^{-1}. Thus, the estimates by Moosdorf et al. (2011) underestimate the total fluvial DSi flux by 8.6% within the area, for which retention of DSi was assumed to be negligible and thus DSi fluxes were assumed to represent the DSi mobilized from the terrestrial system into the fluvial system (cf. Jansen et al., 2010). If this underestimation was assumed to represent a general bias in the estimation of DSi mobilization within the entire monitored area considered in this study, the total DSi retention estimate would have to be corrected up to a value of 22%. This value is about the estimate from Beusen et al. (2009).

On the other hand, some theoretical considerations argue for the DSi retention in the fluvial system of North America to be probably lower than estimated by Beusen et al. (2009). Beusen et al. (2009) assumed DSi retention rates in large reservoirs to equal the retention rates of dissolved inorganic phosphorous (DIP) as estimated by Harrison et al. (2005b). However, studies investigating retention of DSi as well as DIP indicate that retention rates of DIP are generally higher. The mass balances of

dissolved matter within five reservoirs in the western USA give retention rates for DSi that are at least 2.5 times lower than that of DIP in each case (Kelly, 2001; cf. Table 4). DIP retention rates that are substantially higher than DSi retention rates were also reported for the highly perturbed Red River (China/Vietnam) (Le Thi Phuong et al., 2010; factor 2.3), a semiarid riverine lake systems in Australia (Cook et al., 2010; factor 2.0), and three reservoirs in the upper Seine Basin (Garnier et al., 1999; factors 1.1 to 1.7). No studies reporting DSi retention rates higher than that of DIP are known to the author.

Table 4: Examples for silica retention within lakes, reservoirs, and whole rivers.

Lake/River	Silica retention		Reference (Method)
	g SiO_2 $m^{-2}a^{-1}$	rel.	
Oligotrophic lakes with crystalline catchment	<10	-	Campy and Meybeck (1995) (compilation from literature)
Volcanic lakes + partially mesotrophic lakes	>20	-	
Lake Mead (Colorado R.)	28.5	13%	After Kelly (2001) (based on DSi fluxes, inflow, outflow)
Lake Powell (Colorado R.)	16.4	8%	
Falcon reservoir (Rio Grande R.)	26.6	17%	
Amistad reservoir (Rio Grande R.)	-76.0	-66%	
Lower Columbia River reservoirs	-	-20%	
Lake St. Croix (Mississippi R.)	-	10%	Triplett et al. (2008) (mass balance of DSi and BSi, inflow, outflow)
Lake Pepin (Mississippi R.)	-	20%	
Lake Michigan	3.0	80%	Schelske (1985) after Parker et al. (1977) (mass balance DSi + BSi, inflow, atmospheric deposition, outflow, permanent loss to sediments)
Lake Superior	3.6	65%	Schelske (1985) after Johnson and Eisenreich (1979) (mass balance DSi + BSi, inflow, outflow, atmospheric deposition, shoreline erosion, sediment deposition, silicate authigenisis, redissolution from sediments)
Lake Texoma (Red River, USA)	22.2	30%	This study (mass balance based on DSi concentrations and instantaneous discharge from USGS data at inflows and outflow)
Marne reservoir (Seine River basin)	-	48%	Garnier et al. (1999) (mass balance of DSi inflows and outflows, based on three year time series)
Aube reservoir (Seine River basin)	-	57%	
Seine reservoir (Seine River basin)	-	43%	
Seine River in 2001 (wet year)	-	9%	Sferratore et al. (2006) (mass balance based on DSi and BSi measurement from different sampling locations, atmospheric inputs, estimates of anthropogenic point sources)
Seine River in 2003 (dry year)	-	6%	
Red River (China/Vietnam)	-	23%	Le Thi Phuong et al. (2010) (based on Seneque/Riverstrahler model)
Lower lakes (Murray Rive, Australia)	-	39%	Cook et al. (2010) (mass balance, DSi inflows and outflows)
Lake Biwa (Japan)	30	80%	Goto et al. (2007) (mass balance, DSi inflows and outflows)

For the particular examples of the Great Lakes, the DSi retention rates estimated in this study are very close to that reported by Schelske (1985) (cf. Table 2, Table 4). For the St. Mary River basin, which comprises Lake Superior, a DSi retention of 67% or 3.3 g SiO_2 m^{-2} a^{-1} (refers to lake area) was estimated here. In her mass balance comprising fluvial fluxes of DSi and BSi as well as atmospheric inputs after Johnson and Eisenreich (1979), Schelske (1985) estimated a silica retention of 65% or 3.6 g SiO_2 m^{-2} a^{-1} for Lake Superior.

The here estimated DSi retention of 18.8 g SiO_2 m^{-2} a^{-1} in lakes and reservoirs within the Mississippi River Basin (referring to sampling location at Vicksburg, Mississippi) is well within the range of DSi retention calculated for Lake Texoma (mass balance solely based on USGS data), Lake Mead, Lake Powell, and Falcon Reservoir (after Kelly, 2001) and the average DSi retention within lakes after Campy and Meybeck (1995) (cf. Table 4). Thus, it is concluded that the here estimated DSi retention for the Mississippi River is reasonable as well.

2.4.2 Uncertainties due to methods

The uncertainties of DSi retention estimates are the sum of the uncertainties related to estimation of DSi mobilization and calculation of fluvial DSi fluxes. They may further be related to additional sources of DSi not addressed here, the non-availability of BSi data at a regional scale, and the steady state assumptions that might not be valid for the investigated systems. These issues are addressed in the following subsections.

2.4.2.1 Estimates of DSi mobilization

Within the training catchments, the DSi mobilization estimation raster from Moosdorf et al. (2011) explained 89% of the variance of calculated DSi fluxes. This variance was explained by the predictors runoff and lithology. Other potential factors of DSi mobilization not included in the respective mobilization function, i.e. temperature, land cover, slope gradient, and physical denudation rates, were discussed by Jansen et al. (2010). Uncertainties due to the spatially explicit application and the extrapolation to the entire North American continent were discussed by Moosdorf et al. (2011).

Generally, the estimates of DSi mobilization tend to overestimate specific fluxes with low DSi concentration and underestimate specific DSi fluxes with high DSi concentrations within the training catchments (Fig. 7a). As the statistical distribution of DSi concentrations derived from hydrochemical data is similar for the training and non-training catchments, this correlation is not expected to bias the

estimates of average silica retention. Albeit, there is no significant correlation between under- and overestimation of specific DSi fluxes and runoff (Fig. 7b).

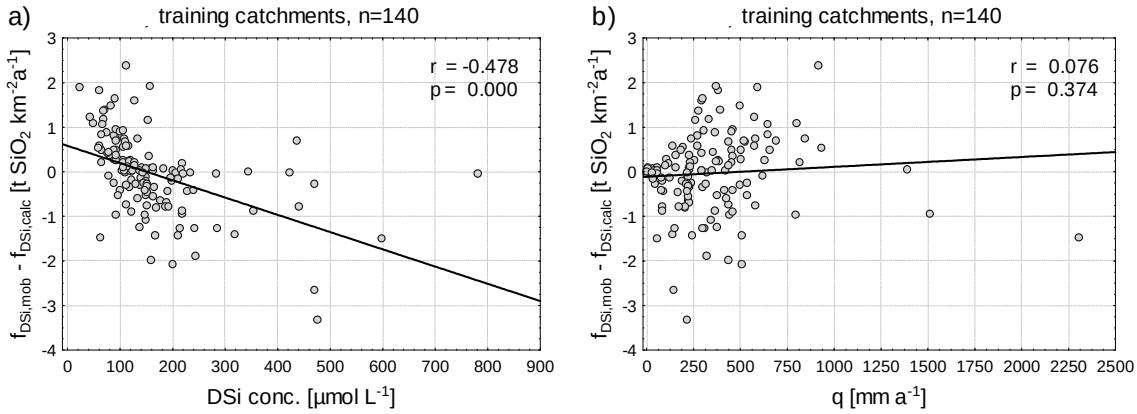

Fig. 7: Difference between estimated mobilization and calculated DSi fluxes vs. a) DSi concentrations derived from hydrochemical monitoring data and b) the runoff data used for flux calculations – both within the training catchments. Note that for the training catchments the calculated DSi fluxes are assumed to represent the DSi mobilized from the terrestrial system.

Despite the fact that the range of runoff values and DSi concentrations within training catchments fully cover those within the other subsets of catchments, the maximum values for $f_{DSi,mob}$ and $f_{DSi,calc}$ within the non-training catchments exceed those within the training catchments substantially (cf. Table B.1). However, only three of the 484 non-training catchments show $f_{DSi,mob}$ and $f_{DSi,calc}$ values exceeding the respective maxima of the training catchments. The same is the case for two of the 161 non-overlapping catchments, which were used to calculate total DSi fluxes and a representative estimate of DSi retention for the monitored area considered here. If these two catchments are discarded from the analyses, the estimated DSi mobilization and the calculated DSi fluxes decrease by only 0.4%, while the thereupon estimated DSi retention remains 13%.

Note that temperature as a possibly important factor was not included in the DSi mobilization equation, because it was not possible to isolate temperature as a statistically significant predictor based on the training catchments (Jansen et al., 2010). The DSi mobilization estimates show a tendency to overestimate DSi mobilization in colder regions and underestimate DSi mobilization in warmer regions (Jansen et al., 2010; Moosdorf et al., 2011a). As the training catchments are on average only slightly colder than the whole monitored area (-0.6℃) (cf. Table. B.1), no notable bias in the estimated total DSi mobilization and thus DSi retention from this tendency is expected.

With regard to land cover, a weak tendency of underestimating DSi mobilization from agricultural lands and grasslands was identified (Jansen et al., 2010; Moosdorf et al., 2011a). In this study, this tendency is confirmed by a low negative correlation of DSi retention (r_{DSi}) to agricultural lands (r=-0.22) and grasslands (r=-0.28) within the training catchments, for which minimum retention effects are expected. However, as there is a strong positive intercorrelation between areal proportions of both land cover classes (r=0.67, cf. Table B.3), it is not easy to distinguish between the effects of both land cover classes. However, as average land cover composition of the training catchments and the monitored area is similar (cf. Table B.2), it is not expected that the total DSi mobilization estimated for the study area and the thereupon derived estimate of total DSi retention is biased by land cover effects.

2.4.2.2 Calculation of DSi fluxes

Uncertainties in the calculation of fluvial DSi fluxes depend on uncertainties and the representativeness of the hydrochemical data and runoff data used for flux calculations. DSi fluxes calculated from series of monthly measurements have specific uncertainties as well as a positive bias (Stelzer and Likens, 2006). The uncertainty is related to the question how well the seasonality in DSi concentrations is represented by monthly sampling and the interannual variability of total DSi fluxes. This uncertainty decreases with increasing sampling frequency (Stelzer and Likens, 2006) and with the length of the times series considered. Positive biases are likely to occur, because short-termed peak-flows, which are characterized by decreased DSi concentrations (also cf. Hornberger et al., 2001), might not be captured well by the sampling frequency but are present in the runoff data (Stelzer and Likens, 2006). The hydrochemical data set used here is based on a monthly sampling, with on average 3.3 twelve-month-series per sampling location. For 136 of the sampling locations, only one twelve-month-series was retrieved. For the 488 sampling locations with two or more twelve-month-series, the average DSi concentration for distinct twelve-month-series show an average coefficient of variance (COV) of 12.0%. For 10% of the respective sampling locations, the COV is lower than 2.55%, for 90% it is lower than 24.8%. However, there is no significant correlation between the number of twelve-month-series and the COV of annual mean DSi concentration (r=0.07, p=0.119). Moreover, the COV of mean DSi concentrations calculated for distinct years is positively correlated to the COV of the annual means of the instantaneously measured discharge (r=0.495, p=0.000). These findings confirm that uncertainties in DSi flux calculations are especially high for intensively fluctuating discharges, which are predominantly found in semi-arid regions (cf. Stelzer and Likens, 2006).

It has to be expected that, due to the positive bias, fluvial DSi fluxes are likely overestimated in this study. For a sampling frequency of 28 days, which is close to that of the monthly data used here, Stelzer and Likens (2006) estimated this bias to be about 13% on average for twenty river catchments distributed throughout the conterminous USA. This value is expected to be representative for the study area. However, these rivers have catchment areas ranging from 0.13 to about 696 km² (Stelzer and Likens, 2006), i.e. rather small compared to the catchments used here (cf. Table B.1). Because the bias increases with the temporal variability of the discharge (Stelzer and Likens, 2006), and because this temporal variability of discharge can be expected to be lower in large rivers with extensive catchments, the bias for the catchments used in this study is probably lower. As the empirical equation by Jansen et al. (2010) is based on a similar data set, the positive bias likely affects the DSi mobilization estimates as well.

UNH/GRDC runoff composites were derived from long-term average discharge taken from gauging stations with at least twelve years of measurement and the conterminous USA is well covered with such sampling locations (cf. Fekete et al., 2002), it can be concluded that the data represent the long-term annual runoff well for larger river basins. Because the runoff was routed over a stream network with 30' resolution and only gauging stations with contributing areas of at least 10,000 km² were considered (Fekete et al., 2002), the data are expected to be more uncertain for river catchments of less than 10,000 km². However, as the same runoff data were used for the estimation of DSi mobilization (Jansen et al., 2010; Moosdorf et al., 2011a) and calculation of DSi fluxes from hydrochemical data, no direct impact of uncertainties in the runoff data on the DSi retention estimate is expected. Furthermore, the same is true for uncertainties in the delineation of catchments. The same catchment delineations were used to calculate the average DSi mobilization from the spatially explicit estimates from Moosdorf et al. (2011) and the average UNH/GRDC runoff for each catchment. Thus, the maximum tolerated deviation of 20% between the catchment size reported by the USGS and that calculated in this study has no direct effect on the estimated DSi retention.

2.4.2.3 Additional sources of DSi

Two potential sources of DSi are neglected in this study: atmospheric inputs and anthropogenic point sources. Atmospheric depositions of silica onto the water surface is usually negligible in the silica budget of freshwater ecosystems (cf. Ladouche et al., 2001; Hofmann et al., 2002). As it can be expected that atmospheric deposition makes up a higher proportion of total silica inputs the larger the

water surface is compared to fluvial inputs, it is most probable to find substantial atmospheric inputs for the Great Lakes. However, the ratio of fluvial silica imports (DSi+BSi) to atmospheric depositions is 16:1 for Lake Superior (Johnson and Eisenreich, 1979) and more than 25:1 for Lake Michigan (Parker et al., 1977). Thus, it is concluded that direct atmospheric inputs to the fluvial systems are generally negligible within the study area.

For Europe, the contribution by anthropogenic point sources to fluvial silica fluxes are estimated to be 2% on average (Van Dokkum et al., 2004). Within the Seine River basin, anthropogenic silica is estimated to make up as much as 8% of total inputs in dry years, when terrestrial ecosystems as diffuse sources contribute less (Sferratore et al., 2006). The average domestic contribution according to the budget by Sferratore et al. (2006) is about 781 g SiO_2 a^{-1} $inhabitant^{-1}$.

Anthropogenic point sources were avoided for the DSi mobilization estimation by using rather pristine training catchments (Jansen et al., 2010). The 140 training catchments considered here have an average population density of 9.2 inhabitants per km². Taking the values given by Sferratore et al. (2006) as first-order approximation, an average anthropogenic contribution of 7.2 kg DSi per km^{-2} a^{-1} from domestic sources would result, i.e. less than 0.3% of the average estimated DSi mobilization of 2.57 t SiO_2 km^{-2} a^{-1}. The total monitored area considered here has an average population density of 26.5 inhabitants per km². Adding this domestic silica, the DSi mobilization within the monitored area could be estimated to be 1.3% higher, and the estimated total retention would increase from 13% to 14%. However, as Sferratore et al. (2006) states, these assumptions on domestic DSi inputs cannot be easily transferred.

Although silica inputs from point sources are minor compared to natural diffuse inputs from the terrestrial system, industrial inputs, especially from pulp and paper mills, can be substantial (Van Dokkum et al., 2004). However, at a regional scale, no appropriate data set on industrial sources is available. Despite being generally a minor source of DSi, anthropogenic sources contribute to the uncertainties in the estimation of DSi retention in some areas.

2.4.2.4 Limitations due to scarce BSi data

A major problem of the mass balance calculations is the scarcity of data on BSi concentrations, as DSi is transformed to BSi by biotic uptake and a major part of BSi is redissolved to DSi within aquatic ecosystems.

The approach to calculate silica retention based on DSi alone requires the assumption that the concentrations of BSi relative to DSi are negligible or, at least, that BSi concentrations relative to DSi concentrations would be similar for different catchment sizes. However, according to the data compiled by Conley (1997), BSi contributes about 16% of the global fluvial silica export. The data further suggest that in small catchments BSi/DSi ratios tend to be lower than in larger catchments. This could cause the approach presented here to overestimate silica retention.

On the other hand, other studies show that small impoundments with very short residence times act mainly as trap for riverine diatoms and decrease BSi concentrations downstream whereas DSi concentrations upstream and downstream of the impoundments can be quite similar (cf. Humborg et al., 2006; Triplett et al., 2008). In these cases, retention of silica can be significant but would not be detected by a budget based on DSi concentrations alone.

The proportions of BSi fluctuate seasonally due to diatom growth, with about 50-70% during diatom blooms and 10-20% throughout the rest of the year (Conley, 1997). Besides the general seasonal patterns, abundance of diatom BSi in the water can fluctuate significantly on even shorter timescales responding to short-term changes in nutrient concentration and light conditions, substantially adding to the uncertainty related to sampling frequency and flux estimation (cf. Triplett et al., 2008).

Furthermore, soil erosion can be a substantial source of terrestrial BSi, mainly consisting of plant phytoliths (e.g. Cary et al., 2005; Smis et al., 2010). The dissolution of such terrestrial BSi is considered a potential source of DSi within the fluvial system (e.g. Triplett et al., 2008). However, to the author no study quantifying such a contribution is known. The in-river dissolution of terrestrial BSi would be a possible explanation for the underestimation of fluvial DSi fluxes within agricultural and grasslands, as these are accumulating large amounts of phytoliths and/or can be susceptible to soil erosion (cf. e.g. Conley, 2002).

2.4.2.5 Assumption of steady state

Additional uncertainties in the approach presented here are due to the assumption of a steady state for the DSi mobilization from the terrestrial system as well as for DSi retention within freshwater systems. For their empirical DSi mobilization equation, Jansen et al. (2010) identified runoff and lithology as major predictors. Thus, the empirical equation suggests that DSi liberation by chemical rock weathering directly determines the DSi mobilization into rivers. Indeed, it was shown that in most

ecosystems substantial plant and soil storages of amorphous silica exist and cycling of silica between these storages is likely to be in the order of magnitude of DSi exports and often exceeds them (Alexandre et al., 1997; Conley, 2002; Fulweiler and Nixon, 2005; Blecker et al., 2006; Street-Perrott and Barker, 2008; Borrelli et al., 2010; Cornelis et al., 2010; Fraysse et al., 2010; Struyf et al., 2010a). Thus, tracing DSi fluxes in rivers back to weathering presupposes that the terrestrial ecosystems are in a steady state with no net changes in BSi storages. However, disturbances in terrestrial ecosystems, likely due to anthropogenic perturbation, may lead to changes in terrestrial silica storages, and thus may influence the rate of DSi exports to rivers (Conley et al., 2008; Melzer et al., 2010; Struyf et al., 2010b). Such effects might have biased the empirical mobilization equation by Jansen et al. (2010) and could be a reason for the tendency to underestimate DSi mobilization from agricultural lands and grasslands. In order to assess such impacts, more research and data on soil and plant BSi pools as well as detailed information on recent land cover changes are needed.

Calculating estimates of DSi retention in the approach presented here also assumes steady state conditions in freshwater ecosystems with constant annual rates of biotic DSi uptake and net-losses of BSi to sediments. However, the variability and complexity of environmental controlling factors causes interannual variations in diatom growth and thus DSi retention that are not easily predictable (e.g. Koch et al., 2004; Ferris and Lehman, 2007). Furthermore, the ecological status of a freshwater ecosystem may be in transition due to changes in its trophic level (c.f. Conley et al., 1993; Hartmann et al., 2010b) and alterations in hydrology due to dams and locks (c.f. Humborg et al., 2006). For such a transition due to eutrophication, Schelske (1985) gives an example for the Great Lakes which was characterized by a negative mass balance with silica outflows exceeding silica inflows. This transition has led from a steady state with N and P limiting diatom growth to a new steady state with DSi limitation and was characterized by a lasting depletion in DSi storages within the water column. Such a transition is a possible reason for negative mass balances for distinct reservoirs calculated by Kelly (2001) (cf. Table 4). However, longer time series of inflows and outflows of DSi and BSi to/from lakes and reservoirs as well as in-reservoir/in-lake silica cycling would be needed to confirm such a hypothesis, at present not available for a continental-scale data base.

2.5 Conclusion

The approach presented here to estimate DSi retention from spatially explicit estimates of DSi mobilization and DSi fluxes calculated from hydrochemical monitoring data was found to be appropriate to estimate total DSi retention within the fluvial system of the conterminous USA. The here estimated DSi retention of 13% is lower than the first-order estimates from previous studies using different approaches.

Uncertainties of DSi retention estimates that arise from uncertainties related to the DSi mobilization estimates and the calculation of DSi fluxes are large compared to expected DSi retention rates. Thus, the approach presented here does not allow deriving reasonable DSi retention rates for individual rivers catchments. However, comparison to literature values suggests that the estimated DSi retention is reasonable for the St. Lawrence River Basin (r_{DSi}=91%), which comprises the Great Lakes and is thus characterized by very high retention times, and for the Mississippi River Basin (at Vicksburg, MS) (r_{DSi}=13%), which is the largest of the here considered catchments (6.6 mio. km², 44% of the monitored area considered here). In summary the main sources of uncertainty encountered in this study are:

1) The uncertainties of the DSi mobilization estimates are large compared to expected DSi retention, which led to negative estimates for nearly half of the river catchments considered. Factors on DSi retention like catchment size, nutrient concentrations, land use, and lake area proportions are probably obscured by these uncertainties.
2) Further uncertainties arise from the non-availability of BSi data, because BSi might be a non-negligible proportion of silica transported by rivers in the study area.
3) The monthly sampling frequency does not capture short-term variations due to peak flows or weather-dependent diatom growth.

For earth system models incorporating land-ocean silica fluxes, it is recommended to account for the spatial variability of fluvial silica fluxes. To assess anthropogenic perturbations of the silica cycle, the factors controlling the retention of silica within the fluvial system and probably explaining the spatial variability in silica retention need to be understood. To provide an empirical basis, more research on the biogeochemical cycling and retention of silica within distinct rivers is needed, which explicitly

distinguishes the mobilization of silica from the catchment into the fluvial system. Furthermore, the BSi pools and fluxes within terrestrial and aquatic ecosystems need to be addressed in more detail.

3 Loss of dissolved organic carbon within the fluvial system of North America

3.1 Introduction

Rivers are the major pathway for land-ocean carbon fluxes which are an important part of the global carbon cycle. Moreover, rivers are biogeochemical reactors with net fluxes of CO_2 to the atmosphere and carbon burial in sediments (cf. Cole et al., 2007; Battin et al., 2008). It has been estimated that globally about 2,700 Mt C a^{-1} are exported from the terrestrial system to inland waters whereas only 900 Mt C a^{-1} are further exported to the marine system (Battin et al., 2009). The mass balance is closed by an accumulation of 600 Mt C a^{-1} in inland waters and a net-efflux of 1,200 Mt C a^{-1} from inland waters to the atmosphere (Battin et al., 2009). Streams and rivers contribute about half of this CO_2 evasion (Aufdenkampe et al., 2011).

Dissolved organic carbon (DOC) accounts for about 29% of the total fluvial carbon exports to the coasts (Ludwig et al., 1996a), the main part stemming from soil drainage (e.g. Mulholland, 1997; Guéguen et al., 2006). From the DOC being flushed from the terrestrial system into streams and rivers, a substantial part can be lost mainly due to respiration and photo-oxidation during fluvial transport or after being adsorbed to suspended or bed sediments, increasing the proportion of refractory, less decomposable components (Battin, 1999; Cole and Caraco, 2001; Dawson et al., 2001; Duan et al., 2007; Worrall et al., 2007; Battin et al., 2008; Rasera et al., 2008; Dubois et al., 2010). Thus, lateral DOC fluxes calculated from data sampled at the rivers' mouths underestimate terrestrial DOC exports (Worrall et al., 2007).

Studies analyzing the spatial variability of fluvial DOC fluxes and its controlling factors identified drainage intensity (Ludwig et al., 1996b) or discharge (Harrison et al., 2005a), slope (Mulholland, 1997), soil organic carbon content (Aitkenhead et al., 1999), C/N ratios of soils (Aitkenhead and McDowell, 2000; Aitkenhead-Peterson et al., 2005), and specific land cover (Mattsson et al., 2009) as potential predictors for a spatially explicit estimation. All these studies assume fluvial DOC fluxes to be conservative, and thus disregard in-stream/in-river losses of DOC. However, the fact that similar predictors can be identified from local to global scale is supporting this assumption (cf. Aitkenhead and McDowell, 2000).

On the other hand, recent global estimates of carbon losses during the lateral transport from terrestrial systems to the coasts (Cole et al., 2007; Battin et al., 2008; Battin et al., 2009) were based on literature reviews and did not account for the spatial variability of carbon fluxes. At the regional scale, Worrall et al. (2007) made an attempt to assess the spatial variability in DOC losses within the fluvial system of England and Wales, calculating estimates of DOC respiration from measurements of the biochemical oxygen demand.

In this study, the in-river DOC loss is estimated for North America applying empirical, spatially explicit flux estimation techniques. For this, an empirical equation is set up, by which fluvial DOC fluxes are estimated from geospatial data representing potential controlling factors. The empirical equation is trained on two different sets of river catchments, divided by catchment size into smaller and larger catchments. Assuming that the large training catchments have already experienced more in-stream/in-river DOC losses than the small catchments, it is hypothesized that spatially explicit estimates of in-river DOC losses can be calculated as the difference between the respective estimates. Further, the applied predictors and their different quantitative effects in both empirical fits of the estimation equation are analyzed and discussed.

3.2 Methods and data

3.2.1 Data processing

Hydrochemical data of 453 sampling locations from various sources (Government of Alberta - Environment; Ontario - Ministry of the Environment; USGS; Alexander et al., 1997; Environment Canada, 2009; Environment Canada, 2010) and the UNH/GRDC runoff data set (Fekete et al., 2002) were used to calculate long-term annual DOC fluxes.

The sampling locations were selected following three criteria: (i) DOC concentrations for at least 12 consecutive months were available; (ii) the sampling location could be positioned on the stream network (Hydrosheds by Lehner et al., 2008, 15" resolution) and the derived catchments were consistent with satellite imagery (no rivers crossing the catchments boundaries), and (iii) the sampling location was not within an urban area nor was the catchment dominated by urban or industrial areas.

From the time series of each sampling location, as many non-overlapping series of twelve consecutive monthly measurements as possible were identified (on average 3.1 years per station). Long-term

mean monthly DOC fluxes were calculated from mean monthly DOC concentrations and monthly UNH/GRDC runoff data, representing long-term average runoff modeled from climatic data and forced by gauging data (Fekete et al., 2002). The mean monthly DOC fluxes were then summed up to mean annual DOC fluxes. By this procedure, the monthly DOC concentrations are implicitly weighted by UNH/GRDC runoff data. It was considered the best feasible practice, as instantaneously measured discharges were often missing or inconsistently reported in the used hydrochemical datasets.

Based on different sets of geodata (Table 5), the catchments for each of the sampling locations were delineated and their catchment properties were calculated. For this, all of the used raster data sets were projected to Lambert Azimuthal Equal Area projection and resampled to a resolution of 1 km x 1 km cell size. Data sets with a similar or coarser resolution in decimal degrees were resampled to 1 km x 1 km resolution using the nearest neighbor method. Data sets with a finer resolution in decimal degrees were first resampled to cell sizes corresponding to the original cell size (GlobCover: 200 m, SRTM DEM: 100 m, Worldclim: 200 m), also using the nearest neighbor technique. The resulting raster cells were then aggregated to 1 km x 1 km raster cells assigned the average of the aggregated cells.

Within the study area, the Global Lake and Wetland Data Base (GLWD) (Lehner and Döll, 2004) distinguishes a certain number of some coherent wetland types, while for extensive parts, only the proportion range of total wetland cover (‘25% to 50%’ and ‘50% to 100%’) is given. To gain a consistent wetland proportion data set, it was assumed that each of the distinguished wetland types take an areal proportion of 1 within the respective raster cells. For the wetland proportion classes, the means of the given ranges, i.e. 0.375 and 0.75, were assigned.

Table 5: Geodata used to derive catchment properties.

Parameter	Data set	Source	Scale/Resolution
Flow directions	Hydrosheds DEM	Lehner et al. (2008)	15''
Runoff	UNH/GRDC runoff composites	Fekete et al. (2002)	30'
Slope gradient	SRTM DEM	Jarvis et al. (2006)	3''
Land cover	GlobCover	Arino et al. (2007)	300 m
Wetlands	GLWD	Lehner and Döll (2004)	30''
Annual precipitation	Worldclim	Hijmans et al. (2005)	30''
Mean air temperatur			
Lakes	SRTM Water Body Data Set	NASA/NGA (2003)	Based on SRTM DEM with 3'' resolution

3.2.2 Statistical analyses

3.2.2.1 DOC flux estimation

Multiple linear regression analysis was used to identify catchment properties as predictors of the spatial variability in DOC fluxes (applying the software Statistica 9.0). The set of 453 training catchments was subdivided into one subset with catchment areas below 2,000 km² (n=246, 'small catchments') and one subset with catchment areas above 2,000 km² (n=207, 'large catchments') (Fig. 8). The threshold of 2,000 km² was chosen in order to gain two subsets of similar sample size. Note that the 'small catchments' have an average area of 494 km². They are several times larger than catchments of small headwater streams which were often studied in local studies (Aitkenhead et al., 1999; Dawson et al., 2001). The 'large catchments' have a mean area of 26,525 km² and are thus on average more than 53 times larger than the 'small catchments'. The regression equation (Eq. 2) was fitted to each subset of catchments.

Eq. 2

$$f_{DOC} = b_1 * x_1 + \ldots. + b_n * x_n$$

Predictors (x_i) were stepwise added to the regression equation. For each predicting variable x_i a factor b_i (b-estimate) was derived during regression analysis, expressing the variable's effect on the specific DOC fluxes f_{DOC} [t C $km^{-2}a^{-1}$]. The predictors were chosen in order to optimize the correlation coefficient of the fitted regression equation and the significance of b-estimates assigned to predictor variables ($p<0.05$-significance level) for both sets of training catchments.

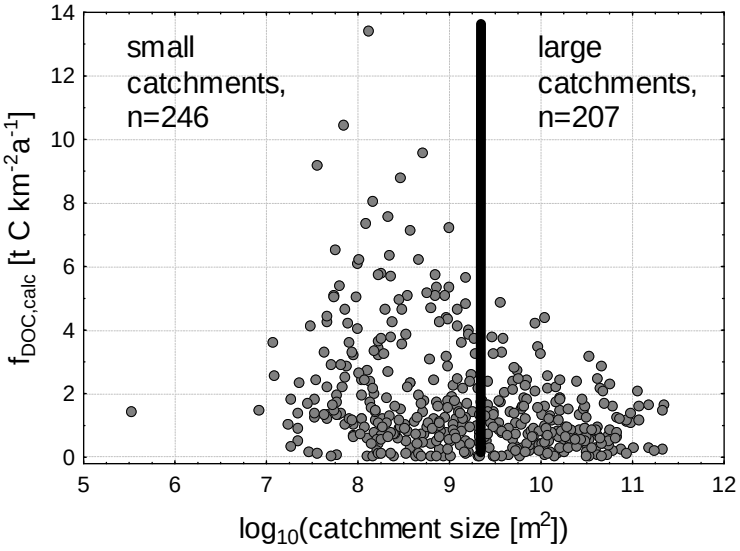

Fig. 8: Specific DOC fluxes vs. catchment size. The whole set of 453 training catchments was divided into two subsets, one with catchments smaller than 2,000 km² ('small catchments') and one with catchments larger than 2,000 km² ('large catchments'). The threshold of 2,000 km² (straight vertical line) was chosen to gain subsets of similar sample size.

The most appropriate regression equations were used to calculate spatially explicit estimates of f_{DOC} from the geospatial source data of the predictors (1 km x 1 km raster for continental North America south of 60°N). This geographical restriction was necessary, as the applied digital elevation data (SRTM) are only available up to this latitude. Negative values in the resulting rasters, which can occur if one or more of the predicting variables have a negative influence on the expected variable, were forced to 0 t C km^{-2}a^{-1}, because negative mobilization (i.e. DOC flux from the fluvial system to the terrestrial system) was not expected. As mobilization of DOC from the terrestrial system into surface waters was focused, the estimated DOC mobilization within mapped lake areas (according to NASA/NGA, 2003) was also forced to 0 t C km^{-2}a^{-1}. In the following, the spatially explicit estimates of fluvial DOC fluxes derived from the small catchments are denoted as $f_{DOC,mod}$[S]. Estimates derived from the large catchments are denoted as $f_{DOC,mod}$[L].

3.2.2.2 DOC loss estimation

Constraints on DOC loss within the fluvial system was calculated in two different budget approaches. For the large catchments the in-river DOC loss was estimated as the difference between $f_{DOC,mod}$[S] and the f_{DOC} calculated from the hydrochemical source data ($f_{DOC,calc}$) (Eq. 3). For the extrapolation area, the in-river loss was estimated based on $f_{DOC,mod}$[L] and $f_{DOC,mod}$[S] (Eq. 4).

Eq. 3

DOC loss rate = ($f_{DOC,mod}$[S] - $f_{DOC,calc}$) / $f_{DOC,mod}$[S]

Eq. 4

DOC loss rate = ($f_{DOC,mod}$[S] - $f_{DOC,mod}$[L]) / $f_{DOC,mod}$[S]

Note that these budgets address the DOC loss within river stretches along which the contributing area increases from the size of the 'small catchments' to the size of the 'large catchments'. As DOC losses within smaller streams and the lower reaches of larger rivers remain unaccounted for, these budgets represent conservative constraints on DOC losses within the fluvial system.

3.3 Results

3.3.1 Set up of empirical DOC flux equations

3.3.1.1 Regression fitting and identification of predictors

During the step-wise set up of the regression equations, runoff (q [ma^{-1}]) was identified as first predictor (1) (Table 6), followed by slope gradient (s [°]) (2), areal proportions of coniferous forests (A_{CF}), broadleaved forests (A_{BF}), herbaceous vegetation (A_{HV}) (3), and areal proportions of wetlands (A_{WL}) (4). Using this method, only predictors were considered that are significant for both the small and the large catchments. Note that the retained predictors are to some part intercorrelated (Table 7).

Runoff as single independent variable explains 22% of the variance in $f_{DOC,calc}$ for the small catchments (Table 6, regression equation S.1, note that the r^2 given here represent the explained proportion of the variance of the predicted variable). For the large catchments (Table 6, regression equation L.1), the explanatory power of this parameter is substantially higher with 33% of the variance of $f_{DOC,calc}$ explained. For the regression equations including more variables, the explained proportion of the variance of specific DOC fluxes is higher and does not differ much between both subsets of training catchments.

Table 6: Correlation coefficients and b-estimates for multiple linear regression equations using different sets of predictors.[a]

			q [m a^{-1}]			s [°]			A_{CF} [1]			A_{BF} [1]			A_{HV} [1]			A_{WL} [1]		
	r	r^2	b	Std. Err.	p	b	Std. Err.	p	b	Std. Err.	p	b	Std. Err.	p	b	Std. Err.	p	b	Std. Err.	p
small catchments (< 2,000 km²), n=246																				
S.1	0.47	0.22	3.72	0.18	0.00															
S.2	0.59	0.35	4.78	0.23	0.00	-0.14	0.02	0.00												
S.3	0.74	0.54	3.21	0.26	0.00	-0.22	0.02	0.00	3.12	0.31	0.00	0.99	0.30	0.00	2.27	0.62	0.00			
S.4	0.75	0.55	3.09	0.26	0.00	-0.21	0.02	0.00	2.95	0.32	0.00	0.82	0.30	0.01	1.99	0.62	0.00	1.68	0.63	0.01
large catchments (> 2,000 km²), n=207																				
L.1	0.58	0.33	3.25	0.14	0.00															
L.2	0.61	0.37	3.73	0.2	0.00	-0.03	0.01	0.00												
L.3	0.75	0.56	2.68	0.22	0.00	-0.11	0.01	0.00	1.76	0.24	0.00	0.79	0.20	0.00	1.64	0.27	0.00			
L.4	0.78	0.60	2.74	0.21	0.00	-0.09	0.01	0.00	1.32	0.24	0.00	0.50	0.19	0.01	1.07	0.28	0.00	1.81	0.37	0.00

[a]The b-estimate of each predictor represents its contribution to the estimated f_{DOC} in t C $km^{-2}a^{-1}$ per unit of the predictor. For A_{CF}, A_{BF}, A_{HV}, and A_{WL} this refers to a 100% proportion.

q	runoff
s	slope gradient
A_{BF}	areal proportion of broadleaved forests
A_{CF}	areal proportion of coniferous forests
A_{HV}	areal proportion of herbaceous vegetation
A_{WL}	areal proportion of wetlands

Table 7: Intercorrelation of the applied predictors within both subsets of training catchments.[a]

	Mean	Std. dev.	q	s	A_{BF}	A_{CF}	A_{HV}	A_{other}	A_{WL}
small catchments, n=246									
q	536	387	1						
s	5.17	5.61	**0.28**	1					
A_{BF}	0.34	0.28	0.07	**-0.15**	1				
A_{CF}	0.32	0.33	**0.27**	**0.34**	**-0.52**	1			
A_{HV}	0.13	0.12	**-0.33**	**-0.16**	**-0.14**	**-0.64**	1		
A_{other}	0.20	0.21	**-0.32**	**-0.25**	**-0.41**	**-0.52**	**0.61**	1	
A_{WL}	0.09	0.15	0.12	**-0.2**	0.09	-0.01	-0.05	-0.07	1
large catchments, n=207									
q	297	228	1						
s	6.63	4.79	**0.21**	1					
A_{BF}	0.28	0.22	**0.34**	**-0.23**	1				
A_{CF}	0.30	0.26	**0.24**	**0.66**	**-0.41**	1			
A_{HV}	0.17	0.12	**-0.33**	**-0.23**	**-0.27**	**-0.48**	1		
A_{other}	0.25	0.20	**-0.49**	**-0.46**	**-0.42**	**-0.56**	**0.33**	1	
A_{WL}	0.08	0.12	-0.03	**-0.27**	0.09	-0.07	0.12	-0.08	1

[a] Pearson correlation coefficients r. Statistically significant correlations ($p<0.05$) are highlighted in bold.

q	runoff
s	slope gradient
A_{BF}	areal proportion of broadleaved forests
A_{CF}	areal proportion of coniferous forests
A_{HV}	areal proportion of herbaceous vegetation
A_{other}	areal proportion of other land cover
A_{WL}	areal proportion of wetlands

Adding slope gradient increased the explained proportion of the variance of $f_{DOC,calc}$ to 35% (regression equation S.2) and 37% (regression equation L.2) (Table 6). The negative b-estimate for slope gradient indicates a negative functional relation to $f_{DOC,calc}$. This negative effect is counterbalanced by an increased b-estimate for runoff.

Adding A_{CF}, A_{BF}, and A_{HV} increased the explained proportion of the variance of $f_{DOC,calc}$ to 54% (regression equation S.3) and 56% (regression equation L.3) (Table 6). All of these land cover class proportions were assigned positive b-estimates. Note that land cover classes not included in the regression equation were combined as reference land cover class (A_{other}), for which f_{DOC} solely depends on runoff and slope gradient. A_{other} is mainly composed of agricultural land (small catchments: 73%, large catchments: 65 $\%_r$) and shrubland (small catchments: 6%, large catchments: 25%).

Areal proportions of the three explicitly included land cover classes add to f_{DOC} according to the related b-estimates. Coniferous forests (A_{CF}) yield most f_{DOC}, followed by herbaceous vegetation (A_{HV}) and broadleaved forests (A_{BF}). Compared to regression equations S.2 and L.2 (cf. Table 6), the positive effects of runoff are decreased and the negative effects of slope gradient are increased, both counterbalancing the positive effects of the three land cover classes.

Adding wetland proportions (A_{WL}) as independent variable increased the proportion of the variance of $f_{DOC,calc}$ only weakly (regression equation S.4: r^2=0.55; L.4: r^2=0.60, Table 6), likely due to on average low areal proportions (72% of the small and 65% of the large catchments are characterized by an A_{WL} of less than 5%). However, according to the b-estimates, wetlands have a notable positive effect on f_{DOC}. Compared to regression equations S.3 and L.3, b-estimates of A_{CF}, A_{BF}, and A_{HV} are decreased, although these predictors show no significant correlation to A_{WL}.

Regression equations S.4 and L.4 (Table 6) were considered the most appropriate for spatial extrapolation. They show the highest r^2 and all b-estimates are significant and reasonably interpretable. The residuals (observed – predicted values) of the fitted regression equations show nearly normal distribution (Fig. 9), indicating that the conditional expected values fit the conditional mean values of $f_{DOC,calc}$ well over the value range of the applied predictors within the training catchments.

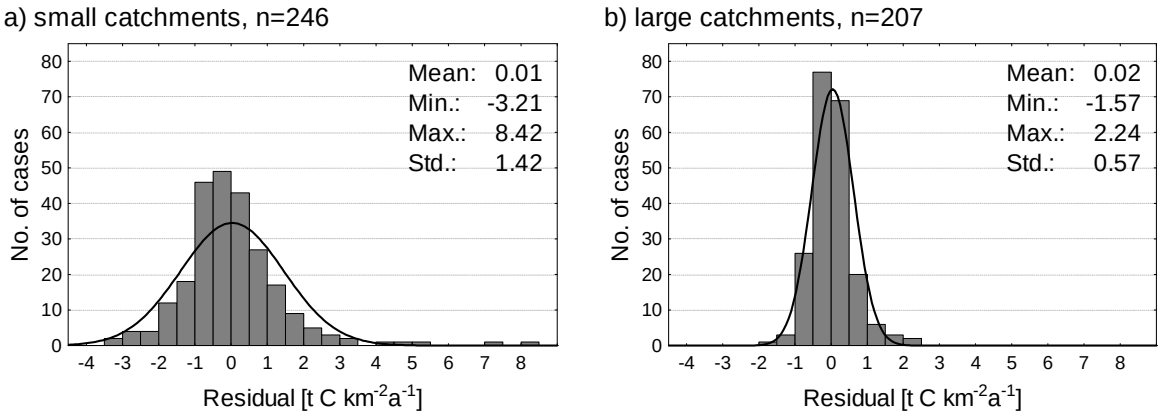

Fig. 9: Histograms of residuals of the regression equations a) S.4 (small catchments) and b) L.4 (large catchments). Means, minima, maxima, and standard deviations of this difference are reported in units of the x-axis. The curve indicates the theoretical normal distribution based on the mean and the standard deviation.

3.3.1.2 Analysis of predictors' effects on estimated DOC fluxes

According to the structure of the multiple linear regression equations S.4 and L.4, an increase in one of the predictors would cause a proportional increase or, in the case of slope gradient, decrease in estimated $f_{DOC.}$ The b-estimates (Table 6) give the amount of estimated f_{DOC} in t C $km^{-2}a^{-1}$ that the respective predictors contribute per reported unit.

Assuming all other predictors to be 0, for a runoff of 100 mm a^{-1}, a specific DOC flux of 0.31 t C $km^{-2}a^{-1}$ (regression equation S.4) or 0.27 t C $km^{-2}a^{-1}$ (regression equation L.4) would be estimated (Table 6). Increasing the average slope gradient by 1° would r educe this specific flux by 0.21 t C $km^{-2}a^{-1}$ (regression equation S.4) or 0.09 t C $km^{-2}a^{-1}$ (regression equation L.4). Thus, each increase of 1° in the average slope gradient would counterbalance the effect of an increase in runoff by 67 mm a^{-1} (regression equation S.4) or 33 mma^{-1} (regression equation L.4) (Table 8).

Compared to slope and runoff, the areal proportions of the distinguished land cover classes and wetlands have a theoretically more constraint value range, with 0 as minimum proportion and 1 as maximum proportion. For instance, a land cover of 100% coniferous forests would add 2.95 t C $km^{-2}a^{-1}$ (regression equation S.4) or 1.32 t C $km^{-2}a^{-1}$ (regression equation L.4) to the estimated f_{DOC} compared to a land cover with 0% of the distinguished land cover classes. Thus, the effect of a 100% areal proportion of coniferous forests on estimated f_{DOC} is equivalent to the effect of an increase in runoff by 953 mma^{-1} (regression equation S.4) or 481 mma^{-1} (regression equation L.4) (Table 8), or would counterbalance the negative effect of an increase in average slope gradient by about 14° for both regression equations. If the negative effect of slope gradient is not fully counterbalanced by the combined positive effects of the other predictors, the estimated specific DOC flux becomes negative. However, that was the case for only 18 of the 246 small catchments (using regression equation S.4) and 11 of the 207 large catchments (using regression equation L.4).

Relative to runoff (Table 8), the predictors slope gradient and areal proportions of coniferous forests (A_{CF}), broadleaved forests (A_{BF}), and herbaceous vegetation (A_{HV}) have substantially lower effects on the estimated f_{DOC} within the large catchments than within the small catchments. The effects of wetland proportions on the estimated f_{DOC}, on the contrary, are rather similar within both sets of training catchments. However, these results underline that the comparison of small and large catchment predictions can be used for DOC loss estimation (see below).

Table 8: Comparison of effects the retained predictors take on the estimated specific DOC flux in the regression equations S.4 or L.4.[a]

	q [mm a^{-1}]	s [‰]	A_{CF} [1]	A_{BF} [1]	A_{HV} [1]	A_{WL} [1]
small catchments, regression equation S.4						
q [mm a^{-1}]	1	-67	953	267	642	543
s [‰]	-0.015	1	-14.2	-4.0	-9.6	-8.1
large catchments, regression equation L.4						
q [mm a^{-1}]	1	-33	481	184	392	662
s [‰]	-0.030	1	-14.4	-5.5	-11.7	-19.8

[a]For each predictor, the effects per unit are expressed in equivalent values of q and s taking the same effect on the estimated specific DOC fluxes. Note that for q the unit mm a^{-1} is used instead of m a^{-1} that is used in the regression equations. For the areal proportions of the distinguished land cover classes (A_{CF}, A_{BF}, A_{HV}), the equivalents refer to a proportion of 100% of the considered land cover class compared to a 100% proportion of the reference land cover (A_{other}, see text). For A_{WL} this refers to 100% wetland proportion compared to 0% wetland proportion.

3.3.2 Spatially explicit application of the regression equations

The regression equations S.4 and L.4 were applied spatially explicitly to the area of continental North America south of 60°N (Fig. 10a,b). In the following, the respective estimates are denoted as $f_{DOC,mod}[S]$ (regression equation S.4) and $f_{DOC,mod}[L]$ (regression equation L.4). The general spatial patterns of $f_{DOC,mod}[S]$ and $f_{DOC,mod}[L]$ (Fig. 10a,b) are quite similar, with low values in the dry south western part and high values in the north western part (Hudson Bay low land area and Eastern Canada) and along the East Coast and West Coast of the US.

For the whole extrapolation area, the averages of $f_{DOC,mod}[S]$ and $f_{DOC,mod}[L]$ are 1.82 t C $km^{-2}a^{-1}$ and 1.40 t C $km^{-2}a^{-1}$, respectively. The estimated total DOC fluxes within the study area are 25.8 Mt C a^{-1} (referring to $f_{DOC,mod}[S]$) and 19.9 Mt C a^{-1} (referring to $f_{DOC,mod}[L]$), giving a total DOC loss of 5.9 Mt C a^{-1} and an average DOC loss rate of 23% within respective river stretches.

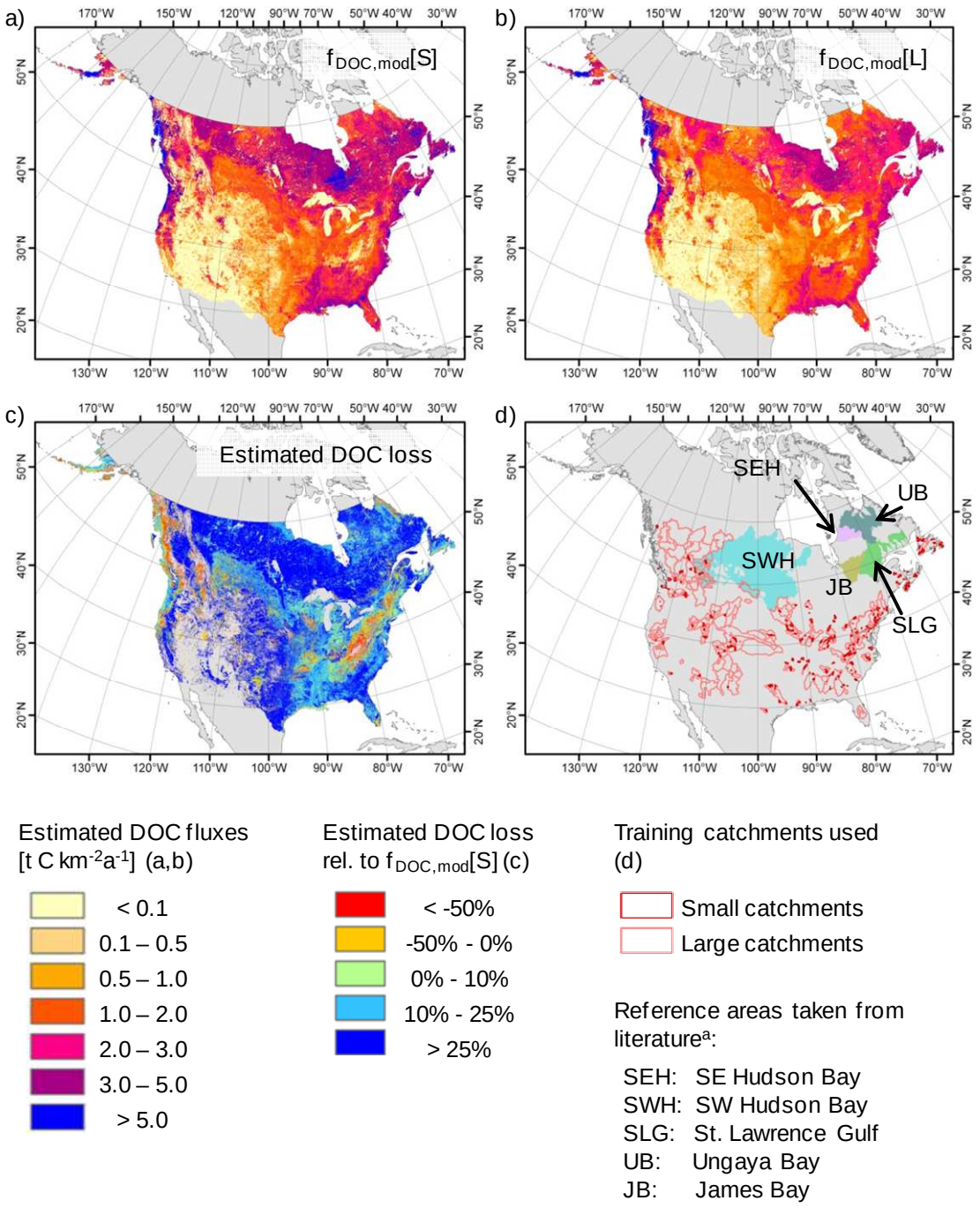

Fig. 10: Spatial variation of a) $f_{DOC,mod}$[S] and b) $f_{DOC,mod}$[L], c) calculated in-river DOC loss, and d) distribution of training catchments. Note that in the spatially explicit estimates, negative values and lake areas were forced to 0 t C km^{-2}a^{-1}. Non-valid values of DOC loss rates due to division by 0 are assigned no data (grey).

[a]Literature values of DOC fluxes for the depicted areas are discussed in section 3.4.1.1.

The calculated DOC loss rate (Fig. 10c) is mainly positive (70.3% of the area). An increased DOC loss rate is particularly visible in the northern parts of the extrapolation area. The reverse case, i.e. $f_{DOC,mod}$[S] being lower than $f_{DOC,mod}$[L] (14.4% of the extrapolation area), is mainly restricted to areas characterized by steep slopes (cf. Fig A.6, Appendix). Areas with $f_{DOC,mod}$[S] < $f_{DOC,mod}$[L] have on

average a slope gradient of 10.3°, which is substan tially higher than the average slope gradients of the training catchments (small catchments: 5.2°, large catchments: 6.6°) and the whole extrapolation area (4.2°) (cf. Table C.1 in Appendix). This suggests, that the applied extrapolation of a budget on DOC fluxes between the small and large catchments fails for high slope gradients, which are not well covered by the training catchments.

The maximum slope gradient covered by both sets of training catchments is 22.6° (Table C.1). Only about 2.8% of the extrapolation area shows higher slope gradients. If these were discarded from the spatial explicit application of the regression equations, the mean value of $f_{DOC,mod}[L]$ would remain 1.40 t C $km^{-2}a^{-1}$ whereas the mean value of $f_{DOC,mod}[S]$ would slightly increases by 1.7% to 1.85 t C $km^{-2}a^{-1}$. The calculated DOC loss would also slightly increase by 0.3 Mt C a^{-1} to 6.2 Mt C a^{-1} in total, giving an average DOC loss rate of 24%. However, as these differences are rather negligible, a notable bias for the DOC loss estimation is not expected.

3.3.3 Budget based on estimated and calculated specific DOC fluxes

Using the set of large training catchments, estimates of in-river DOC loss can also be derived from $f_{DOC,mod}[S]$ and calculated specific DOC fluxes ($f_{DOC,calc}$) (Eq. 3, Table 9). Note that in-river DOC loss is calculated here from the averages of modeled and calculated fluxes. For the small catchments, on which the empirical estimation equation for $f_{DOC,mod}[S]$ was trained, these estimates represent the calculated DOC fluxes quite well. The 2% 'estimated DOC loss' (Table 9) can be interpreted as a minor negative bias for DOC loss calculations. For the large catchments, the estimated DOC loss is 19%. Further dividing the large catchments in such smaller than 10,000 km² (L1) and such larger than 10,000 km² (L2) reveals that this difference is even higher for the latter subset (Table 9). While from small catchments (S) to L1 and from L1 to L2 the average catchment size increase by about one order of magnitude, the increase in the derived DOC loss rate is rather linear.

For both subsets of large catchments, the differences $f_{DOC,mod}[S]$ - $f_{DOC,calc}$ per catchment show a bell-shaped distribution around a positive mean value (Fig. 11), indicating that there is a general tendency of $f_{DOC,mod}[S]$ to overestimate $f_{DOC,calc}$ within both subsets of large catchments. This justifies the applied approach to calculate in-river DOC loss.

Table 9: Averages of calculated ($f_{DOC,calc}$) and estimated ($f_{DOC,mod}[S]$) specific DOC fluxes and estimated DOC loss for different catchment size classes.[a]

Subsets of catchments	N	avg. catchment size [km²]	avg. $f_{DOC,calc}$ [t C km^{-2}a^{-1}]	avg. $f_{DOC,mod}[S]$ [t C km^{-2}a^{-1}]	Estimated DOC loss
Small catchments (S) <2,000 km²	246	494	2.24	2.29	2%
Large catchments (L) >2,000 km²	207	26,525	1.09	1.35	19%
L1) 2,000 - 10,000 km²	90	4,880	1.22	1.38	11%
L2) >10,000 km²	117	43,175	0.99	1.33	25%

[a]The estimated DOC loss was calculated from the averages of calculated ($f_{DOC,calc}$) and estimated specific DOC fluxes ($f_{DOC,mod}[S]$) (Eq. 3).

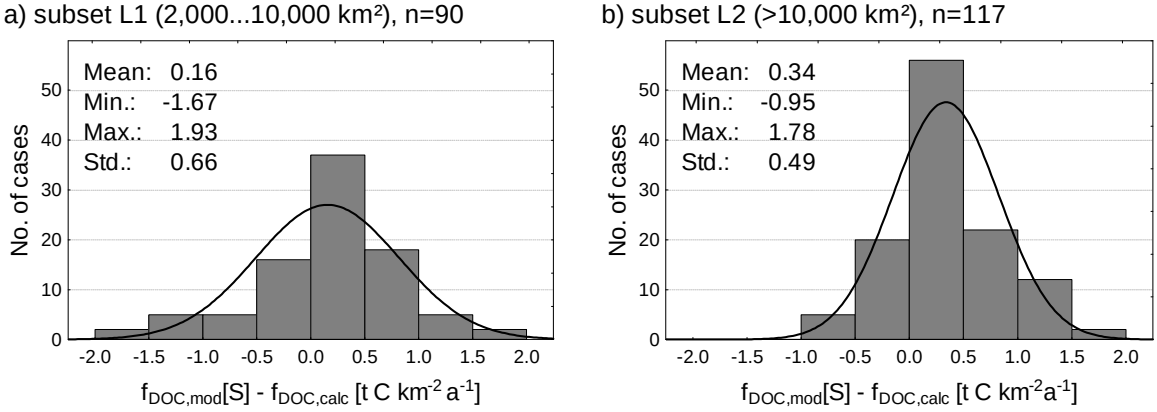

Fig. 11: Histograms of the difference $f_{DOC,mod}[S] - f_{DOC,calc}$ for two subsets of the large catchments. Means, minima, maxima, and standard deviations are reported in units of the x-axis. The curve indicates the theoretical normal distribution based on the mean and the standard deviation.

3.4 Discussion

3.4.1 Validity of empirical models

3.4.1.1 Specific DOC fluxes

Ludwig et al. (1996b) estimated an average specific DOC flux of 1.79 t C km^{-2}a^{-1} for the whole North American continent. This estimate is based on measured DOC fluxes of the Mississippi, Columbia, St. Lawrence, Yukon, Mackenzie, and Brazos Rivers and a spatially explicit estimation for the remaining area using a globally trained regression equation (Ludwig et al., 1996b). As these DOC fluxes refer to the mouths of large world rivers (avg. catchment size 1.13 mil km²), the proportion of terrestrial DOC retained or oxidized within the fluvial network is likely higher than within the 'large catchments' used

here. The fact that the average specific DOC flux estimated by Ludwig et al. (1996b) is still substantially higher than that derived from the 'large catchments' in this study (1.40 t C $km^{-2}a^{-1}$) is probably due to the relatively high DOC yields from areas north of 60°N, which are not covered by this study. For tundra and taiga ecosystems, which dominate this area, Ludwig et al. (1996b) reported a global average DOC flux of 2.0 t C $km^{-2}a^{-1}$, being notably higher than their estimate of the North America average (1.79 t C $km^{-2}a^{-1}$). The relatively high specific DOC fluxes, which are characteristic for high latitudes (e.g. Cooper et al., 2008), can be explained by a high soil carbon storage combined with a considerable amount of runoff (Ludwig et al., 1996b), and by the permafrost related abundance of wetlands (e.g. Striegl et al., 2007; Frey and McClelland, 2009). Indeed, also for the northern parts of the study area, which can already be referred to as taiga, estimated fluvial DOC fluxes are clearly above average (cf. Fig. 10).

The maximum specific DOC fluxes estimated in this study are 17.6 t C $km^{-2}a^{-1}$ ($f_{DOC,mod}$[S]) and 15.2 t C $km^{-2}a^{-1}$ ($f_{DOC,mod}$[L]). These values, which were estimated for 1 km x 1 km raster cells, are not much higher than the highest specific DOC flux of 13.4 t C $km^{-2}a^{-1}$ derived from the hydrochemical data and referring to a whole catchment. These maximum values are still substantially lower than the fluvial DOC export of 32.5 t C $km^{-2}a^{-1}$ reported by Worrall et al. (2007) for a hot spot region at the English West Coast. Therefore, it is concluded that the spatially explicit estimates are well within the natural range of specific DOC fluxes.

Areas in which high values of $f_{DOC,mod}$[S] and $f_{DOC,mod}$[L] predominate (cf. Fig. 10a,b) are underrepresented by the training catchments (cf. Fig. 10d). This is especially true for the Hudson Bay lowland area and Eastern Canada. However, for these areas, literature values can be used for a comparison (Table 10, Fig. 10d). Note that because the average size of the considered river catchments are in the order of magnitude of the here used 'large catchments', $f_{DOC,mod}$[L] is taken as reference.

Table 10: Comparison of spatially explicit estimates of fluvial DOC flux, the applied runoff data (UNH/GRDC runoff), and implicitly derived mean DOC concentrations with literature values for different areas in eastern Canada.[a]

Area defined by river basin outlets	Rivers	Average catchment size [10^6 km²]	Literature values			Spatially explicit estimates $f_{DOC,mod}$[L]		
			q [mm a^{-1}]	DOC [mg L^{-1}]	f_{DOC} [t $km^{-2}a^{-1}$]	q [mm a^{-1}]	DOC [mg L^{-1}]	f_{DOC} [t $km^{-2}a^{-1}$]
SE Hudson Bay	Great Whale R., Little Whale R., R. du Nord, Nastapoka R.	21	484[b,c]	3.6[b,c]	1.76[b,c]	457 (-5%)	4.2 (+15%)	1.91 (+9%)
Ungaya Bay	R. aux Feuilles, R. aux Melezes, R. Caniapiscau, Whale R., Georges R.	62	555[b]	2.5[b]	1.37[b]	518 (-7%)	3.8 (+55%)	1.99 (+45%)
St. Lawrence Gulf	Petit Mecatina, Olomane, Natashquan, Romaine, Magpie, Moisie, Manicouagan, Aux Outardes, Bersimis, Saguenay	25	674[b]	5.3[b]	3.57[b]	648 (-4%)	3.5 (-34%)	2.27 (-36%)
SW Hudson Bay	Churchill R., Nelson R., Hayes R., Winisk R.	370	259[d,c]	10.5[d,c]	2.72[d,c]	108 (-58%)	14.1 (+33%)	1.51 (-44%)
James Bay	Nottaway R., Broadback R., Rupert R.	43	663[c]	7.1[c]	4.67[c]	536 (-19%)	4.4 (-37%)	2.38 (-49%)

[a]The values from this study and that from the literature refer to the same river basins listed in the table. All values are flux-weighted averages. The over/underestimations of the literature values by this study are given in brackets.
[b] after Hudon et al. (1996)
[c] after Mundy et al. (2010)
[d] after Granskog et al. (2007)

For the rivers tributary to the South Eastern Hudson Bay, $f_{DOC,mod}[L]$ reproduces the literature values well (Table 10). The lateral DOC fluxes in the rivers tributary to the St. Lawrence Gulf, the South Western Hudson Bay, and James Bay are substantially underestimated by $f_{DOC,mod}[L]$, whereas the fluvial DOC fluxes in rivers draining to the Ungaya Bay are substantially overestimated by $f_{DOC,mod}[L]$. Note that for the rivers tributary to the South Western Hudson Bay and James Bay, the long-term average annual runoff of the UNH/GRDC data is substantially lower than the annual runoff reported in the literature (cf. Table 10), contributing to the underestimation of specific DOC fluxes by this study. Moreover, for the rivers draining to the South Western Hudson Bay, the flux weighted average DOC concentration derived from $f_{DOC,mod}[L]$ is even higher than that derived from the literature values (cf. Table 10). However, it is not clear from the literature, in how far the reported DOC fluxes are representative for the long-term DOC fluxes.

3.4.1.2 Discussion of predictors

Runoff as single factor was found to have the highest explanatory power (Table 6), well in accordance with previous studies (e.g. Ludwig et al., 1996b; Harrison et al., 2005a; Worrall and Burt, 2007). This is not surprising, as specific DOC fluxes are calculated from DOC concentrations and runoff. Interestingly, the effect of runoff identified in this study, especially for the small catchments, is comparatively low (cf. Ludwig et al., 1996b). A reason for this may be uncertainties in the applied runoff data set (UNH/GRDC) that shows the by far coarsest resolution (0.5°) of the applied predictor data sets. Uncertainties in the UNH/GRDC runoff data are specifically expected for river basins smaller than 10,000km² (Fekete et al., 2002). Indeed, 75% of the here used 453 river catchments are smaller than 10,000 km². For 181 of the considered sampling locations, daily discharge time series of at least 5 years are available. Taking these data as reference, the correlation between UNH/GRDC and gauged runoff is not very high but still satisfactory (r=0.76). The UNH/GRDC data overestimate the long-term annual runoff by 6.6% on average, with a 10^{th} percentile of -54% and a 90^{th} percentile of +53%. However, a relation between these deviations and catchment size could not be confirmed.

Negative effects of slope gradient on specific DOC fluxes were also identified by Ludwig et al. (1996b) and Mulholland (1997). Mulholland (1997) attributed those to a generally higher abundance of wetlands in flat areas. For wetlands, high soil organic carbon contents and terrestrial flowpaths close to the surface through organic-rich soil horizons are characteristic, which are the most important natural controlling factors of DOC inputs to streams and rivers (Mulholland, 1997). In this study, a

weak negative relation between slope gradient and areal proportions of wetlands (A_{WL}) was found as well (Table 7).

According to their b-estimates, each of the here distinguished land cover classes (coniferous forest, broadleaved forest, and herbaceous vegetation) adds to the specific fluvial DOC fluxes compared to the remaining area, mainly comprised of agricultural land and shrubland. Coniferous forests add most DOC, followed by herbaceous vegetation and broadleaved forests. A higher specific fluvial DOC export from coniferous forest in comparison to broadleaved forest and grassland was also estimated by Aitkenhead and McDowell (2000) at the global scale. In a local study in France, however, natural deciduous forests have been found to yield twice as much fluvial DOC than planted coniferous forests (Amiotte-Suchet et al., 2007). From agricultural areas, Royer and David (2005) expect generally lower specific DOC exports than from forests, which is supported by a negative correlation (r=-0.36) between DOC concentrations and agricultural land reported for stream systems across Europe (Mattsson et al., 2009). A probable explanation for low DOC exports from agricultural land may be lower soil organic carbon contents due to soil erosion, aeration caused by agricultural tilling, and removal of plant litter (cf. e.g. Follett, 2001). No study is known to the author dealing with fluvial DOC fluxes from shrublands. However, as shrublands dominate the arid to semi-arid western part of the conterminous USA, DOC exports from these ecosystems are expected to be low.

Although only slightly adding to the explained proportion of variance of specific DOC fluxes, areal proportions of wetlands have been identified as a robust predictor. Areal proportions of wetlands were previously identified as highly important predictor in local studies, for which detailed information on wetland distribution exists (eg. Aitkenhead et al., 1999; Creed et al., 2008; Johnston et al., 2008). Harrison et al. (2005a) used wetland proportions as the only predictor besides discharge in their model of fluvial DOC exports to coastal zones at the global scale. Within this study, the relative importance of the predictor wetland proportion is higher within the large training catchments whereas the importance of the land cover classes was decreased compared to the small catchments. It is hypothesized here, that this predictor becomes even more important if catchments larger than used in this study are considered.

However, the partly coarse classification of wetland proportions in the data set used is a considerable source of uncertainty. Further, considering probably substantial DOC inputs from riparian wetlands (cf. Mulholland, 1997; Aitkenhead and McDowell, 2000; Preiner et al., 2008), DOC concentration do not

necessarily decrease downstream despite substantial in-river respiration of DOC. As typology and exact position of wetlands were not distinguished, the specific contribution of riparian wetlands to fluvial DOC fluxes could not be identified in this study.

Although soil organic carbon content was previously identified as an important predictor (eg. Ludwig et al., 1996b; Mulholland, 1997; Aitkenhead et al., 1999), it was not applied in this study due to the weak detail and coarse resolution of available data sets (SOTER by Batjes, 2008; HSWD, cf. Fischer et al., 2008). Land cover and wetland proportions were used as surrogate here, as they are closely related to soil properties like soil organic carbon content and soil organic matter quality. However, especially as the here applied land cover classification is quite coarse, a high variance in soil organic carbon content and soil organic matter quality can be expected within the distinguished land cover classes (cf. Aitkenhead-Peterson et al., 2005; Homann et al., 2007; Moore et al., 2008), which adds uncertainty to the prediction.

Climatic variables like precipitation and air temperature, which were not found to be significant predictors in this study, were previously identified as controlling factors for smaller study areas and in analysis of temporal variations of DOC fluxes within specific river catchments (eg. Worrall et al., 2004; Raymond and Oh, 2007; Creed et al., 2008). In this study, annual precipitation was not identified to add explanatory power to the DOC flux predictions, probably because of its close relation to runoff.

Mean annual air temperature [℃] was considered a potential predictor. However, added to the regression equation using the small catchments, this parameter only slightly increased the explained variance in f_{DOC} (from r^2=0.55 to r^2=0.57). If included in the regression equation, this predictor would have a negative effect, theoretically causing a decrease in estimated DOC fluxes of 0.07 t C km^{-2} a^{-1} per 1℃ increase in mean annual air temperature. For the large catchments, this parameter was not found to improve the regressions. Consequently, there is a weak negative correlation for this predictor with model residuals (Eqs. 5, 6) of regression equation S.4 but not of regression equation L.4 (Fig. 12). This implies a tendency for $f_{DOC,mod}$[S] to underestimate specific DOC fluxes in colder regions and overestimate it in warmer regions.

Eq. 5

Residual = $f_{DOC,calc}$ – predicted f_{DOC}

Eq. 6

Relative residual = ($f_{DOC,calc}$ – predicted f_{DOC}) / $f_{DOC,calc}$

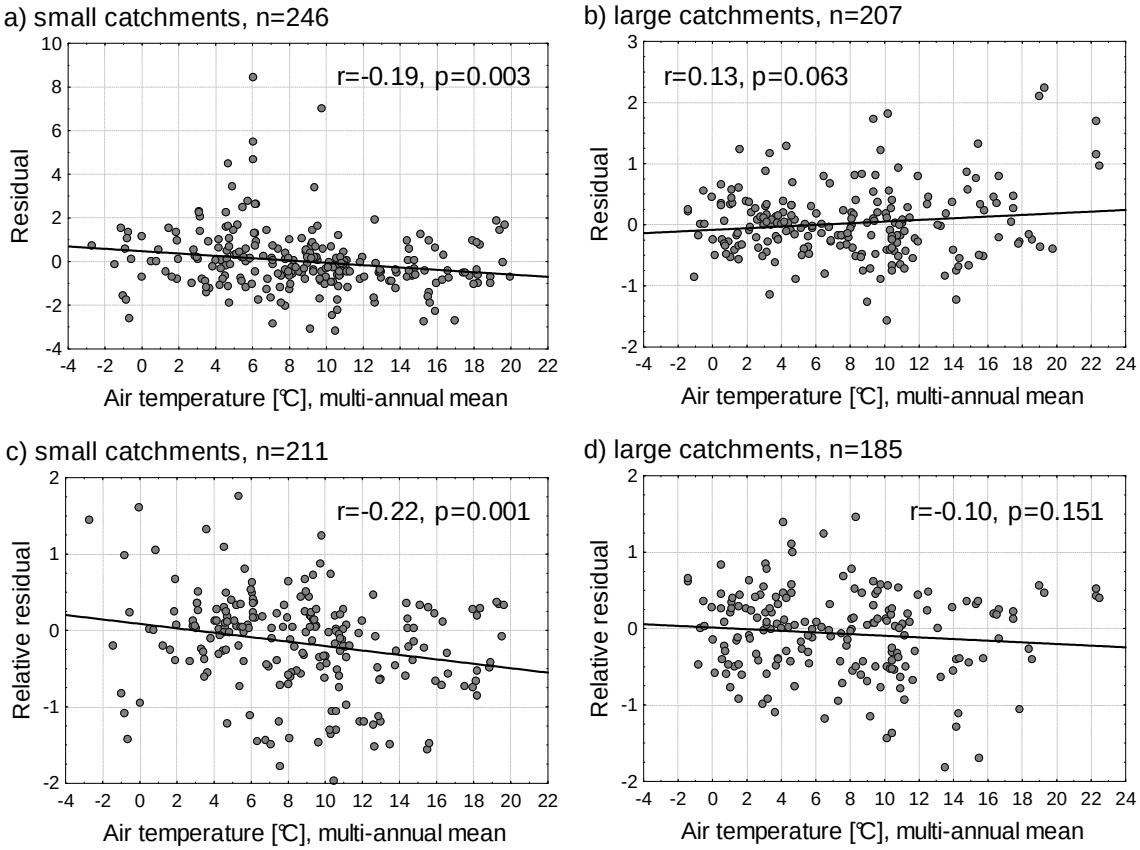

Fig. 12: Scatter-plots of absolute and relative residuals (Eqs. 5,6) of the applied regression equations vs. multi-annual means of air temperature [℃]. As relative residuals partly take extreme values, the respective scatter-plots are restricted to catchments with relative residuals of -2…2.

As catchment size is discussed in this study (see below) for its correlation to calculated DOC losses, this parameter would be of potential interest as predictor for fluvial DOC flux estimation. However, it was not possible to include catchment size in a robust regression equation. For relative residuals (Eq. 6) of the regression equations S.4 and L.4 no significant correlation to this factor was found (Fig. 13). Although for small catchments, the correlation is only slightly beyond the 5% uncertainty level ($p=0.058$), the correlation is very low ($r=0.13$, $r^2=0.02$). Thus, for the here considered catchment sizes, the direct influence of catchment size on DOC flux is rather small and might be obscured by the effects of other factors.

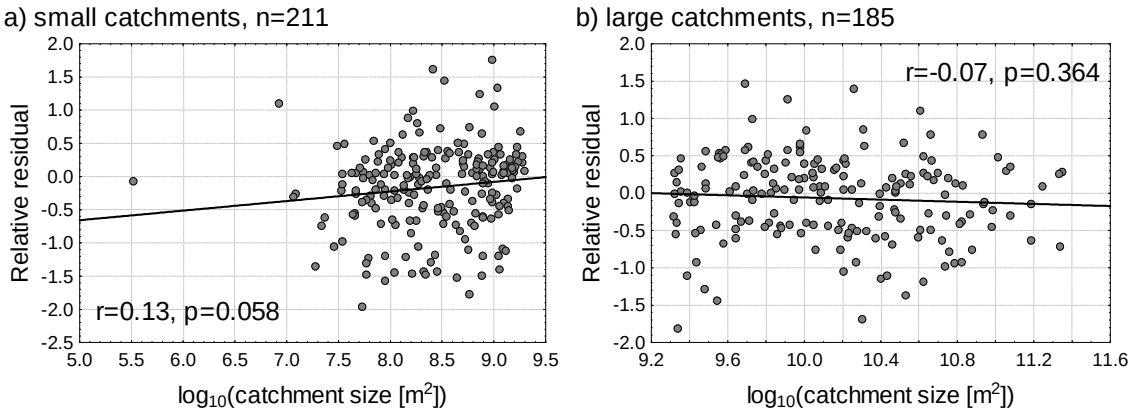

Fig. 13: Scatter-plots of relative residuals of the regression equations S.4 and L.4 vs. decadic logarithm of catchment size [m²]. As relative residuals partly take extreme values, these plots and correlation coefficients are restricted to subsets of the training catchments having relative residuals -2…2.

Two sources of DOC not addressed by this study are autochthonous production of DOC and anthropogenic point sources. Mulholland (1997) demonstrated that lateral DOC fluxes in rivers across North America are governed by catchment processes and thus terrestrial DOC sources whereas no significant contribution of autochthonous DOC production could be identified. Anthropogenic point sources of DOC, which can substantially contribute to fluvial DOC fluxes in densely populated areas (eg. Tipping et al., 1997), are expected to be negligible in this study. Artificial areas, including urban areas, are scarce (below 1.6% for 90% of all training catchments) and sampling locations within or directly downstream of urban areas were discarded from the analysis. Further, as wastewater DOC is more labile than terrestrial DOC (cf. e.g. Garcia-Esteves et al., 2007), the effects from upstream anthropogenic point sources are expected to vanish quickly downstream.

3.4.2 Implications for in-river losses of DOC

The specific fluvial DOC fluxes estimated in this study refer to points within the fluvial network with contributing areas similar in size to the training catchments. Thus, an average DOC flux of 1.82 t C $km^{-2}a^{-1}$ for the study area represents specific DOC fluxes from 'small catchments' ($f_{DOC,mod}[S]$) with an average size of 494 km². For catchment sizes similar to the 'large catchments' (avg. size 26,525 km²), an substantially lower average specific DOC flux of 1.40 t C $km^{-2}a^{-1}$ ($f_{DOC,mod}[L]$) was estimated for the study area, and the difference between both of 23% was consequently attributed to in-river losses of DOC . The plausibility of that number is supported by literature, reporting a downstream DOC loss of 24.5% in the Pearl River (Mississippi/Louisana, catchment size: 22,700 km²) (Duan et al., 2007) and 28% in the lower Hudson River (New York, catchment size: 33,500 km²) (Cole and Caraco, 2001). Based on the estimates of fluvial DOC exports and in-river respiration of DOC,

Worrall et al. (2007) concluded that at least 32% of the terrestrial DOC exports are mineralized within the fluvial network of England and Wales. As it can be expected that sinks other than respiration and photo-oxidization are negligible (cf. e.g. Worrall et al., 2007), the total DOC loss of 5.9 Mt C a^{-1} estimated for North America south of 60° is assumed to be lost as CO_2 from respective river stretches to the atmosphere.

Results from the budget approach averaging $f_{DOC,mod}$[S] and $f_{DOC,calc}$ for three catchment size classes suggest a non-linear relationship between in-river DOC losses and catchment area (cf. Table 9). A downstream decrease of DOC losses can be explained by the preferred degradation of the more labile proportion of DOC while the proportion of refractory DOC increases (cf. e.g. Worrall et al., 2007).

According to the global estimates by Battin et al. (2008), respiration within small headwater streams is of the same magnitude as respiration within rivers, distinguishing streams from rivers by a mean discharge lower than 0.5 m^3 s^{-1}. As only 15% of the 'small catchments' used in this study can be attributed to streams according to this definition (average discharge of the 246 small catchments: 7.3 m^3s^{-1}), the DOC losses estimated here can be fully attributed to losses within rivers, and the total in-stream/in-river losses within the study area might be considerably higher. On the other hand, the fact that similar predictors of fluvial DOC fluxes are reported in literature from local to global scales suggest that still a substantial proportion of terrestrial DOC behaves rather conservative during fluvial transport.

3.4.3 Uncertainties

Due to the nearly normal distribution of residuals of the used regression equations (cf. Fig. 9) no general bias is expected from the estimation of fluvial DOC fluxes. However, as only 55% (regression equation S.4, small catchments) or 60% (regression equation L.4, large catchments) of the variance of $f_{DOC,calc}$ is statistically explained, there is a certain tendency to overestimate low values and underestimate high values (Fig. 14).

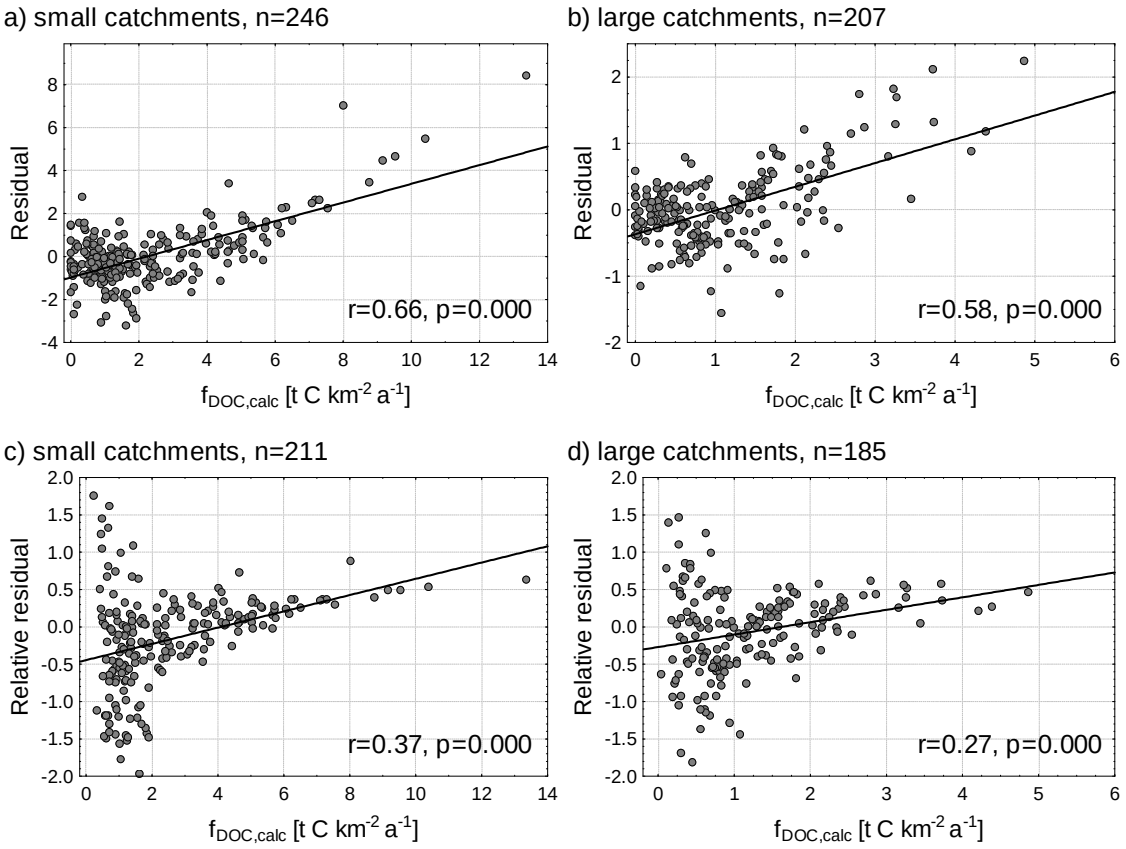

Fig. 14: Scatter-plots of absolute and relative residuals (Eqs. 5,6) of the applied regression equations vs. calculated specific DOC fluxes ($f_{DOC,calc}$) [t C $km^{-2}a^{-1}$]. As relative residuals partly take extreme values, the respective scatter-plots are restricted to catchments with relative residuals of -2 to 2.

For a small proportion of the training catchments (small catchments: 18 of 246, large catchments: 11 of 207 catchments, cf. Fig. 15 a,b), the lumped estimation of f_{DOC} (i.e. for each catchment based on averages of the applied predictors) gave negative specific DOC fluxes. After applying the fitted regression equations spatially explicitly, raster cells with negative values were forced to 0 t C $km^{-2}a^{-1}$ as negative fluvial DOC fluxes were not expected. This procedure affected 16.1% ($f_{DOC,mod}$[S]) and 12.5% ($f_{DOC,mod}$[L]) of the raster cells. However, for the larger proportion of these areas ($f_{DOC,mod}$[S]: 69%, $f_{DOC,mod}$[L]: 82%) the UNH/GRDC data gave average annual runoffs below 10 mm a^{-1}. Thus, specific DOC fluxes from the affected areas are negligible at the scale addressed by this study, even if DOC concentrations in the river water would be high.

Lake areas were forced to 0 t C $km^{-2}a^{-1}$, because only terrestrial sources of DOC were addressed by the applied predictors and lakes are rather sinks of fluvial DOC (cf. Sobek et al., 2005; Sobek et al., 2007). Within the training catchments, lake area proportions are generally small (average: 1.3% within

both sets of training catchments; higher than 5% only in about 10% of the small and 5 % of the large catchments). Thus, no substantial bias from this procedure is expected.

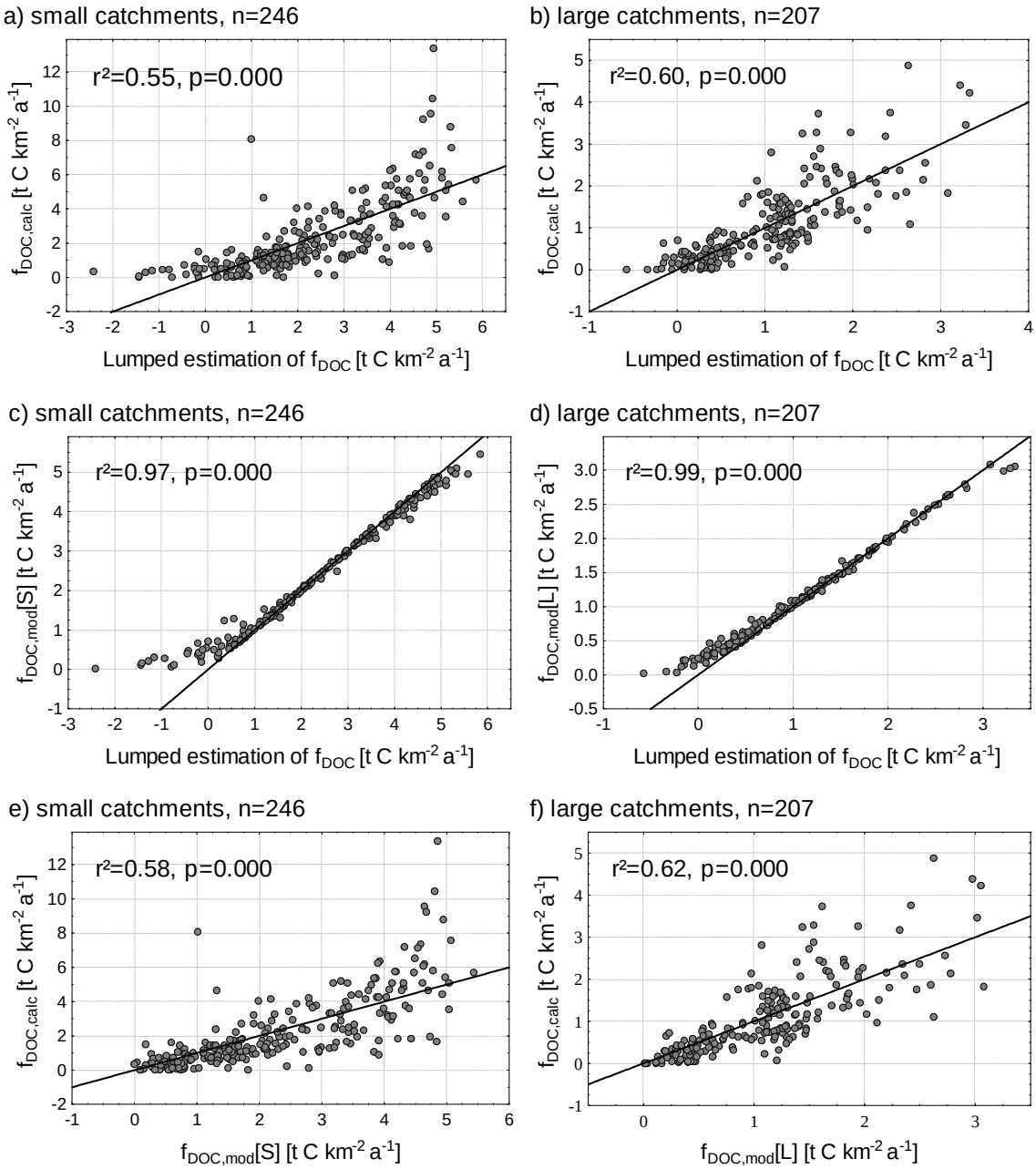

Fig. 15: Scatter-plots of a,b) lumped estimates vs. calculated specific DOC fluxes, c,d) lumped estimates vs. spatially explicit estimates of specific DOC fluxes, and e,f) spatially explicit estimates vs. calculated specific DOC fluxes. Straight lines represent the theoretical 1:1 ratios.

The spatially explicit estimates reproduce those derived from the lumped estimation quite well for estimated specific DOC fluxes above 0.5 t C $km^{-2}a^{-1}$ (cf. Fig. 15 c, d). For lumped estimates below 0.5 t C $km^{-2}a^{-1}$, spatially explicit estimates are mostly higher, mainly due to forcing negative cell values to 0 t C $km^{-2}a^{-1}$. The correlations with fluxes calculated from the hydrochemical data ($f_{DOC,calc}$) are

similar for spatially explicit estimates and lumped estimates (Fig. 15 e,f). This confirms the validity of the spatially explicit application of the regression equations, at least for the area represented by the training catchments.

The validity of the spatial extrapolation of the DOC flux estimation depends on whether the training catchments are representative for the extrapolation area, especially with regard to physiographic properties which were used as predictors (Table C.1 in Appendix). The maximum runoff covered by both sets of training catchments is 1,035 mm a^{-1}. Within the extrapolation area, runoff reaches values of up to 4,738 mm a^{-1}. However, only 3.6% of the extrapolation area shows runoff values above 1,035 mm a^{-1}. The maximum average slope gradient covered by both sets of training catchments is 22.6° (Table C.1). Only about 2.8% of the extrapolation area show higher slope gradients. As still 94.6% of the extrapolation area shows values for both predictors which are covered by the range of per-catchment-averages within both sets of training catchments, it is concluded that a probable bias due to a non-valid extrapolation to the remaining area is negligible for the overall results.

The averages and distributions of land cover classes and wetlands are comparable among the two sets of training catchments (cf. Table C.1). Notable proportions of the training catchments are dominated (>60% cover) by coniferous forests (A_{CF}) (small c.: 62/243, large c.: 38/207) or broad-leaved forests (A_{BF}) (small c.: 57/243, large c.: 30/207). It is concluded, that the effects of these land cover classes are well distinguished from effects of the other land cover. On the contrary, there are no training catchments dominated by wetlands (A_{WL}) or herbaceous vegetation (A_{HV}). With regard to the extrapolation area, especially A_{WL} is underrepresented by the training catchments (Table C.1). However, as the comparison with literature values for wetland dominated river catchments in Canada did not reveal a general over- or underestimation of fluvial DOC fluxes (cf. Table 10), a general bias from this predictor is excluded at least for $f_{DOC,mod}[L]$.

The statistical distribution of predictors A_{CF}, A_{BF}, A_{HV}, and A_{WL} are similar within both sets of training catchments. The value ranges of the predictors runoff and slope gradient are larger within the small catchments and fully cover those within the large catchments. Thus, it is concluded that the DOC loss estimation based on $f_{DOC,mod}[S]$ and $f_{DOC,calc}$ within the large catchments is valid.

The relative difference between the averages of $f_{DOC,mod}[S]$ and $f_{DOC,mod}[L]$ for the extrapolation area (23%) is close to the relative difference between $f_{DOC,mod}[S]$ and $f_{DOC,calc}$ within the large catchments

(19%). This indicates that for the extrapolation area, the estimated in-river DOC loss and subsequent CO_2 evasion of 5.9 Mt C a^{-1} is reasonable and not generally biased by an invalid extrapolation of the empirical DOC flux equations.

3.5 Conclusion

As expected, the mean and total DOC flux estimated for the study area (North America south of 60°N) are higher using the regression equation for small catchments < 2,000 km² (1.82 t C km^{-2} a^{-1}, 25.8 Mt C a^{-1}) than that for the large catchments > 2,000 km² (1.40 t C km^{-2} a^{-1}, 19.9 Mt C a^{-1}). The total difference of 5.9 Mt C a^{-1} can be interpreted as the DOC loss that occurs in river stretches leading from contributing areas of 494 km² (average size of the 246 small catchments used) over to such of 26,525 km² (average size of the 207 large catchments used), giving an overall DOC loss rate of 23% within respective river stretches.

The identified and applied predictors for the DOC flux estimation confirm those described in the literature: runoff, slope gradient, land cover, and wetland area proportions. Applying the same set of predictors for different catchment size classes allows giving representative estimates of in-river DOC loss at regional to global scales, which is a main advantage of the methodological concept presented here over studies addressing single river systems.

The DOC loss rate estimated here is rather low compared to spatial variability of fluvial DOC fluxes. Thus, direct effects of catchment area on DOC fluxes are probably obscured by the stronger effects of other predictors.

It was shown that from small to large catchments the relative importance of land cover as predictor decreased whereas that of runoff and wetland proportions increased. This hints to differences in the lability of fluvially transported DOC depending on its terrestrial source, with wetland derived DOC being more refractory. However, further research needs to be done to confirm such a hypothesis at a regional to global scale.

As smallest headwaters are not represented in the data set used, and as literature suggests DOC losses in such headwaters to be substantial, the here estimated DOC loss rate is a rather conservative estimate of DOC losses within the whole fluvial system of the study area. Generally, fluvial DOC fluxes

derived from available regional surface water quality data sets will inevitably underestimate the DOC export from the terrestrial system.

To better assess in-stream/in-river DOC losses at regional to global scales, the total exports of DOC from the terrestrial system into streams and rivers need to be assessed in future studies. For this, more data on DOC fluxes are needed which cover smallest headwater catchments and the large variety of land properties. With regard to these smallest headwaters, there is a need for improved geodata sets with a higher spatial resolution, especially for runoff and soil properties. Additionally, more data on the quality of dissolved organic matter are needed, which allow for an evaluation of its susceptibility to decomposition during fluvial transport.

4 Controls of spatial patterns in the carbonate system of North American rivers

4.1 Introduction

4.1.1 Identification of the research gap

The land-ocean transfer of dissolved inorganic carbon (DIC) via rivers is an important part of the global carbon cycle and was assessed at the global scale by various studies (Livingston, 1963; Garrels and Mackenzie, 1971; Kempe, 1979; Meybeck, 1979; Ludwig et al., 1996a), with estimated total fluvial exports ranging from 320 Mt a^{-1} (Ludwig et al., 1996a) to 450 Mt a^{-1} (Kempe, 1979). The fluvial exports of DIC represent about 45% of fluvial exports of carbon to the coastal zones (Ludwig et al., 1996a).

Most of the previous studies at continental to global scale focused on the lateral fluxes of carbon only, and thus regarded rivers as “pipes” in the carbon cycle (cf. Cole et al., 2007), although it has long been recognized that rivers are mostly supersaturated with CO_2 relative to the ambient air and are thus a net source of CO_2 to the atmosphere (eg. Park et al., 1969; Garrels and Mackenzie, 1971; Kempe, 1982).

More recent studies focused on rivers as biogeochemical reactors and as systems with substantial net-fluxes of CO_2 to the atmosphere (Cole et al., 2007; Battin et al., 2008; Battin et al., 2009; Aufdenkampe et al., 2011). At the global scale, the freshwater-atmosphere flux of CO_2 is estimated to amount to 750 to 1,400 Mt C a^{-1} (Aufdenkampe et al., 2011). Streams and rivers contribute about 560 Mt a^{-1} to the CO_2 efflux (Aufdenkampe et al., 2011).

Fluvial carbon fluxes observed at the rivers mouths are not sufficient to assess the exports of carbon from the catchments to the fluvial system (Worrall et al., 2007; Battin et al., 2009). Reasonable estimates of CO_2 evasion from lakes and rivers, which also account for its spatial variability, would help refining carbon budgets of terrestrial ecosystems (cf. Jones and Mulholland, 1998a; Cole and Caraco, 2001; Billett et al., 2004; Jenerette and Lal, 2005; Jonsson et al., 2007).

While latitudinal gradients in CO_2 partial pressures (PCO_2) were stated at global scale (Aufdenkampe et al., 2011) and the spatial variability of river water PCO_2 was already described for the conterminous USA (Jones et al., 2003), the controlling factors of the spatial variability in the carbonate system of

rivers are still unknown. Knowledge about these controls is a basic requirement for the spatially explicit prediction and modeling of the river-atmosphere CO_2-flux.

This study is an attempt to improve our knowledge in this respect, drawing on the example of North America's river network. In the following, some more specific considerations on the carbonate system of rivers are presented, from which the working hypothesis and research questions of this study are deduced.

4.1.2 The carbonate system

4.1.2.1 Hydrochemical basics

DIC consists of free dissolved CO_2 (CO_2(aq)), carbonic acid (H_2CO_3), bicarbonate (HCO_3^-), and carbonate ions (CO_3^{2-}) (Eq. 7). By convention, all free dissolved CO_2 is considered carbonic acid as well, although the by far largest proportion of unionized dissolved CO_2 exists in the form of CO_2(aq) (cf. e.g. Stumm and Morgan, 1981; Drever, 1997). The dissolution of carbonic acid can be illustrated with equation 8. Carbonic acid partly dissociates to bicarbonate (HCO_3^-, Eq. 9) and to carbonate ions (CO_3^{2-}, Eq. 10).

Eq. 7

$$DIC = CO_2(aq) + H_2CO_3 + HCO_3^- + CO_3^{2-}$$

Eq. 8

$$H_2CO_3 = H_2O + CO_2(aq)$$

Eq. 9

$$H_2CO_3 = HCO_3^- + H^+$$

Eq. 10

$$HCO_3^- = CO_3^{2-} + H^+$$

Equations 8-10 indicate that these reactions govern the H^+ concentrations and thus pH ($pH=-\log_{10}([H^+])$). The dissolution of CO_2 in water or the outgassing of CO_2 from water can be explained by Henry's Law (Henry, 1803), a hydrochemical equilibrium equation stating that at equilibrium the concentration of a dissolved gas is proportional to the partial pressure of that gas in the atmosphere with which the solution is in contact (Eq. 11). This proportion is expressed as the equilibrium constant K_{CO2}, which is termed Henry constant. Similar constants exist for the dissociation

of H_2CO_3 (K_1, Eq. 12) and HCO_3^- (K_2, Eq. 13). The constants K_{CO2}, K_1, and K_2 depend on water temperature.

Eq. 11

$[H_2CO_3] = [CO_2(aq)] = K_H * PCO_2(atmosphere)$ (Henry, 1803)

Eq. 12

$K_1 = [H^+] * [HCO_3^-]/[H_2CO_3]$

Eq. 13

$K_2 = [H^+] * [CO_3^{2-}]/[HCO_3^-]$

An important concept of hydrochemistry is the alkalinity (Eq. 14), which expresses the buffering capacity of a solution against acidification, i.e. the increase in $[H^+]$ and thus the decrease in pH. The alkalinity is equal to the charge-sum of anions of weak acids.

Eq. 14

Total alkalinity

$= [HCO_3^-] + 2 * [CO_3^{2-}] + [B(OH)_4^-] + [H_2SiO_4^-] + [HS^-] + [\text{organic anions}] + [OH^-] - [H^+]$

In most freshwater systems with low concentrations of dissolved organic matter (DOM) the total alkalinity is represented mainly by HCO_3^- and CO_3^{2-}. The buffering capacity is caused by a consumption of H^+ while HCO_3^- is transformed to H_2CO_3 or CO_3^{2-} is transformed to HCO_3^- (cf. Eq. 9, Eq. 10). In dilute freshwaters with high concentrations of DOM (blackwater rivers), organic anions can be the main contributor of alkalinity (cf. e.g. Oliver et al., 1983; Driscoll et al., 1994; Edmond et al., 1995; Edmond et al., 1996; Köhler et al., 2001). However, the contribution of organic anions to alkalinity further depends on the quality of DOM and cannot be easily deduced from DOM concentration.

4.1.2.2 Carbonate system of rivers

Sources of DIC in river water are (1) CO_2 from the atmosphere, (2) CO_2 from soil respiration, (3) the dissolution of carbonate rocks, and (4) in-river respiration of organic carbon (e.g. Kempe, 1982; Telmer and Veizer, 1999). The first two of these sources involve the dissolution of CO_2 from the gas phase (Eq. 11). As streams and rivers are mostly CO_2 supersaturated with respect to the ambient air,

there is mainly a net flux of CO_2 from streams and rivers to the atmosphere (e.g. Garrels and Mackenzie, 1971; Kempe, 1982; Aufdenkampe et al., 2011).

In soils and the groundwater system, where a gas exchange with the atmosphere is inhibited, the PCO_2 is one to two orders of magnitude higher than that of the atmosphere (e.g. Miotke, 1974; Brook et al., 1983; Macpherson, 2009). The equilibrium concentration of CO_2 in the soil solution or groundwater is accordingly increased (cf. Eq. 11). When the dissolved CO_2 acts as an agent in chemical rock weathering, it is transformed to HCO_3^- (Eq. 15, Eq. 16), increasing the alkalinity of the solution and concomitantly increasing the pH as H^+ ions are consumed in the weathering process (e.g. Garrels and Mackenzie, 1971; Jones and Mulholland, 1998b).

Eq. 15

$$2NaAlSi_3O_8 + 2CO_2 + 3H_2O = Al_2Si_2O_5(OH)_4 + 2Na^+ + 2HCO_3^- + 4SiO_2$$

Eq. 16

$$CaCO_3 + H_2O + CO_2 = Ca^{2+} + 2HCO_3^-$$

During the weathering of silicates (Eq. 15), all HCO_3^- is derived from the dissolved CO_2 in the soil solution or groundwater. During the weathering of calcium carbonate ($CaCO_3$, Eq. 16), by each mole of $CaCO_3$ dissolved one mole of HCO_3^- of lithogenic origin is released to the solution, which forms the third source of river DIC, as stated above. Because carbonates weather at substantially higher rates than silicates, rivers with carbonate rocks in their catchments show higher alkalinity and thus higher pH values (e.g. Telmer and Veizer, 1999). At the global scale, it is estimated that 36% of the DIC transported to coastal zones are of lithogenic origin (Meybeck, 1993), while less than 11% of the global land surface are covered by carbonate rocks (Dürr et al., 2005).

H_2CO_3 is globally the dominant weathering agent. Contributions by other acids to chemical weathering decrease the CO_2 consumption and might even release CO_2 from the solution of carbonates rocks to the atmosphere (e.g. Zeng and Masiello, 2010). Locally, sulfuric acid is an important weathering agent, formed by the oxidation of sulfides, mainly pyrite (e.g. Millot et al., 2003; Lerman et al., 2007; Li et al., 2008; Hartmann, 2009), or deposited as acid rain (e.g. Li et al., 2008; Xu and Liu, 2010). Nitric acid stemming from fertilizers might also act as weathering agent on agricultural land (e.g. Zeng and Masiello, 2010).

In-river respiration of organic carbon can be a substantial source of dissolved CO_2 decreasing the pH and increasing the PCO_2 of the river, in its intensity controlled by the alkalinity of the river water (e.g. Kempe, 1984; Battin et al., 2008). Sinks of DIC in the fluvial system are (1) photosynthetic activity (uptake of CO_2(aq) or HCO_3^-), (2) precipitation of carbonates, i.e. the reverse reaction of equation 16, and (3) degassing of CO_2 to the atmosphere (c.f. Eq. 11).

Photosynthetic activity might drive PCO_2 temporarily below the atmospheric level, as in the upper layers of stratified lakes, but also in some streams and rivers during low water stages (Kempe, 1982; Kempe, 1984; Tobias and Böhlke, 2011). However, freshwater systems are most often net-heterotrophic, i.e. on average in-river/lake/stream respiration exceeds photosynthesis due to terrestrial inputs of organic matter (e.g. Kempe, 1982; Kempe, 1984; Sobek et al., 2005; Alin and Johnson, 2007; Cole et al., 2007; Battin et al., 2008; Battin et al., 2009).

Besides the PCO_2 gradient between water and air, the rate of CO_2 outgassing from inland waters further depends on the area of the air/water interface, the turbulence in the upper part of the water body, and temperature (e.g. Raymond and Cole, 2001; Alin et al., 2011; Aufdenkampe et al., 2011). The turbulence is controlled by flowing velocities, streambed roughness, and sheer forces exerted on the water surface by wind (e.g. Raymond and Cole, 2001; Aufdenkampe et al., 2011). With regard to the total amounts of CO_2 degassed from the fluvial network, the water residence time within the different compartments of the fluvial network are of importance. Thus, there is a tendency for PCO_2 to be lower in larger rivers than in small streams and further lower within lakes (cf. Teodoru et al., 2009; Aufdenkampe et al., 2011). Riverine lakes and reservoirs can cause the PCO_2 equilibration of the traversing rivers with the atmosphere (e.g. Kempe, 1984; Yang et al., 1996; Wang et al., 2007; Teodoru et al., 2009).

In the literature it has been argued that PCO_2 commonly declines from the headwater to the downstream reaches, while the connectivity between stream/river biogeochemistry and the catchments declines (Hoffer-French and Herman, 1989; Dawson et al., 1995; Jones and Mulholland, 1998b; Finlay, 2003). Especially for headwaters draining wetlands it was found that excess CO_2 from soil-/groundwater contributions evades rather quickly to the atmosphere, already over a few kilometers downstream (Dawson et al., 2001; Worrall and Burt, 2005; Johnson et al., 2008; Davidson et al., 2010). The maintenance of increased PCO_2 within the downstream reaches of streams and rivers is thus mainly attributed to respiration of allochtonous organic matter if significant direct contributions of

fresh soil-/groundwater high in PCO_2 can be excluded. For rivers gaining high loads of labile organic carbon in the lower reaches, e.g. due to pollution, PCO_2 might also substantially increase as e.g. shown for the river Rhine of the 60's and 70's (Kempe, 1982; Kempe, 1984). However, for streams and rivers in Sweden it was found that groundwater contributions and in-stream/river respiration are of similar importance for the spatial and temporal variations in PCO_2, even within the lower reaches of rivers (Humborg et al., 2010), contradicting the hypothesized catchment-river decoupling with regard to the PCO_2.

Many hard water streams, rivers, and lakes are supersaturated with respect to calcite (Kempe, 1984). However, precipitation of calcite only occurs at very high supersaturation which takes place when the solution is highly deprived of dissolved CO_2. This might take place in sources and head water streams, especially when the streamflow is highly turbulent, and results in the formation of travertine (e.g. Kempe, 1984; Kempe, 1985; Herman and Lorah, 1987). Besides, increased photosynthetic activity might temporally drive down the PCO_2 in the upper layer of stratified lakes but also in some hard water streams and rivers at low water stages (e.g. Kempe, 1984; Szramek and Walter, 2004; Tobias and Böhlke, 2011). Significant $CaCO_3$ precipitation due to the mixing of sodium bicarbonate waters with calcium bearing waters was reported for the Huanghe River (Feng and Kempe, 1987). However, carbonate precipitation as sink is thought to be negligible regarding land-ocean DIC fluxes at continental to global scales (e.g. Kempe, 1984; Szramek and Walter, 2004; Moosdorf et al., 2011c).

4.1.3 Objective of this study

The objective of this study is to reveal the spatial patterns in the carbonate system of North America's rivers and to identify the controlling factors behind these spatial patterns. Throughout the study area, hydrochemical data from 1,120 sampling locations are considered. For these sampling locations, the mean values of the main parameters of the carbonate system, i.e. PCO_2, alkalinity, and pH, are analyzed with regard to functional relationships to the related river catchments (Fig. 16). The aim is to set up empirical equations explaining the spatial variability in these parameters based on predictors derived from available geodata on climate, lithology, land cover, and relief. Note that these predictors may be in a functional relation to the river's carbonate system while not directly being the controlling factors.

The feasibility of predicting spatial variations in alkalinity fluxes has been confirmed by previous regional to global scale studies (e.g. Bluth and Kump, 1994; Hartmann, 2009; Moosdorf et al., 2011c).

Note that mean alkalinity instead of alkalinity fluxes is focused in this study. For PCO_2 and pH, in-river biogeochemical processes, i.e. mainly biological activity and gas-exchange with the atmosphere, are thought to have a substantial effect. Thus, the catchment-river coupling with regard to these parameters may be weaker, and thus the spatial predictability of these parameters. In this respect, this study pursues the questions, whether it is possible to identify catchment properties as predictors for these parameters as well, and if their predictability declines with catchment size, as it is hypothesized based on these considerations.

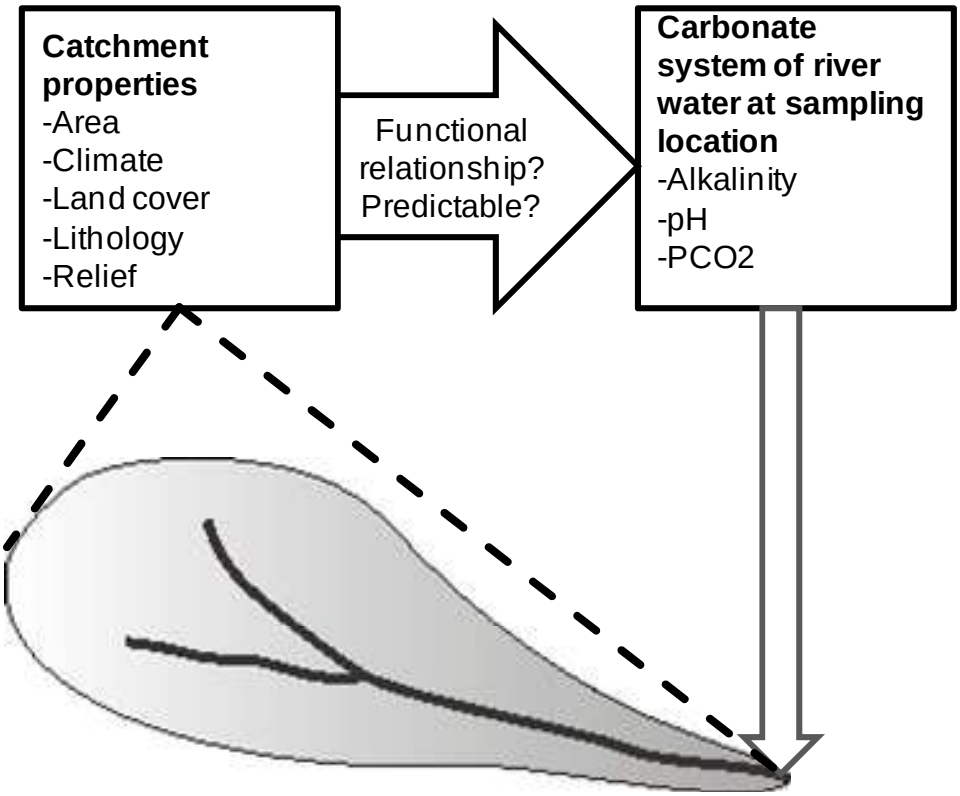

Fig. 16: Methodological concept of this study.

4.2 Methods

4.2.1 Processing of hydrochemical data

Hydrochemical data were taken from various sources (Government of Alberta - Environment; Ontario - Ministry of the Environment; USGS; Alexander et al., 1997; Environment Canada, 2009; Environment Canada, 2010). From these data bases, all samples having at least measurements of water temperature, pH, and alkalinity were selected. If available, additional information on the concentrations

of major ions, dissolved silica, dissolved organic carbon (DOC), or suspended matter (SPM) concentrations was adopted as well.

For each sample, the partial pressure of CO_2 (PCO_2) was calculated from water temperature, pH, and alkalinity using the program PhreeqC v2 (Parkhurst and Appelo, 1999). As far as available, concentrations of other major solutes and their effects on the hydrochemical equilibrium were taken into account. If Ca^{2+} concentrations were available, the saturation index for calcite $SI_{calcite}$ was calculated.

To gain representative mean values of all hydrochemical parameters for each sampling location, the following procedure was applied.

1) For the aggregation of hydrochemical parameters, it was necessary to avoid logarithmic values. Thus, pH values were transformed to H^+-concentration values. Similarly, $SI_{calcite}$, which is considered in its logarithmic form (Eq. 17), was recalculated to the saturation $\Omega_{calcite}$ (Eq. 18) before the aggregation procedure.

   Eq. 17

   $$SI_{calcite} = \log_{10}(IAP/K_{Calcite})$$

   Eq. 18

   $$\Omega_{calcite} = IAP/K_{Calcite}$$

   With:
   IAP ion activity product
   $K_{calcite}$ solubility constant for calcite

2) The calculation of PCO_2 is very sensitive to uncertainties in the source data, especially with regard to pH (cf. Kempe, 1982). This circumstance partly led to unreasonably extreme PCO_2 values. As an objective and reproducible strategy to cope with this problem, for each sampling location only samples with calculated PCO_2 values between the 10^{th} and 90^{th} percentile of the respective time series were selected for the following procedure steps and analyses.
3) With the remaining data, for each sampling location long-term monthly means of each hydrochemical parameter were calculated (Eq. 19).

Eq. 19

$$C_m = \frac{\sum_{i=1}^{k} C_{m,i}}{k}$$

With:
C_m average monthly value of a hydrochemical parameter, for months m=1-12
k number of values per month, i.e. the same month over all years

4) For 814 catchments, an average PCO_2 could be calculated for each month of the year. For the other sampling locations, gaps within the annual cycle of up to three months were filled via linear interpolation between the last reported value before the gap and the first reported value after the gap (Eq. 20, Fig. 17).

Eq. 20

$$C_m = \frac{y * C_{m-x} + x * C_{m+y}}{x + y}$$

With:
C_m missing value of month n that is calculated
m number of month
m-x number of first month in left hand direction for which a value C exists
m+y number of first month in right hand direction for which a value C exists

Month n	1	2	3	4	5	6	7	8	9	10	11	12
Value	C_1	C_2	…	…	C_5	C_6	…	…	…	C_{10}	C_{11}	C_{12}

Fig. 17: Scheme of an 'annual cycle' of mean monthly values and potential gaps to be filled.

According to the size of the gaps within the ‘annual cycle’, one of four quality levels was assigned to each sampling location (Table 11).

Table 11: Quality levels for stations concerning the coverage of the annual cycle by available parameter values.

Quality code	Description	Number of sampling locations
1	All twelve months	814
2	No gaps larger than 1 month	226
3	No gaps larger than 2 months	53
4	No gaps larger than 3 months	32

5) For those sampling location and parameters, for which a complete cycle of twelve monthly values was present after this procedure, a mean parameter value was calculated (Eq. 21).

Eq. 21

$$C_{ann} = \frac{\sum_{m=1}^{12} C_m}{12}$$

With:
C_{ann} average value of a hydrochemical parameter
C_m average monthly value of a hydrochemical parameter, for months m=1-12

Note that by the steps 4 and 5 a seasonal weighting is applied, which accounts for the seasonality in the variability of the hydrochemical parameters. For $\Omega_{calcite}$, geometric means have been used for aggregation, being the appropriate averaging technique for ratios. Five of the 1,125 sampling locations had to be discarded from the following analyses, because of unrealistic average PCO_2 values (>15,000 ppmv) that were still present after the procedure described above.

4.2.2 Calculation of catchment properties

For deriving the catchments' boundaries, the position of each sampling location was adjusted to fit the stream network of the applied digital elevation model (DEM), i.e. the Hydrosheds DEM in a resolution of 15''. Note that this DEM just covers areas south of 60°N, which restricts the study area accordingly.

The catchment properties were derived as mean values of geodata (Table 12) overlain by each catchment. For this, all of the used raster data sets were projected to Lambert Azimuthal Equal Area projection and resampled to a resolution of 1 km x 1 km cell size. Data sets with a similar or coarser resolution in decimal degrees were resampled to a 1 km x 1 km resolution using the nearest neighbor

method. Data sets with a finer resolution in decimal degrees were first resampled to cell sizes corresponding to the original cell size (GlobCover: 200 m, SRTM DEM: 100 m, worldclim: 200 m, cf. Table 12), also using the nearest neighbor technique. The resulting raster cells were then aggregated to 1 km x 1 km cells; each 1 km x 1 km cell assigned the average value of the aggregated cells. For deriving catchment averages of subsoil and topsoil pH, the raster data were first recalculated to H^+-concentrations, similar to the aggregation of river water pH (cf. previous section). The catchment averages of the H^+-concentrations were then re-transformed to pH-value.

Table 12: Geodata used to derive catchment properties.

Parameter	Data set	Source	Scale/Resolution
Flow direction	Hydrosheds DEM	Lehner et al. (2008)	15''
Runoff	UNH/GRDC data set	Fekete et al. (2002)	30'
Slope gradient	SRTM DEM	Jarvis et al. (2006)	3''
Land cover	GlobCover data set	Arino et al. (2007)	300 m
Wetlands	Global Lake and Wetland Data Base	Lehner and Döll (2004)	30''
Annual Precipitation	worldclim	Hijmans et al. (2005)	30''
Annual avg. air temperature			
Lakes	SRTM Water Body Data Set	NASA/NGA (2003)	Vector, Based on SRTM DEM with 3'' resolution
Lithology	Lithological map of North America v1	Jansen et al. (2010)	Vector, Scale of the geologic source maps: 1:5,000,000 and higher
Topsoil C org.	Harmonized World Soil Data Base (HWSD)	FAO/IIASA/ISRIC/ISS-CAS/JRC (2009)	30''
Topsoil $CaCO_3$			
Subsoil $CaCO_3$			
Topsoil pH			
Subsoil pH			

4.2.3 Statistical analyses

The statistical and spatial distributions of mean pH, alkalinity, PCO_2, and $SI_{calcite}$ values were obtained using basic statistics and maps. Catchment properties derived from geodata were analyzed with regard to their potential as predictors of the spatial variation in the carbonates system of rivers. For this, a functional relationship between catchment properties and pH, alkalinity, or PCO_2 is required. Note that a potential predictor does not necessarily represent a controlling factor itself, but might be an indicator for environmental factors controlling both, the predictor and the variable to be predicted.

For the set up of empirical equations describing the spatial variability in alkalinity, pH, and PCO_2, multiple linear regression analysis was used, applying catchment properties as predicting variables. For each predicting variable x_i, a factor b_i (b-estimate) was derived by the regression analysis, expressing the predictor's effect on the variable to be predicted (Eq. 22). The predictors were chosen in order to optimize the correlation coefficient of the fitted regression equations and the significance of b-estimates assigned to the predictor variables ($p<0.05$-significance level).

Eq. 22

$$PCO_2, \text{ Alkalinity, or } pH = b_0 + b_1 * x_1 + \ldots. + b_n * x_n$$

Using scatter-plots, functional relationships between predictors and predicted variables were visually analyzed and discussed with regard to controlling mechanisms lying behind specific patterns. Generally, it is hypothesized that the relationship between catchment properties and the carbonate system of the rivers decrease downstream, due to in-river biogeochemical processes and gas-exchange with the atmosphere, and thus should be stronger in smaller than in larger catchments. To test this hypothesis, the multiple linear regression equations set up for pH, alkalinity, and PCO_2 were refitted for three subsets of catchments of similar sample size: 'small catchments' (<1,000 km², n=367), 'medium catchments' (1,000 – 10,000 km², n=360), and 'large catchments' (>10,000 km², n=393).

For all statistical analyses, the software Statistica 9.0 (Statsoft®) was applied. All statistical correlations between parameters were given as Pearson correlation coefficients. If not stated otherwise, the correlation coefficients given in the text are significant with respect to the $p<0.05$ significance level.

4.3 Results and discussion

4.3.1 Statistical and spatial distribution

The vast majority of the 1,120 sampling locations show an average partial pressure of CO_2 (PCO_2) that is well above the PCO_2 of the atmosphere (at Mauna Loa, 2010, annual mean 389.78 ppmv after Tans, 2011), i.e. the rivers are supersaturated with respect to atmospheric CO_2. Only 8 sampling locations show a mean PCO_2 below 390 ppmv. The calculated average PCO_2 values range from 223 ppmv to 14,168 ppmv, with a mean of 2,091 ppmv (Table 13) that is quite close to the mean river PCO_2 of 2,109 ppmv reported earlier for the conterminous US (Jones et al., 2003). Compared to the average PCO_2 of rivers (3,200 ppmv) and streams (3,500 ppmv) estimated by Aufdenkampe et al. (2011) for the whole temperate zone (25° - 50° latitude), the average PCO_2 in the study area is relatively low.

Values of mean alkalinity per sampling location vary from 6 µeq L^{-1} to 13,378 µeq L^{-1}, with a mean value 2,122 µeq L^{-1} (Table 13). This mean value is substantially higher than the global mean alkalinity of 852 µeq L^{-1} (after Meybeck, 1979), which refers to large world rivers. It is also substantially higher than the mean alkalinity of 1,066 µeq L^{-1} (after Livingston, 1963) reported for North American rivers. However, the literature data are not directly comparable as they are discharge weighted and here, for the purpose of this study, arithmetic means of hydrochemical properties are considered. Mean pH values per sampling location range from 5.1 to 8.9, with a mean value of 6.9.

Table 13: Statistical distribution of mean PCO_2, alkalinity, pH, and $SI_{calcite}$ per sampling location for the set of 1,120 sampling locations.

	N	Mean	Median	Min.	Max.	10th Perc.	90th Perc.	Std.Dev.
PCO_2 [ppmv]	1,120	2,091	1,567	223	14,168	709	4,042	1,756
Alkalinity [µeq L^{-1}]	1,120	2,122	1,864	6	13,378	254	4,348	1,665
pH	1,120	6.9	7.8	5.1	8.9	6.6	8.2	6.3
$SI_{calcite}$	1,070	-0.73	-0.15	-6.52	1.50	-2.92	0.72	0.41

For 1,070 of the 1,120 sampling locations, the mean saturation index of calcite ($SI_{calcite}$) was calculated. Values of mean $SI_{calcite}$ range from -6.52 (highly undersaturated) to 1.50 (highly supersaturated). For 487 sampling locations, the river water is on average supersaturated with respect to calcite ($SI_{calcite} > 0$). Only 14 sampling locations show a mean supersaturation of more than 10 times

the equilibrium ($SI_{calcite}$ > 1). This is quite consistent with the study by Tobias and Böhlke (2011) who found about 40% of the 652 'WQN' monitoring stations throughout the conterminous US to be supersaturated with respect to calcite.

The spatial distribution of mean PCO_2, alkalinity, pH, and $SI_{calcite}$ shows distinct patterns (Figs. 18-21). While the western part of the study area is characterized by lower PCO_2 values, increased PCO_2 values are predominantly located in the Atlantic plains (Fig. 18). Similarly, low pH (Fig. 20) and alkalinity (Fig. 19) values are predominantly located in these coastal plains, but also found alongside the west coast, in the foreland of the Cascade range. Sampling locations with $SI_{calcite}$ < 0, indicating undersaturation, are predominately located in coastal areas and in the south-east of the study area (Fig. 21). Sampling locations in the remaining, more central part of the study area most often show a calcite supersaturation. This is consistent with the spatial patterns in mean $SI_{calcite}$ per sampling location reported previously (Tobias and Böhlke, 2011).

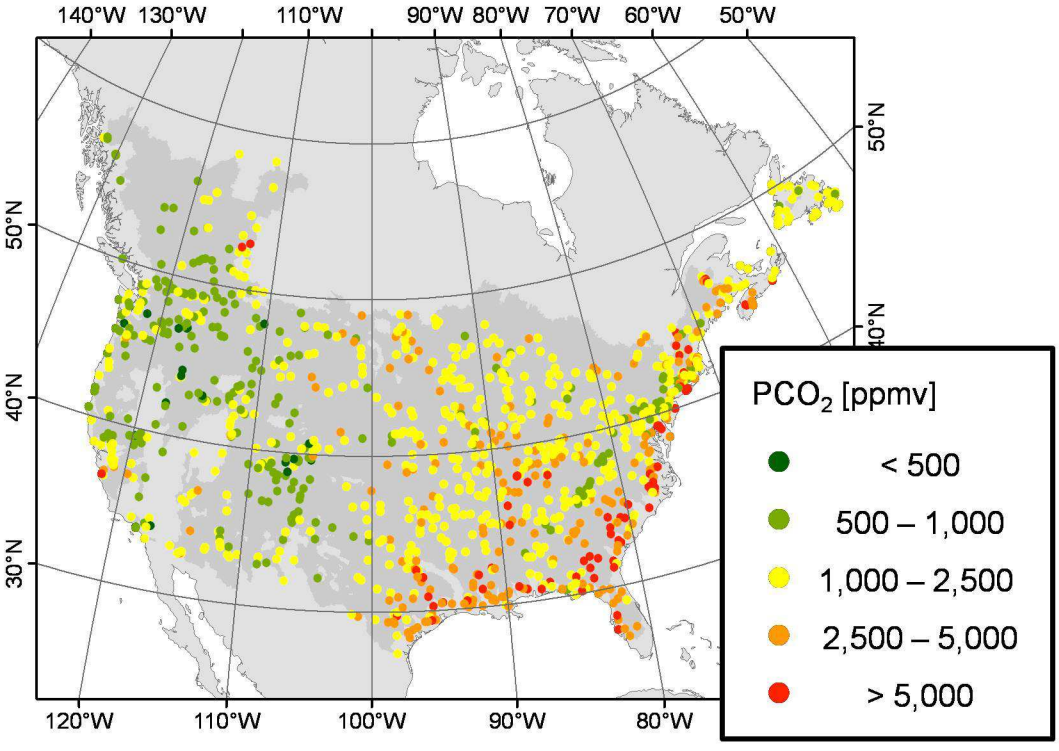

Fig. 18: Spatial distribution of mean PCO_2 of river water per sampling location.

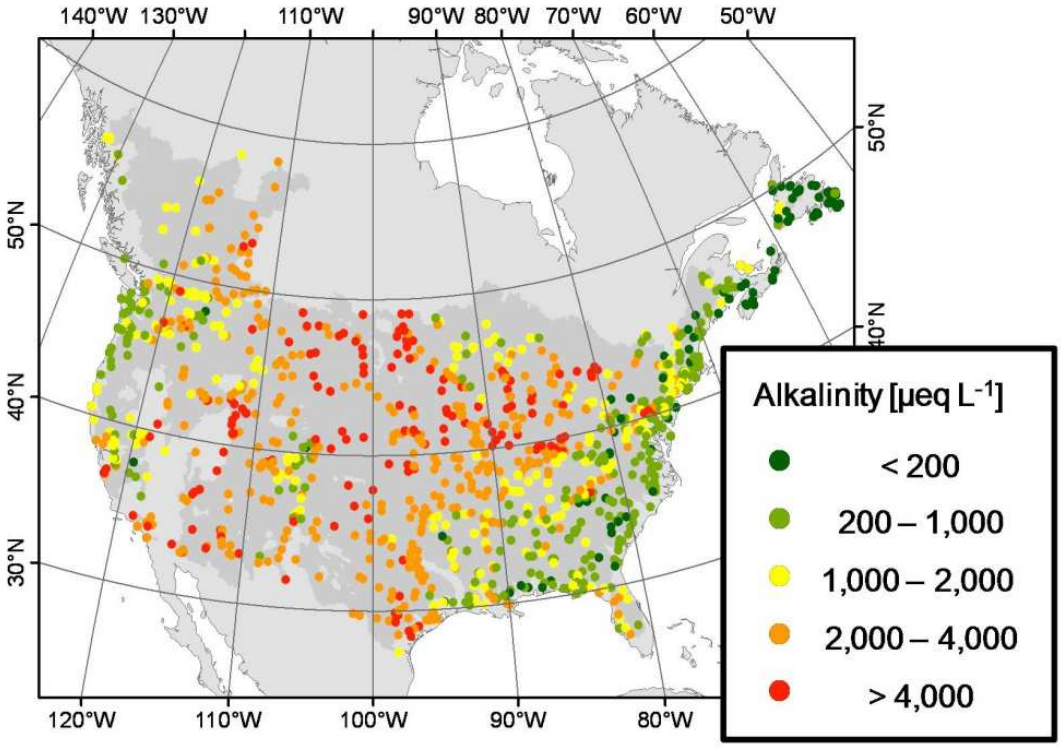

Fig. 19: Spatial distribution of mean alkalinity of river water per sampling location.

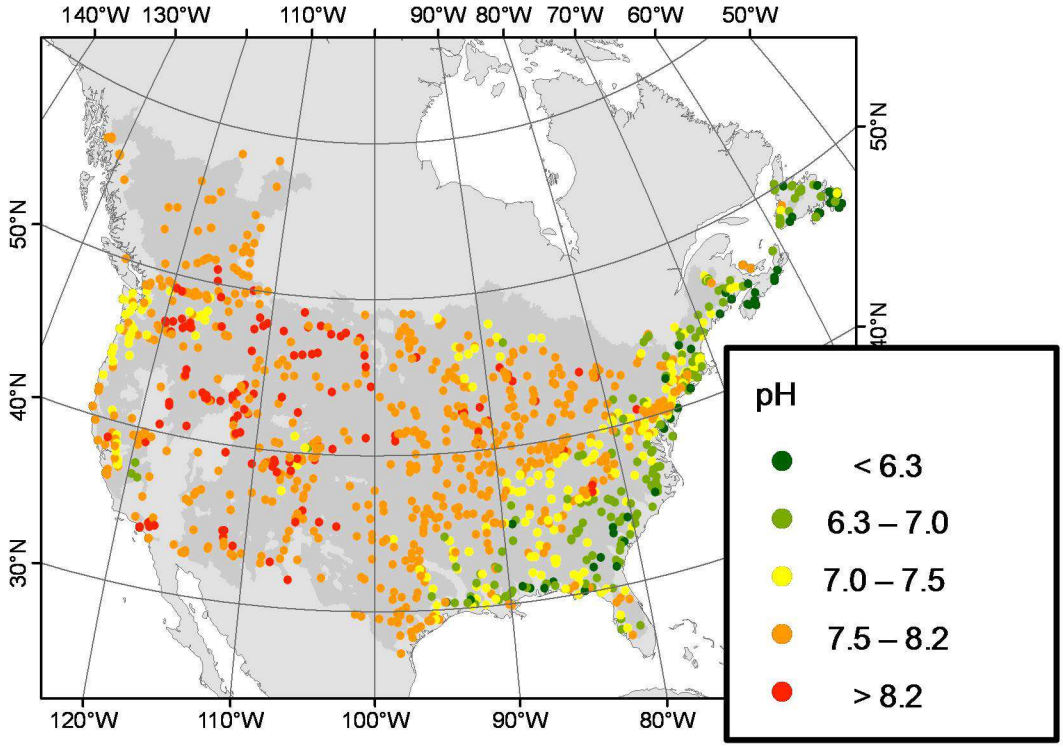

Fig. 20: Spatial distribution of mean pH of river water per sampling location. Mean pH was derived from mean H^+ concentrations.

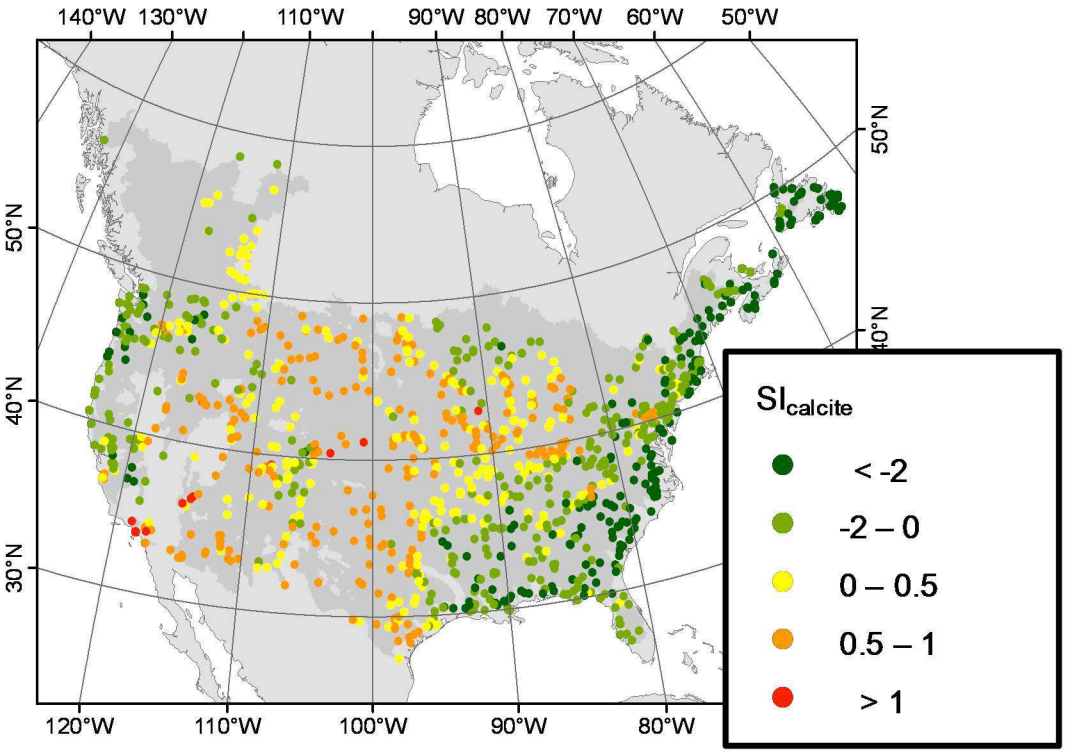

Fig. 21: Spatial distribution of mean saturation index of calcite ($SI_{calcite}$) per sampling location.

In the calculation of PCO_2, pH is linearly related to the negative decadic logarithm of PCO_2 ($pPCO_2$) (cf. Stumm and Morgan, 1981). Figure 22 illustrates the relations between $pPCO_2$, pH, and alkalinity of the 1,120 sampling locations considered here. It becomes visible that for a given range of alkalinity values, the $pPCO_2$ is clearly related to the pH. Nevertheless, increased PCO_2 values (low $pPCO_2$ values) occur at a broad variety of mean pH or alkalinity values (90^{th} percentile about 4,000 ppmv, i.e. $pPCO_2 \approx 2.4$).

4.3.2 Controls of the carbonate system of rivers

The parameters $pPCO_2$, pH, and alkalinity show distinct patterns when plotted against mean annual precipitation per catchment (P) (Fig. 23 - Fig. 25). For P up to 1.7 m a^{-1}, there is a substantial negative correlation with alkalinity (r=-0.61) and pH (r=-0.71), and a lower but still notable correlation with $pPCO_2$ (r=-0.30). For the 18 cases with P>1.7 m a^{-1}, no further trend is visible and the value ranges of PCO_2, pH, and alkalinity are rather narrow (Table 14). Thus, this subgroup was discarded from the multivariate statistics, leaving a set of 1,102 sampling locations/catchments (cf. Tables D.1 & D.2 in Appendix). P was identified as a predictor for all three parameters: PCO_2 (as $pPCO_2$), pH, and alkalinity (Table 15).

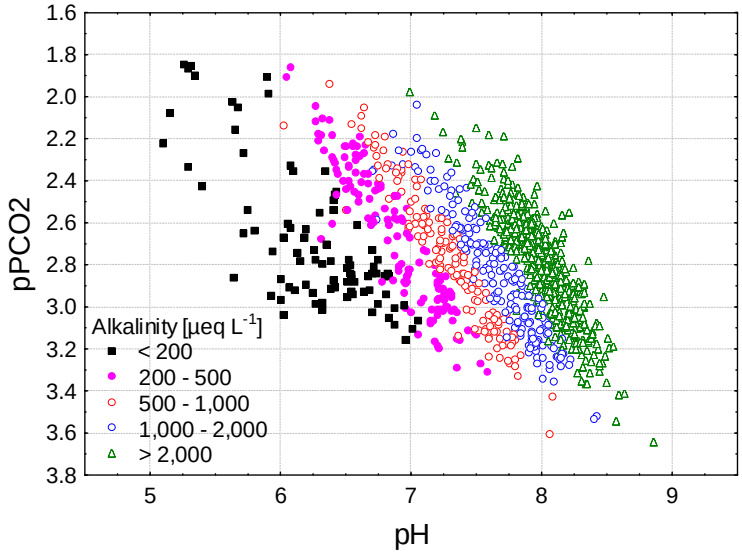

Fig. 22: Relations between mean PCO_2, alkalinity and pH per sampling location (n=1,120) used in this study.

Table 14: Statistical distribution of mean PCO_2, alkalinity, and pH of sampling locations having a mean annual catchment precipitation (P) of more than 1.7 m a^{-1} (n=18).

	Mean	Median	Minimum	Maximum	10th percentile	90th percentile	Std.Dev.
PCO_2 [ppmv]	1,019	957	485	1,984	631	1,488	346
Alkalinity [µeq L^{-1}]	465	444	266	736	304	677	133
pH	7.3	7.3	7.2	7.7	7.2	7.6	7.8

The multiple linear regression analysis revealed that the variation in alkalinity values can best be explained by P, the areal proportion of carbonate rocks per catchment (SC), the average subsoil pH (S_pH), and the areal proportions of agricultural land (A_{AL}) (r^2=0.66, Table 15). For the variations in pH, only two of these parameters, P and SC, were identified as predictors (r^2=0.60). S_pH was not identified as predictor though showing a substantial correlation to pH (r=0.60, Fig. 26). This is probably due to the high correlation with the stronger predictor P (r=-0.73, Fig. 26), leaving S_pH redundant for the multiple linear regression. A probable explanation for the intercorrelations between these two potential predictors is that under high annual precipitation, soils are deeply weathered and the subsoil is more deprived of bases and easily weatherable minerals, leaving the soil solution at a rather low pH compared to more arid conditions. Interestingly, subsoil pH does not show a notable correlation to the areal proportion of carbonate rocks (SC) (r=0.10).

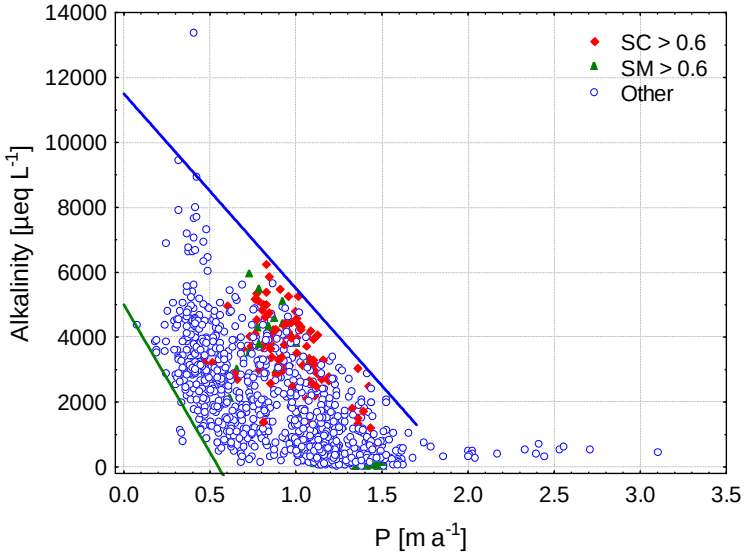

Fig. 23: Scatter-plot of mean annual precipitation per catchment (P) vs. mean alkalinity of river water at the related sampling location. For P<1.7 m a^{-1} (n=1,102), there is a substantial negative correlation (r=-0.62). Highlighted are catchments which are dominated (>60%) by carbonate rocks (SC) or mixed sedimentary rocks (SM). The blue and green lines represent suggested constraints on expectable value ranges (cf. Table D.4).

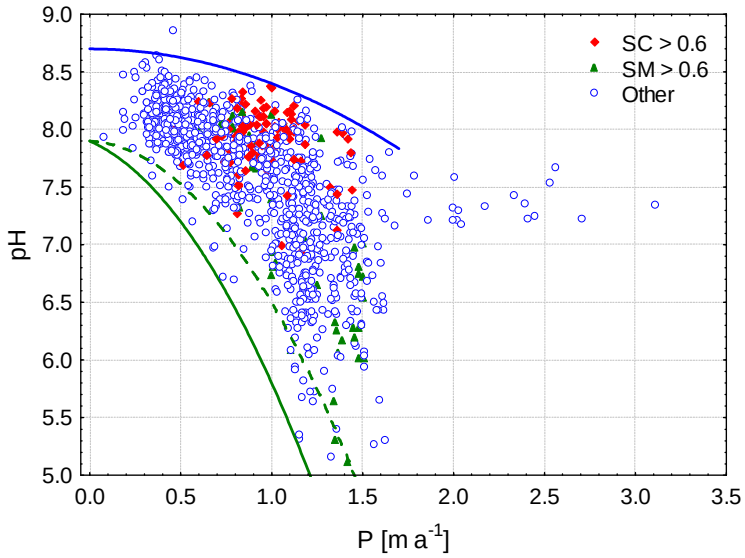

Fig. 24: Scatter-plot of mean annual precipitation per catchment (P) vs. mean pH of river water at the related sampling location. For P<1.7 m a^{-1} (n=1,102), there is a substantial negative correlation to pH (r=-0.71). Highlighted are catchments which are dominated (>60%) by carbonate rocks (SC) or mixed sedimentary rocks (SM). The blue and green lines represent suggested constraints on expectable value ranges (cf. Table D.4).

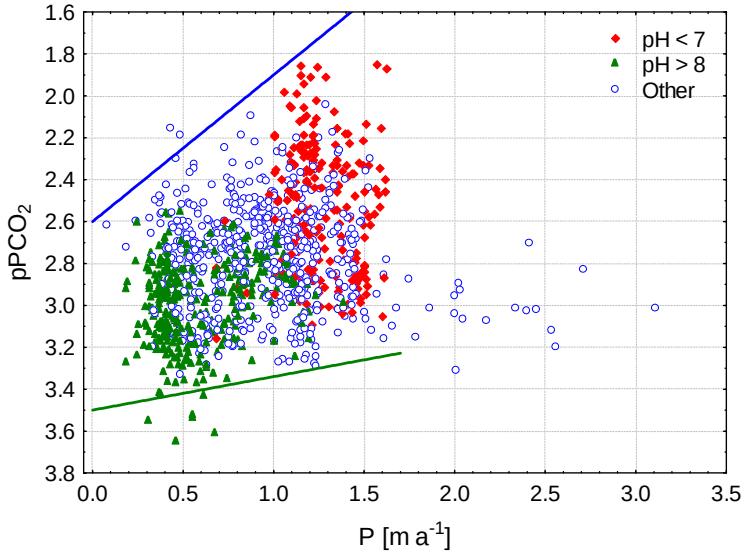

Fig. 25: Scatter-plot of mean annual precipitation per catchments (P) vs. $pPCO_2$ at the related sampling location. For P<1.7 m a^{-1} (n=1,102), there is a low correlation to $pPCO_2$ (r=-0.30). For cases with P>1.7 m a^{-1} (n=18), no further trend with P is observable in this data set. Subsets selected by average pH are highlighted to illustrate the intercorrelation between this parameter and P. The blue and green lines represent suggested constraints on expectable value ranges (cf. Table D.4).

Table 15: Results of multiple linear regression analyses for alkalinity, pH, and pCO_2 as predicted variables[a]

Training catchments	r^2	Intercept	P [m a^{-1}]	SC [1]	S_pH	A_{AL} [1]	$T_{air,mean}$ [℃]	ln(s [°])
Alkalinity [µeq L^{-1}]								
all	66%		-1,715± 64	1,510±126	524±12	2,453±187		
small	63%		-1,719±130	1,767±206	526±28	2,336±355		
medium	65%		-1,795±120	1,266±225	549±23	2,668±318		
large	69%		-1,693±106	970±269	515±16	2,497±295		
pH								
all	60%	8.630±0.033	-1.310±0.034	0.808±0.048				
small	53%	8.665±0.094	-1.423±0.084	0.852±0.087				
medium	54%	8.563±0.061	-1.174±0.062	0.744±0.083				
large	69%	8.580±0.031	-1.200±0.041	0.759±0.077				
pCO_2								
all	43%	2.911±0.025	-0.167±0.020				-0.015±0.001	0.119±0.008
small	47%	2.848±0.056	-0.082±0.041				-0.020±0.003	0.140±0.015
medium	45%	2.870±0.041	-0.180±0.037				-0.009±0.003	0.131±0.013
large	40%	3.008±0.037	-0.266±0.036				-0.013±0.002	0.083±0.013

[a]Reported values are the b-estimates of the predictors ± the standard error. Note that only catchments with mean annual precipitation below 1.7 m a^{-1} are considered (n=1,102, see text). As catchment size could not be identified as predictor but is hypothesized to have an effect on the carbonate system of rivers, and more specifically on the relationship between catchment properties and the carbonate system of rivers, the regression equations have also been fitted for subsets of small, medium, and large catchments (see below) in order to identify these effects. Note that in the regression analysis for alkalinity, one medium sized catchment missing a value for S_pH had to be discarded.

P mean annual precipitation
SC areal proportion of carbonate rocks
S_pH subsoil pH
A_{AL} areal proportion of agricultural land
$T_{air,mean}$ mean annual air temperature
ln(s [°]) logarithm of mean slope gradient

Training catchments:
all n=1,102
small < 1,000 km², n=356
medium 1,000 - 10,000 km², n=353
large > 10,000 km², n=393

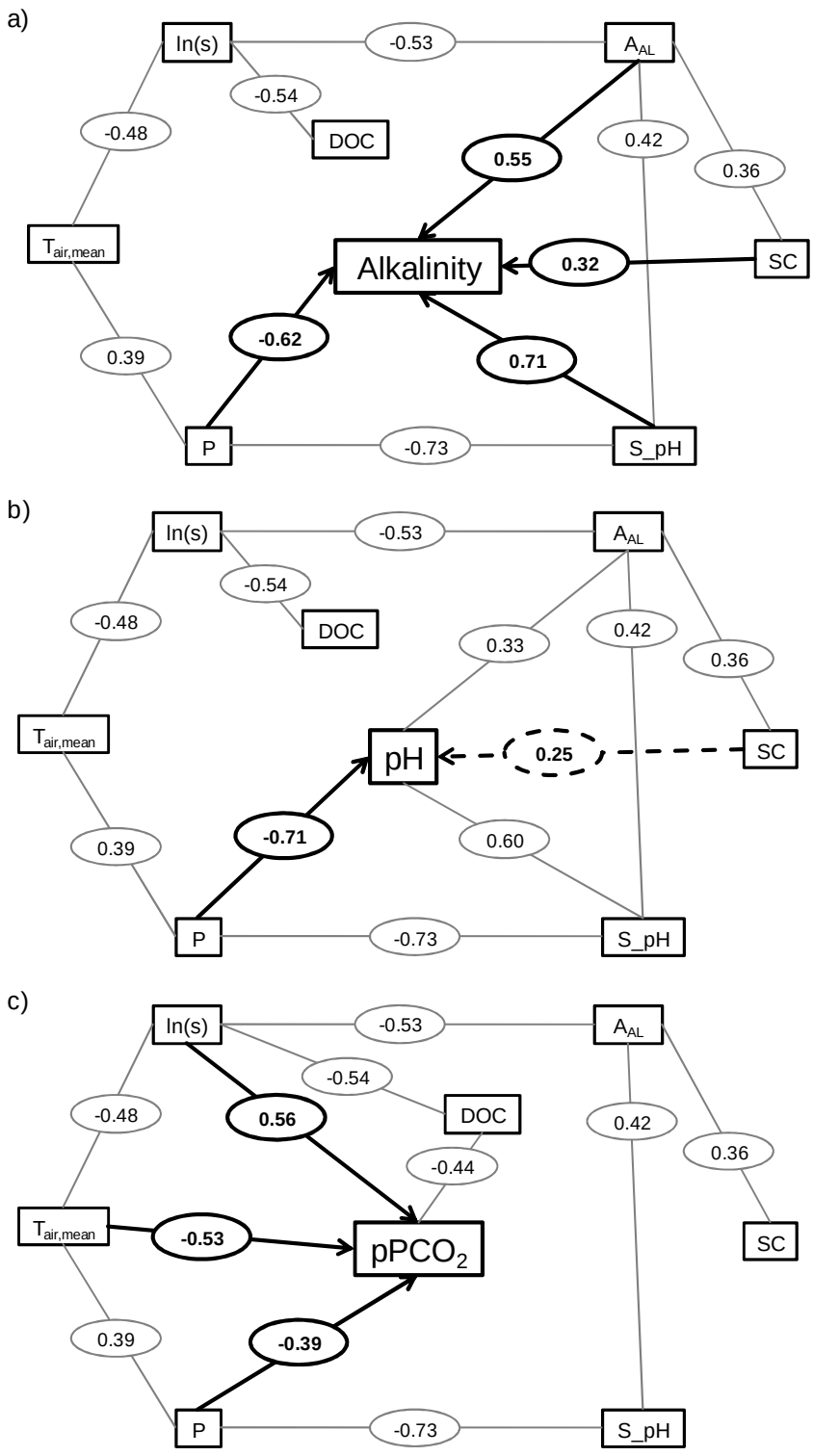

Fig. 26: Correlations between catchment properties and means of a) alkalinity, b) pH, and c) $pPCO_2$ per sampling location. Pearson correlation coefficients r > 0.3 are given in the oval shapes. For explanation of abbreviations used see Table 15. Correlations of predictors applied in the regression analyses are highlighted with bold lines. Only for the correlation between SC and pH a lower correlation coefficient is reported (dashed bold line), because SC is used in the multiple linear regression analysis to predict mean pH per sampling location. Besides catchment properties, DOC is analyzed in its potential as predictor. Note that only for 707 sampling locations a mean DOC concentration could be calculated. The correlations for DOC thus refer to this subset of sampling locations. Similarly, the correlations of S_pH with other parameters refer to a subset of 1,101 sampling locations (see text).

SC as individual predictor shows a rather low correlation to alkalinity (r=0.32) and pH (r=0.25) (cf. Fig. 26). However, SC shows a modulating effect on the relation between P and pH. For catchments dominated by carbonate rocks (SC>0.6, n=99), pH generally remains at rather high levels even for high P (Fig. 24). The effect of SC on alkalinity increases with P; for P>1 m a^{-1} (n=500) it is indeed substantial (r=0.74) (Fig. 27). Similarly, the correlation between SC and pH is substantial for P>1 m a^{-1} (r=0.55); for P<1 m a^{-1} (n=602), there is no significant correlation between SC and pH (Fig. 28). With one single exception, very low pH values of 6.5 and lower (n=78) only occur where P exceeds 1 m a^{-1} and no notable proportion of carbonate rocks is present within the catchment (SC<2%) (Fig. 28). The highest pH (Fig. 24, Fig. 28) and alkalinity (Fig. 23, Fig. 27) values were found for rivers draining catchments with low P. Among these catchments, such with notable proportions of carbonate rocks are however rare in the data set.

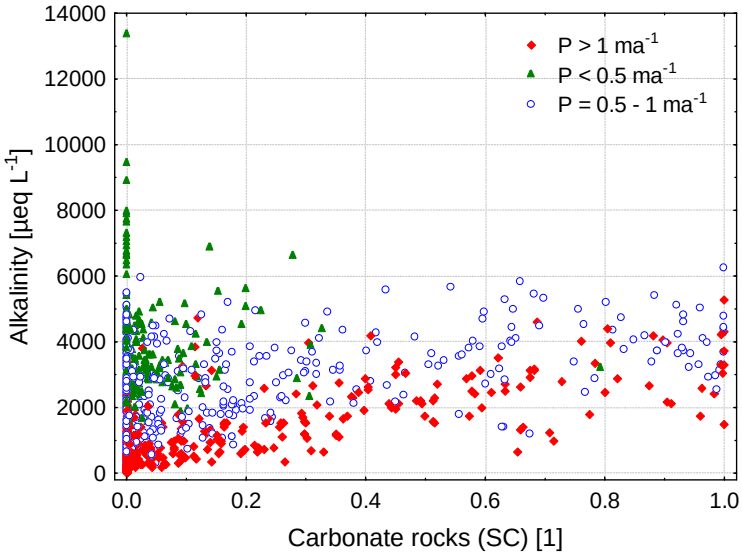

Fig. 27: Scatter-plot of areal proportion of carbonate rocks (SC) per catchment vs. mean alkalinity of river water at the related sampling location (n=1,120, r=0.31). Subsets selected by mean annual precipitation (P) are highlighted. For catchments with a higher P (P>1 m a^{-1}: n=500, r=0.74; P=0.5 - 1 m a^{-1}: n=404, r=0.47), the positive correlation between SC and alkalinity is clearly increased.

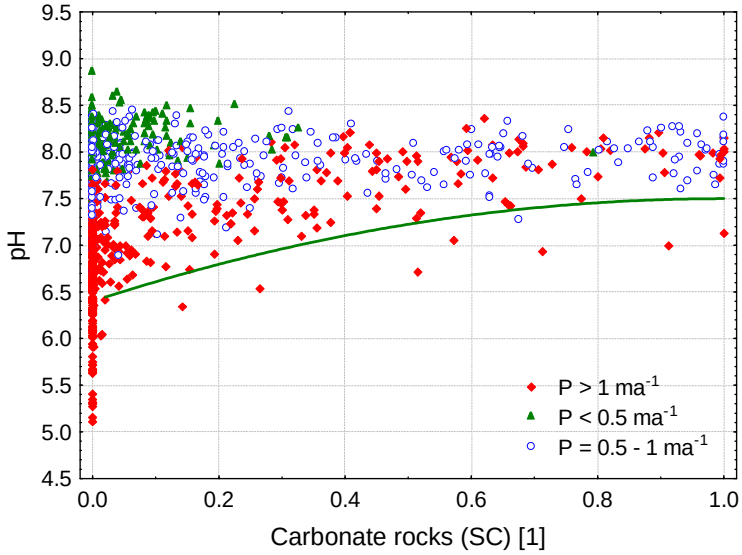

Fig. 28: Scatter-plot of areal proportion of carbonate rocks (SC) per catchment vs. mean pH of river water at the related sampling location (n=1,120, r=0.26). Subsets selected by mean annual precipitation (P) are highlighted. For catchments with P>1 m a^{-1} (n=500, r=0.55), there is a substantial positive correlation between SC and pH. For catchments with P<1 m a^{-1} (n=620), there is no significant correlation between SC and pH. The green line represents a suggested constraint on expectable value ranges (cf. Table D.4).

The negative correlations between P and pH and between P and alkalinity can be explained by dilution effects, when increasing P leads to higher runoff and on average shorter mineral-water interaction times (cf. Pinol and Avila, 1992; Jones and Mulholland, 1998b; Moosdorf et al., 2011b). The strong negative intercorrelation with subsoil pH suggests as well that under high precipitation soils are probably already deeply weathered and deprived of bases, forming a superficial substrate in which actual weathering rates are generally low. If chemical weathering is limited, the weathering related production of alkalinity and consumption of H^+ from the soil solution are also limited. Consequently, the dilution effects are modulated by the catchment bedrock lithology, specifically by the proportion of carbonate rocks, which show by far higher weathering rates than silicate rocks (cf. Moosdorf et al., 2011c).

For the areal proportions of mixed sedimentary rocks (SM), from which substantial contributions by carbonate weathering are expected as well (Moosdorf et al., 2011c), no significant correlation with alkalinity was found. This is in contrast to the findings by Moosdorf et al. (2011c), who estimated similar HCO_3^- fluxes from SM and SC under comparable hydroclimatic conditions.

The identification of areal proportions of agricultural lands (A_{AL}) as a predictor for alkalinity hints at an anthropogenic increase in the rivers' alkalinity related to agricultural land use (Williams et al., 2005; Raymond et al., 2008; Barnes and Raymond, 2009), which can partly be attributed to agricultural liming (Oh and Raymond, 2006).

For PCO_2 (as $pPCO_2$), multiple linear regression reveals that the spatial variations mainly depend on P, mean air temperature ($T_{air,mean}$), and slope gradient (s) (Table 15). However, the explained proportion of the variation in $pPCO_2$ of 43% (r^2=0.43) is lower than that for alkalinity and for pH (r^2=0.66 and r^2=0.60, respectively). $T_{air,mean}$ shows a substantial negative correlation (r=-0.56, Fig. 30), s a substantial positive correlation (as ln(s): r=0.53, Fig. 29) to $pPCO_2$. Both catchment properties do not show a notable correlation to alkalinity or pH (Fig. 26). Neither do SC, S_pH, or A_{AL} show notable correlations to $pPCO_2$ (Fig. 26).

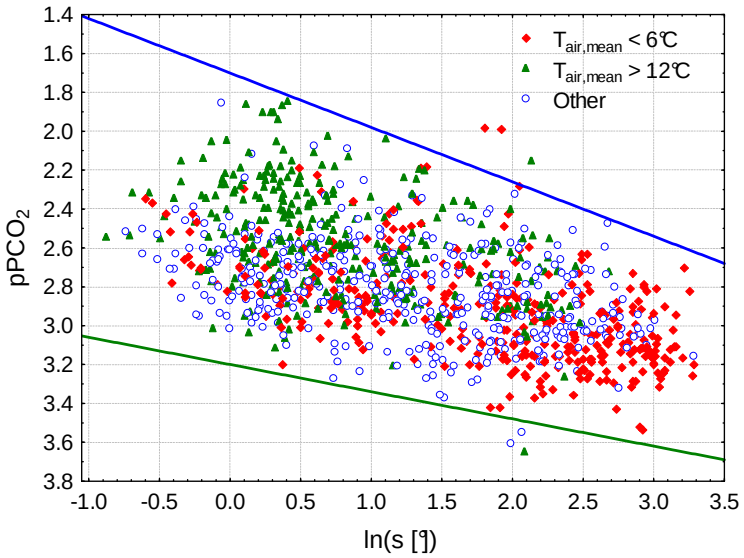

Fig. 29: Scatter-plot of $pPCO_2$ vs. logarithm of slope gradient ln(s [°]) (n=1120, r=0.56). Subsets selected by $T_{air,mean}$ are highlighted to illustrate the inter-correlation between this parameter and ln(s [°]) (r=-0.48). The blue and green lines represent suggested constraints on expectable value ranges (cf. Table D.4).

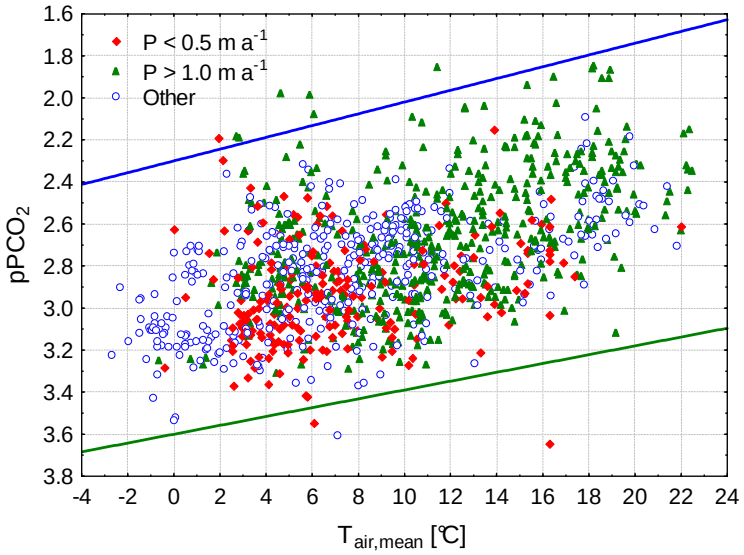

Fig. 30: Scatter-plot of $pPCO_2$ vs. mean air temperature per catchment ($T_{air,mean}$) (n=1120, r=-0.56). Subsets selected by mean annual precipitation P illustrate the inter-correlation between this parameter and $T_{air,mean}$ (r=0.33). The blue and green lines represent suggested constraints on expectable value ranges (cf. Table D.4).

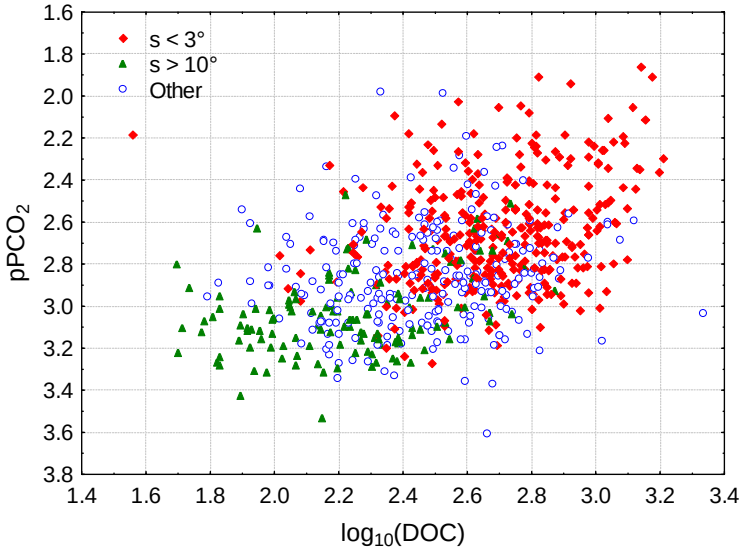

Fig. 31: Scatter-plot of $pPCO_2$ vs. log_{10}(DOC) (r=-0.46). Subsets selected by average slope gradient s illustrate the correlation between s and DOC (r=-0.49), and the correlation between ln(s [°]) and log_{10}(DOC) (r=-0.63), respectively.

The probable explanations for the positive correlations of s to $pPCO_2$ (i.e. negative correlation between s and PCO_2) are a tendency for the occurrence of shallower soils in steeper environment and the higher flowing velocities and thus more turbulent discharges in steeper terrain fostering CO_2 evasion from streams and rivers. The negative correlation between $T_{air,mean}$ and $pPCO_2$ (i.e. positive correlation between $T_{air,mean}$ and PCO_2) may be explained by increased respiration within soils and aquatic ecosystems under higher temperature, but also thermodynamically by the positive effect of water temperature on the PCO_2 in the water. Indeed, $T_{air,mean}$ is – as expected - highly correlated with average water temperatures derived from the hydrochemical data set (r=0.89).

For an increase in water temperature from 5°C to 25°C, the PCO_2 estimated by the regression equation in Table 15 (all catchments' fit) would increase by about 100%. Due to the thermodynamic dependence on water temperature, over this temperature range, the PCO_2 would theoretically increase by about 30% (derived from test calculation with PhreeqC). Thus, it can be concluded that increased respiration is the major link between $T_{air,mean}$ and PCO_2.

The residuals of the regression equations for alkalinity, pH, and $pPCO_2$ are more or less close to a normal distribution (Fig. 32), indicating that there is no general bias in the prediction. Only for pH, there exists a notable bias concerning very low pH values. For P<1.7 m a^{-1}, the lowest pH estimate possible is 6.4. Indeed, 61 of the 1,102 sampling locations (ca. 5.5%) have average pH values below 6.4. Thus, with the predictors used here, it is not possible to explain those lowest pH values. Very low pH values are mainly distributed along the coastal plains (Fig. 20) and could be expected for blackwater rivers draining wetlands (cf. e.g. Beck et al., 1974). However, for most of the sampling locations with very low pH, such a hypothesis could not be confirmed by increased proportions of wetlands within the catchments or by increased DOC concentrations.

The substantial correlations of PCO_2 (as $pPCO_2$), pH, and alkalinity with catchment properties suggest that to a substantial proportion, the rivers' carbonate system is controlled by catchment processes. For PCO_2 there is also a substantial correlation to DOC ($pPCO_2$ vs. $\log_{10}$(DOC): n=717, r=-0.44, Fig. 31), hinting at a substantial contribution of in-river respiration to PCO_2. As DOC is intercorrelated with the average slope gradient s (cf. Fig. 31, Fig. 26), one of the important mechanism behind the negative effect of s on PCO_2 may be the decreased export of DOC from steeper areas (cf. Mulholland, 1997). For pH and alkalinity no notable correlation with DOC or $\log_{10}$(DOC) was found.

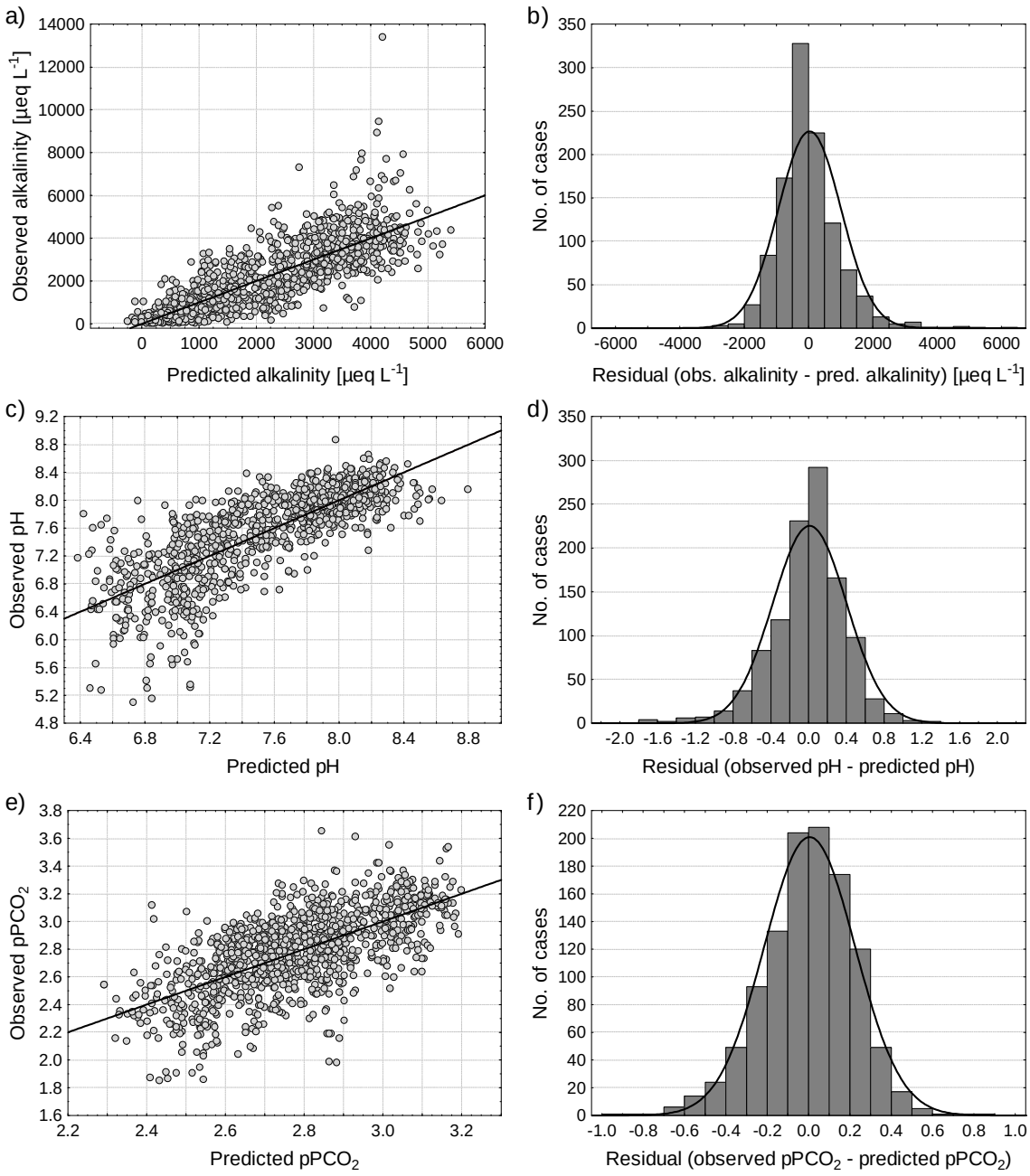

Fig. 32: Scatter-plots of observed vs. predicted values and frequency distribution of residuals from the regression equations for a,b) alkalinity, c,d) pH, and e,f) $pPCO_2$ (cf. Table 15). Straight lines represent hypothetical 1:1 ratios. The curves represent the theoretical normal distributions of the residuals based on their means and standard deviations.

4.3.3 Effects of catchment size

Catchment size was not found to show any significant correlation or distinct pattern with alkalinity, pH, or PCO_2 (as $pPCO_2$). This finding is supported by local studies showing that the main changes in PCO_2 and, subsequently, pH occur below springs and in the uppermost headwaters where most of the excess CO_2 evades rather quickly (e.g. Kempe, 1985; Choi et al., 1998; Johnson et al., 2008). To estimate the CO_2 evasion of soil and groundwater that enters rivers directly, it would be necessary to

assess the PCO_2 of the soil- and groundwater before it enters surface waters. That was attempted in a regional scale study for England and Wales (Worrall et al., 2007). At continental to global scale, groundwater contributions have mostly been neglected in the assessment of CO_2 evasion from fluvial systems (cf. Battin et al., 2008; Battin et al., 2009; Aufdenkampe et al., 2011). However, CO_2 evasion from rivers due to the net-heterotrophy is still a substantial source of CO_2 to the atmosphere, as shown by the studies quoted above.

In the literature it is hypothesized that catchment-river coupling with regard to the rivers' carbonate system attenuates downstream, i.e. with increasing catchment size. Consequently, the effects of catchment properties used as predicting variables in multiple linear regression analyses should decrease. By refitting the regression equations for alkalinity, pH, and $pPCO_2$ to three subsets of catchments representing three different catchment size classes, this hypothesis was tested (Table 15, small, medium, and large catchments).

For alkalinity, r^2 slightly increases from the small (<1,000 km²) to the large catchments (>10,000 km²) (Table 15). The b-estimates assigned to the predictors mean annual precipitation (P), areal proportions of agricultural land (A_{AL}), and subsoil pH (S_pH) do not vary substantially between these three versions of the regression equation, confirming that alkalinity is a rather conservative property less affected by in-river processes. The effect assigned to the areal proportions of carbonate rocks (SC), on the contrary, decreases substantially from the small to the large catchments, with the large catchments' fit showing the highest deviation from the fit for the total set of 1,102 catchments, i.e. -540 µeq L^{-1} for SC = 100% (Table 15). However, while the statistical distributions of P, S_pH, and A_{AL} are quite similar for the three catchment size classes, catchments with substantial proportions of carbonate rocks become more rare from the small to the large catchments (90^{th} percentile of SC: small c.: 78%, medium c.: 60%, large c.: 31%, Table D.3). Thus, for 90% of the large catchments, the difference in the b-estimate assigned to SC results in a total difference of less than 167 µeq L^{-1} in the estimated mean alkalinity, which is quite low compared to the mean alkalinity of 2,515 µeq L^{-1} of rivers with large catchments. At the continental scale addressed by this study, alkalinity can be considered a conservative property which can be well predicted by just addressing catchment processes, and $CaCO_3$ precipitation within the fluvial network is considered negligible for the land-ocean transfer.

For pH, r^2 is substantially higher for the large catchments (69%) than for small (53%) and medium catchments (54%) (Table 15). This can possibly be explained by the fact that in only 4 of 393 cases

(about 1%) observed pH is below the minimum predictable value (for this version: 6.54). For the re-fits for the small and medium catchments (Table 15), about 7.6% and 9.3% of the mean observed pH values were lower than the minimum predictable pH value. The b-estimates ascribed to the predictors do not vary substantially, also indicating the absence of notable differences in the catchment-river coupling between the distinguished catchment size classes. The predictors P and SC indicate that spatial patterns in river pH can best be explained by catchment processes controlling groundwater contributions to stream flow and groundwater chemistry. Thus, even if pH increases rapidly due to CO_2 evasion when groundwater enters surface waters, the initial chemistry of the groundwater has a strong influence on the average river water pH if different river systems are compared.

For $pPCO_2$, there is a slight decrease in the r^2 from the small to the large catchments, which may reveal that the river-catchment decoupling increases downstream (Table 15). However, this effect is rather weak. The effects of s and $T_{air,mean}$ are substantially lower for the larger than for the smaller catchments. On the contrary, the effects of P substantially increase from the small to the large catchments, hinting at a probably increasing importance of P as a predictor for $pPCO_2$ with increasing catchment size.

The PCO_2 of rivers of the sizes considered here does obviously not depend on the initial PCO_2 of soil and groundwater. This is confirmed by the rather low correlation with P, compared to the correlation of P with pH and alkalinity, and the missing correlation to lithology, specifically to carbonate rocks. On the other hand, the substantial correlation to DOC hints at in-river respiration as a major factor controlling spatial variations in mean PCO_2.

However, even if it is assumed that PCO_2 of rivers with catchment sizes addressed here is mainly governed by in-river processes and direct groundwater contribution can be neglected, a correlation between catchment properties and the PCO_2 in the rivers at continental to global scales is still probable, because in-river processes themselves may be related to catchment properties. In-river respiration depends on terrestrial exports of organic carbon which have been shown to depend on catchment properties, for instance slope gradient (Ludwig et al., 1996b; Mulholland, 1997), and water temperature (Demars et al., 2011), which was here found to be highly correlated to the $T_{air,mean}$ of the catchments. Similarly, in-river photosynthesis depends on terrestrial exports of nutrients and light-limitation by transported sediments, which are related to catchment processes and thus to catchment properties also at regional to global scales (cf. e.g. Humborg et al., 2004; Syvitski et al., 2005;

Mayorga et al., 2010). The rather indirect effects of the identified predictors on the PCO_2 are a probable explanation for the lower correlation coefficient of the multiple linear regression, compared to the multiple linear regression analysis' results for alkalinity and pH (cf. Table 15).

4.3.4 General uncertainties

General uncertainties in the assessment of mean alkalinity, pH, and PCO_2 per sampling location exist with regard to the representativeness of the samples used. Seasonal variations are taken into account by the seasonal weighting of aggregated sample information done in this study. Specifically for pH and PCO_2, diurnal variations should be taken into account, because these are substantial and may even exceed seasonal variations of daily means (Jarvie et al., 2001; Lynch et al., 2010; de Montety et al., 2011). Because samples are mostly taken during the daytime when photosynthesis plays a certain role, it is expected that the majority of measured pH over- and derived PCO_2 values underrepresent average conditions in streams and rivers (Jarvie et al., 2001). Indeed, 98.8% of samples considered were taken between 6 am and 6 pm. Thus, a positive bias for averaged pH values and a negative bias for calculated PCO_2 values is as well to be expected for this study. However, representative estimates of diurnal variation would be needed to quantify this bias.

For more than 78% of the considered samples, pH is reported with a precision of one decimal place. If we expect uncertainties in pH measurements of up to 0.1 pH-units, these uncertainties would imply an uncertainty of calculated PCO_2 values of -21% ($=10^{-0.1}-1$) to +26% ($=10^{+0.1}-1$) (cf. Eqs. 5-7).

By the method of discarding samples with PCO_2 values beyond the 10^{th} and 90^{th} percentile for each time series, unreasonable PCO_2 values, most likely representing erroneous pH values, were excluded. Because the highest PCO_2 values usually differ much more from the mean PCO_2 than the lowest PCO_2 values in each time series, this method implies a rather conservative estimate of mean PCO_2.

Additional uncertainties in the calculation of PCO_2 are related to the non-carbonate contribution to alkalinity, in natural freshwater systems most likely from dissolved inorganic phosphorous (DIP) and organic anions. For most aquatic systems, these non-carbonate contributions are negligible (e.g. Stumm and Morgan, 1981). For samples, for which DIP was measured (54% of all samples), that contribution to alkalinity is taken into account by PhreeqC. Dissolved organic matter (DOM), however, is not taken into account by PhreeqC.

The contribution of DOM to alkalinity depends on the charge density of the DOM, which in turn largely depends on the carboxyl content (cf. Oliver et al., 1983). The role of DOM in buffering pH was mainly investigated for softwater lakes and streams of the boreal zone being rich in DOM (e.g. Driscoll et al., 1994; Roila et al., 1994; Hruška et al., 2001; Köhler et al., 2001; Köhler et al., 2002; Cuss et al., 2010). Generally, it can be expected that DOM may contribute most to alkalinity in blackwater rivers having low mineralization and pH, and being rich in DOM. For two low pH (pH≈4.4) blackwater rivers in boreal Canada, a DOM contribution to alkalinity of 26-28% was reported (Cuss et al., 2010). As PCO_2 is linearly related to alkalinity, this would mean a 26-28% overestimation of PCO_2 if calculated from titrated alkalinity. Especially for the highest PCO_2 values which were calculated here mainly for rivers with on average low pH and alkalinity (cf. Fig. 22), there may be a notable overestimation of real conditions. However, as the respective rivers are mainly located in temperate to subtropical climate zones (cf. Fig. 18 - Fig. 20), literature findings from the boreal zone are not directly comparable (cf. Hruška et al., 2003).

Nevertheless, even if the highest PCO_2 values are affected by such a bias, the spatial patterns can be regarded as reliable. The same is true for the general patterns identified between the parameters of the carbonate system and catchment properties.

4.4 Conclusion

Average PCO_2, alkalinity, and pH of rivers throughout North America show distinct spatial patterns at continental scale. For pH and alkalinity, more than 60% of the spatial variation can be predicted from catchment properties. For both parameters, mean annual precipitation and areal proportions of carbonate rocks within the rivers' catchments have been identified as important predictors. For mean alkalinity, two more predictors have been identified: average subsoil pH and areal proportions of agricultural land; the latter supporting the hypothesis of a land-use related increase in fluvial alkalinity export that was debated in the literature.

For PCO_2, there is still a notable proportion of the variance (> 40%) that can be explained by catchment properties at this spatial scale. The identified predictors are average slope gradient, mean air temperature, and mean annual precipitation.

A direct effect of catchment size on mean pH, alkalinity, or PCO_2 could not be shown for the set of rivers analyzed here. Further, a hypothesized decrease in the river-catchment coupling with increasing catchment size could not be clearly confirmed. It is expected, that PCO_2 and pH rapidly change within the uppermost headwater stretches due to high CO_2 degassing, which are, however, not represented in the data set applied here, or generally in river water quality data sets provided by national and provincial surveys.

It can thus be argued that the increased PCO_2 in the rivers analyzed is maintained by in-river respiration rather than direct groundwater contributions. This is further confirmed by a correlation between DOC and PCO_2.

The empirical prediction equation for PCO_2 should in a next step be used to calculate CO_2 evasion from fluvial systems. For such an enterprise, reasonable estimates of the stream-width and gas-exchange velocities are required; the latter can probably be deduced from estimates of flowing velocities which in turn might be predicted from the slope gradient of the fluvial network.

However, this estimation would mainly address excess CO_2 produced by in-river respiration exceeding in-river photosynthesis. For an assessment of the total CO_2 evasion from the fluvial system, quality and quantity of soil- and groundwater entering the surface waters need to be assessed. Estimates of CO_2 evasion from rivers should be brought together with existing studies on lakes to assess the whole inland water system's role in the carbon cycle.

The patterns revealed by plotting pH, alkalinity, or $pPCO_2$ against potential predictors suggest some constraints on the expectable value ranges of these parameters, which can directly be applied for numerical modeling approaches (Table D.4 in Appendix), which could be the next step in the scientific progress in this field.

More empirical research needs to be done on the quantitative role of DOM in the acid-base system of softwater rivers, specifically outside of the boreal zone. Further, representative values for diurnal variations in PCO_2 are needed to correct for potential biases related to the fact that PCO_2 values are mostly derived from data measured from daytime samples.

5 Concluding remarks

Recent approaches in earth system modeling do not consider the fluvial land-ocean fluxes and processes within the fluvial system. However, it was suggested that these processes may be important for the global carbon and silica cycles (e.g. Cole et al., 2007; Battin et al., 2009; Beusen et al., 2009; Aufdenkampe et al., 2011; Dürr et al., 2011). For an integration of rivers in earth system models, it must be known how to represent the mobilization of matter from the terrestrial system into rivers, the fluvial transport, the in-river processes, and the CO_2 evasion from rivers to the atmosphere.

Drawing on North America as model region, the presented thesis shows that a spatially explicit assessment of the fluvial fluxes of dissolved silica (DSi), dissolved inorganic carbon (DIC), and dissolved organic carbon (DOC) at a continental scale is possible, with a spatial resolution not achieved before. It was proven that spatially explicit, empirical estimation techniques are suitable to derive constraints on DSi and DOC losses during fluvial transport from land to the ocean at a continental scale. Further, it was shown that there are spatial patterns in the carbonate system of North American rivers and that these, to a significant proportion, can be predicted from catchment properties. By this, a basic requirement is given for the feasibility of a spatially explicit approach to assess or model CO_2 evasion from the fluvial system at that scale. It is suggested that this is also possible at the global scale if the required data bases are available. In the following, the main findings of this thesis are briefly summarized, before a short outlook is given.

For the assessment of DSi retention within the fluvial system of the conterminous USA, a budget was calculated based on the spatially explicit DSi mobilization estimates from Moosdorf et al. (2011a) and fluvial DSi fluxes calculated from hydrochemical monitoring data. By this, it was estimated that about 13% of the DSi mobilized from the terrestrial system are retained within the fluvial system of the study area, expecting that DSi retention mainly occurs in riverine lakes and reservoirs. It could be argued, that the existing first-order estimates of DSi retention are probably too high.

The spatially explicitly calculated estimates of DSi retention are more uncertain for individual river catchments. However, for the river catchments comprising the Great Lakes, for which substantial DSi retention can be expected, the DSi estimates could be validated with previous local studies. In these lakes, up to about 90% of the DSi mobilized from the contributing terrestrial area are retained.

For the assessment of the DOC loss within North American rivers, a budget was calculated based on two spatially explicit estimates of fluvial DOC fluxes, representing different catchment size classes. For continental North America south of 60°N, the DOC loss was estimated to amount to at least 5.9 Mt C a^{-1}, i.e. at least 23% of the DOC mobilized from the terrestrial system. This value is representative for the fluvial transport through river stretches, over which the contributing area increases from about 500 km² to such of about 26,500 km². However, as headwater-streams, from which substantial DOC loss is expected (e.g. Battin et al., 2008), are not represented in the data base, this estimate represents a rather conservative constraint on DOC losses during the fluvial land-ocean transfer.

The predictors applied in the spatially explicit estimation of DOC fluxes confirm those stated in the literature: runoff, slope gradient, land cover, and areal proportion of wetlands. Additionally, a shift in the effects of the predictors from smaller to larger catchments was identified, with an increasing relative importance of wetlands. This hints to more refractory DOC stemming from wetlands, compared to terrestrial soils. However, to test such a hypothesis, a worthwhile extension of the approach presented here could be to investigate the quality of dissolved organic matter in rivers and its predictability by catchment properties.

For the analysis of spatial patterns in the carbonate system of North American rivers and its controls, an extensive data set of river monitoring stations and the related catchments (n=1,120) were used. Means of PCO_2, pH, and alkalinity per sampling location were investigated for functional relations to catchment properties.

For pH and alkalinity, ≥60% of the variance could be explained by catchment properties. Identified predictors are mean annual precipitation and areal proportion of carbonate rocks, for alkalinity additionally average subsoil pH and areal proportions of agricultural land. There are significant trends for alkalinity and pH to decrease with increasing mean annual precipitation. These trends are attributed to dilution effects, i.e. for higher annual precipitation the chemistry of the runoff is less influenced by weathering reactions. The areal proportions of carbonate rocks mainly attenuates these dilution effects, likely due to the high weathering rates of carbonate rocks and the lithogenic contribution to carbonate alkalinity. The positive effect of agricultural land on river alkalinity confirms previous local to regional scale studies that report anthropogenically increased alkalinity of rivers, in

part due to agricultural liming (e.g. Williams et al., 2005; Oh and Raymond, 2006; Raymond et al., 2008; Barnes and Raymond, 2009).

For PCO_2 (as $pPCO_2$), about 40% of the variance could be explained by catchment properties. Identified predictors are mean air temperature, average slope gradient, and precipitation. It is expected that in-river respiration is the major source for the increased PCO_2 of rivers of the size analyzed in this study, which was supported by the positive correlation between DOC concentrations and PCO_2. High PCO_2 due to direct ground- and soilwater inputs are expected rather for headwater streams, which are not represented in the data base used.

It is hypothesized that the identified predictors have a rather indirect effect on the PCO_2 by controlling in-river processes like respiration and photosynthesis. Mean air temperature has a positive effect on river PCO_2, which can be explained by its close relation to mean water temperature which controls respiration rates within the rivers. Slope gradient has a negative effect on river PCO_2. Probable mechanisms are an increased CO_2 evasion due to a more turbulent discharge in steeper terrain and a notable negative intercorrelation between slope gradient and DOC concentrations. The indirect effects of the catchment properties used as predictors on river water PCO_2 are a probable explanation for the lower proportion of the explained variance compared to pH and alkalinity.

However, as still a substantial proportion of the variance of PCO_2 can be predicted, the next step should be the spatially explicit estimation of CO_2 evasion from rivers, for which additionally the gas-exchange velocities need to be predicted (cf. e.g. Raymond and Cole, 2001). Such an assessment would enhance our knowledge of CO_2 release from continental waters, because up to now the spatial patterns of CO_2 evasion are not well known, and because a spatially explicit assessment would provide a more representative estimate of total CO_2 evasion from continental waters.

The predictability of spatial patterns in mean alkalinity and pH is of importance for other continental scale studies on the biogeochemistry of rivers, e.g. concerning the susceptibility of surface waters to anthropogenically induced acidification processes. For spatially explicit modeling approaches focusing the carbonate system of rivers, constraints on the expectable value ranges of PCO_2, pH, and alkalinity are provided by this thesis.

Compared to other studies focusing on fluvial matter fluxes at continental to global scale, partly rather small river catchments have been analyzed in this thesis. By this, an important step towards the

assessment of total terrestrial carbon and silica exports to the fluvial system was made. Such an assessment would be important with regard to the evaluation of the carbon budgets of terrestrial ecosystems (cf. e.g. Jones and Mulholland, 1998a; Cole and Caraco, 2001; Billett et al., 2004; Jenerette and Lal, 2005; Jonsson et al., 2007; Battin et al., 2009; Aufdenkampe et al., 2011).

However, specifically with regard to DOC loss and CO_2 evasion, more data on smallest headwaters and also soil- and groundwater chemistry are needed for an assessment of the total carbon inputs from the terrestrial system to streams and rivers. Additionally, the assessment of in-river processes could be improved by including other biogeochemically important parameters, like the biochemical oxygen demand, O_2 concentrations, and the quality of the dissolved organic matter.

Generally, rivers are of a greater importance for the global carbon cycle than it could be assumed from recent scientific compilations (eg. IPCC, 2007). It is suggested to consider the fluvial system, i.e. streams and rivers including connected lakes and wetlands, as a separate part of the earth system besides the terrestrial system, the marine system, and the atmosphere. The integration of fluvial systems into earth system models is recommended.

6 References

Aitkenhead-Peterson, J.A., Alexander, J.E. and Clair, T.A., 2005. Dissolved organic carbon and dissolved organic nitrogen export from forested watersheds in Nova Scotia: Identifying controlling factors. Global Biogeochemical Cycles, 19(4).

Aitkenhead, J.A., Hope, D. and Billett, M.F., 1999. The relationship between dissolved organic carbon in stream water and soil organic carbon pools at different spatial scales. Hydrological Processes, 13(8): 1289-1302.

Aitkenhead, J.A. and McDowell, W.H., 2000. Soil C : N ratio as a predictor of annual riverine DOC flux at local and global scales. Global Biogeochemical Cycles, 14(1): 127-138.

Alexander, R.B., Slack, J.R., Ludtke, A.S., Fitzgerald, K.K. and Schertz, T.L., 1997. Data from Selected U.S. Geological Survey National Stream Water-Quality Monitoring Networks (WQN). USGS Digital Data Series DDS-37.

Alexandre, A., Meunier, J.D., Colin, F. and Koud, J.M., 1997. Plant impact on the biogeochemical cycle of silicon and related weathering processes. Geochimica Et Cosmochimica Acta, 61(3): 677-682.

Alin, S.R. and Johnson, T.C., 2007. Carbon cycling in large lakes of the world: A synthesis of production, burial, and lake-atmosphere exchange estimates. Global Biogeochemical Cycles, 21(3).

Alin, S.R., Rasera, M.D.F.F.L., Salimon, C.I., Richey, J.E., Holtgrieve, G.W., Krusche, A.V. and Snidvongs, A., 2011. Physical controls on carbon dioxide transfer velocity and flux in low-gradient river systems and implications for regional carbon budgets. Journal of Geophysical Research G: Biogeosciences, 116(1).

Amiotte-Suchet, P.A. and Probst, J.L., 1993. CO2 Flux Consumed by Chemical Weathering of Continents - Influences of Drainage and Lithology. Comptes Rendus De L Academie Des Sciences Serie Ii, 317(5): 615-622.

Amiotte-Suchet, P.A. and Probst, J.L., 1995. A Global Model for Present-Day Atmospheric Soil CO2 Consumption by Chemical Erosion of Continental Rocks (GEM-CO2). Tellus Series B-Chemical and Physical Meteorology, 47(1-2): 273-280.

Amiotte-Suchet, P.A., Probst, J.L. and Ludwig, W., 2003. Worldwide distribution of continental rock lithology: Implications for the atmospheric/soil CO2 uptake by continental weathering and alkalinity river transport to the oceans. Global Biogeochemical Cycles, 17(2).

Amiotte-Suchet, P.A., Linglois, N., Leveque, J. and Andreux, F., 2007. C-13 composition of dissolved organic carbon in upland forested catchments of the Morvan Mountains (France): Influence of coniferous and deciduous vegetation. Journal of Hydrology, 335(3-4): 354-363.

Arino, O., Gross, D., Ranera, F., Leroy, M., Bicheron, P., Brockman, C., Defourny, P., Vancutsem, C., Achard, F., Durieux, L., Bourg, L., Latham, J., Di Gregorio, A., Witt, R., Herold, M., Sambale, J., Plummer, S. and Weber, J.L., 2007. GlobCover: ESA service for Global land cover from MERIS, Igarss: 2007 Ieee International Geoscience and Remote Sensing Symposium, Vols 1-12 - Sensing and Understanding Our Planet. IEEE International Symposium on Geoscience and Remote Sensing (IGARSS), pp. 2412-2415.

Aufdenkampe, A.K., Mayorga, E., Raymond, P.A., Melack, J.M., Doney, S.C., Alin, S.R., Aalto, R.E. and Yoo, K., 2011. Riverine coupling of biogeochemical cycles between land, oceans, and atmosphere. Frontiers in Ecology and the Environment, 9(1): 53-60.

Barnes, R.T. and Raymond, P.A., 2009. The contribution of agricultural and urban activities to inorganic carbon fluxes within temperate watersheds. Chemical Geology, 266(3-4): 327-336.

Batjes, N.H., 2008. Mapping soil carbon stocks of Central Africa using SOTER. Geoderma, 146(1-2): 58-65.

Battin, T.J., 1999. Hydrologic flow paths control dissolved organic carbon fluxes and metabolism in an alpine stream hyporheic zone. Water Resources Research, 35(10): 3159-3169.

Battin, T.J., Kaplan, L.A., Findlay, S., Hopkinson, C.S., Marti, E., Packman, A.I., Newbold, J.D. and Sabater, F., 2008. Biophysical controls on organic carbon fluxes in fluvial networks. Nature Geoscience, 1(2): 95-100.

Battin, T.J., Luyssaert, S., Kaplan, L.A., Aufdenkampe, A.K., Richter, A. and Tranvik, L.J., 2009. The boundless carbon cycle. Nature Geoscience, 2(9): 598-600.

Beck, K.C., Reuter, J.H. and Perdue, E.M., 1974. Organic and inorganic geochemistry of some coastal plain rivers of the southeastern United States. Geochimica Et Cosmochimica Acta, 38(3): 341-364.

Berner, R.A., 1992. Weathering, Plants, and the Long-Term Carbon-Cycle. Geochimica Et Cosmochimica Acta, 56(8): 3225-3231.

Beusen, A.H.W., Dekkers, A.L.M., Bouwman, A.F., Ludwig, W. and Harrison, J., 2005. Estimation of global river transport of sediments and associated particulate C, N, and P. Global Biogeochemical Cycles, 19(4).
Beusen, A.H.W., Bouwman, A.F., Dürr, H.H., Dekkers, A.L.M. and Hartmann, J., 2009. Global patterns of dissolved silica export to the coastal zone: Results from a spatially explicit global model. Global Biogeochemical Cycles, 23.
Billett, M.F., Palmer, S.M., Hope, D., Deacon, C., Storeton-West, R., Hargreaves, K.J., Flechard, C. and Fowler, D., 2004. Linking land-atmosphere-stream carbon fluxes in a lowland peatland system. Global Biogeochemical Cycles, 18(1).
Blecker, S.W., McCulley, R.L., Chadwick, O.A. and Kelly, E.F., 2006. Biologic cycling of silica across a grassland bioclimosequence. Global Biogeochemical Cycles, 20(3).
Bluth, G.J.S. and Kump, L.R., 1994. Lithologic and Climatologic Controls of River Chemistry. Geochimica Et Cosmochimica Acta, 58(10): 2341-2359.
Borrelli, N., Alvarez, M.F., Osterrieth, M.L. and Marcovecchio, J.E., 2010. Silica content in soil solution and its relation with phytolith weathering and silica biogeochemical cycle in Typical Argiudolls of the Pampean Plain, Argentina-a preliminary study. Journal of Soils and Sediments, 10(6): 983-994.
Brook, G.A., Folkoff, M.E. and Box, E.O., 1983. A World Model of Soil Carbon-Dioxide. Earth Surface Processes and Landforms, 8(1): 79-88.
Campy, M. and Meybeck, M., 1995. Les sédiments lacustres. In: R. Pourriot and M. Meybeck (Editors), Limnologie Générale. Masson, Paris, pp. 6-59.
Cary, L., Alexandre, A., Meunier, J.D., Boeglin, J.L. and Braun, J.J., 2005. Contribution of phytoliths to the suspended load of biogenic silica in the Nyong basin rivers (Cameroon). Biogeochemistry, 74(1): 101-114.
Choi, J., Hulseapple, S.M., Conklin, M.H. and Harvey, J.W., 1998. Modeling CO2 degassing and pH in a stream-aquifer system. Journal of Hydrology, 209(1-4): 297-310.
CIESIN, C., 2005. Gridded population of the world version 3 (GPWv3): Population grids, CIESIN, Columbia University New York, Palisades, NY.
Cole, J.J. and Caraco, N.F., 2001. Carbon in catchments: Connecting terrestrial carbon losses with aquatic metabolism. Marine and Freshwater Research, 52(1): 101-110.
Cole, J.J., Prairie, Y.T., Caraco, N.F., McDowell, W.H., Tranvik, L.J., Striegl, R.G., Duarte, C.M., Kortelainen, P., Downing, J.A., Middelburg, J.J. and Melack, J., 2007. Plumbing the global carbon cycle: Integrating inland waters into the terrestrial carbon budget. Ecosystems, 10(1): 171-184.
Conley, D.J., Schelske, C.L. and Stoermer, E.F., 1993. Modification of the Biogeochemical Cycle of Silica with Eutrophication. Marine Ecology-Progress Series, 101(1-2): 179-192.
Conley, D.J., 1997. Riverine contribution of biogenic silica to the oceanic silica budget. Limnology and Oceanography, 42(4): 774-777.
Conley, D.J., 2002. Terrestrial ecosystems and the global biogeochemical silica cycle. Global Biogeochemical Cycles, 16(4): 8.
Conley, D.J., Likens, G.E., Buso, D.C., Saccone, L., Bailey, S.W. and Johnson, C.E., 2008. Deforestation causes increased dissolved silicate losses in the Hubbard Brook Experimental Forest. Global Change Biology, 14(11): 2548-2554.
Cook, P.L.M., Aldridge, K.T., Lamontagne, S. and Brookes, J.D., 2010. Retention of nitrogen, phosphorus and silicon in a large semi-arid riverine lake system. Biogeochemistry, 99(1-3): 49-63.
Cooper, L.W., McClelland, J.W., Holmes, R.M., Raymond, P.A., Gibson, J.J., Guay, C.K. and Peterson, B.J., 2008. Flow-weighted values of runoff tracers (delta 18O, DOC, Ba, alkalinity) from the six largest Arctic rivers. Geophysical Research Letters, 35(18).
Cornelis, J.T., Ranger, J., Iserentant, A. and Delvaux, B., 2010. Tree species impact the terrestrial cycle of silicon through various uptakes. Biogeochemistry, 97(2-3): 231-245.
Creed, I.F., Beall, F.D., Clair, T.A., Dillon, P.J. and Hesslein, R.H., 2008. Predicting export of dissolved organic carbon from forested catchments in glaciated landscapes with shallow soils. Global Biogeochemical Cycles, 22(4).
Cuss, C.W., Guéguen, C., Hill, E. and Dillon, P.J., 2010. Spatio-temporal variation in the characteristics of dissolved organic matter in the streams of boreal forests: Impacts on modelled copper speciation. Chemosphere, 80(7): 764-770.
Danielsson, A., Papush, L. and Rahm, L., 2008. Alterations in nutrient limitations - Scenarios of a changing Baltic Sea. Journal of Marine Systems, 73(3-4): 263-283.

Davidson, E.A., Figueiredo, R.O., Markewitz, D. and Aufdenkampe, A.K., 2010. Dissolved CO2 in small catchment streams of eastern Amazonia: A minor pathway of terrestrial carbon loss. Journal of Geophysical Research G: Biogeosciences, 115(4).

Dawson, J.J.C., Hope, D., Cresser, M.S. and Billett, M.F., 1995. Downstream changes in free carbon dioxide in an upland catchment from Northeastern Scotland. Journal of Environmental Quality, 24(4): 699-706.

Dawson, J.J.C., Bakewell, C. and Billett, M.F., 2001. Is in-stream processing an important control on spatial changes in carbon fluxes in headwater catchments? Science of the Total Environment, 265(1-3): 153-167.

de Montety, V., Martin, J.B., Cohen, M.J., Foster, C. and Kurz, M.J., 2011. Influence of diel biogeochemical cycles on carbonate equilibrium in a karst river. Chemical Geology, 283(1-2): 31-43.

Demars, B.O.L., Russell Manson, J., Ólafsson, J.S., Gíslason, G.M., Gudmundsdóttir, R., Woodward, G., Reiss, J., Pichler, D.E., Rasmussen, J.J. and Friberg, N., 2011. Temperature and the metabolic balance of streams. Freshwater Biology, 56(6): 1106-1121.

Derry, L.A., Kurtz, A.C., Ziegler, K. and Chadwick, O.A., 2005. Biological control of terrestrial silica cycling and export fluxes to watersheds. Nature, 433(7027): 728-731.

Drever, J.I., 1997. The Geochemistry of Natural Waters. Prentice Hall, Upper Saddle River, NJ.

Driscoll, C.T., Lehtinen, M.D. and Sullivan, T.J., 1994. Modeling the acid-base chemistry of organic solutes in Adirondack, New York, lakes. Water Resources Research, 30(2): 297-306.

Duan, S.W., Bianchi, T.S., Shiller, A.M., Dria, K., Hatcher, P.G. and Carman, K.R., 2007. Variability in the bulk composition and abundance of dissolved organic matter in the lower Mississippi and Pearl rivers. Journal of Geophysical Research-Biogeosciences, 112(G2).

Dubois, K.D., Lee, D. and Veizer, J., 2010. Isotopic constraints on alkalinity, dissolved organic carbon, and atmospheric carbon dioxide fluxes in the Mississippi River. Journal of Geophysical Research-Biogeosciences, 115.

Dürr, H.H., Meybeck, M. and Dürr, S.H., 2005. Lithologic composition of the Earth's continental surfaces derived from a new digital map emphasizing riverine material transfer. Global Biogeochemical Cycles, 19(4).

Dürr, H.H., Meybeck, M., Hartmann, J., Laruelle, G.G. and Roubeix, V., 2009. Global spatial distribution of natural riverine silica inputs to the coastal zone. Biogeosciences Discussions, 6(1): 1345-1401.

Dürr, H.H., Meybeck, M., Hartmann, J., Laruelle, G.G. and Roubeix, V., 2011. Global spatial distribution of natural riverine silica inputs to the coastal zone. Biogeosciences.

Edmond, J.M., Palmer, M.R., Measures, C.I., Grant, B. and Stallard, R.F., 1995. The fluvial geochemistry and denudation rate of the Guayana Shield in Venezuela, Colombia, and Brazil. Geochimica Et Cosmochimica Acta, 59(16): 3301-3325.

Edmond, J.M., Palmer, M.R., Measures, C.I., Brown, E.T. and Huh, Y., 1996. Fluvial geochemistry of the eastern slope of the northeastern Andes and its foredeep in the drainage of the Orinoco in Colombia and Venezuela. Geochimica Et Cosmochimica Acta, 60(16): 2949-2974.

Einsele, G., Yan, J.P. and Hinderer, M., 2001. Atmospheric carbon burial in modern lake basins and its significance for the global carbon budget. Global and Planetary Change, 30(3-4): 167-195.

Environment Canada, 2009. Pacific and Yukon Water Quality Monitoring & Surveillance Program, http://www.waterquality.ec.gc.ca/EN/navigation/search.htm, accessed on 2009-05-25.

Environment Canada, 2010. Atlantic Environdat Water Quality Database., http://map.ns.ec.gc.ca/envirodat/root/main/en/extraction_page_e.asp, accessed on 2010-05-20.

FAO/IIASA/ISRIC/ISS-CAS/JRC, 2009. Harmonized World Soil Database (version 1.1). FAO, Rome.

Fekete, B.M., Vörösmarty, C.J. and Grabs, W., 2002. High-resolution fields of global runoff combining observed river discharge and simulated water balances. Global Biogeochemical Cycles, 16(3).

Feng, J.-X. and Kempe, S., 1987. The concentration and transportation of major ions in the lower Huanghe. In: E.T. Degens, S. Kempe and G. Weibin (Editors), Transport of Carbon and Minerals in Major World Rivers, Pt. 4. Mitt. Geol.-Paläont. Inst. Univ. Hamburg, SCOPE/UNEP Sonderband 64, Hamburg, pp. 161-170.

Ferris, J.A. and Lehman, J.T., 2007. Interannual variation in diatom bloom dynamics: Roles of hydrology, nutrient limitation, sinking, and whole lake manipulation. Water Research, 41(12): 2551-2562.

Finlay, J.C., 2003. Controls of streamwater dissolved inorganic carbon dynamics in a forested watershed. Biogeochemistry, 62(3): 231-252.

Fischer, G., Nachtergaele, F., Prieler, S., van Velthuizen, H.T., Verelst, L. and Wiberg, D., 2008. Global Agro-ecological Zones Assessment for Agriculture (GAEZ 2008), IIASA, Laxenburg, Austria and FAO, Rome, Italy.

Follett, R.F., 2001. Soil management concepts and carbon sequestration zin cropland soils. Soil and Tillage Research, 61(1-2): 77-92.

Fraysse, F., Pokrovsky, O.S. and Meunier, J.D., 2010. Experimental study of terrestrial plant litter interaction with aqueous solutions. Geochimica Et Cosmochimica Acta, 74(1): 70-84.

Frey, K.E. and McClelland, J.W., 2009. Impacts of permafrost degradation on arctic river biogeochemistry. Hydrological Processes, 23(1): 169-182.

Friedl, G., Teodoru, C. and Wehrli, B., 2004. Is the Iron Gate I reservoir on the Danube River a sink for dissolved silica? Biogeochemistry, 68(1): 21-32.

Fulweiler, R.W. and Nixon, S.W., 2005. Terrestrial vegetation and the seasonal cycle of dissolved silica in a southern New England coastal river. Biogeochemistry, 74(1): 115-130.

Gaillardet, J., Dupré, B., Louvat, P. and Allègre, C.J., 1999. Global silicate weathering and CO2 consumption rates deduced from the chemistry of large rivers. Chemical Geology, 159(1-4): 3-30.

Garcia-Esteves, J., Ludwig, W., Kerherve, P., Probst, J.L. and Lespinas, F., 2007. Predicting the impact of land use on the major element and nutrient fluxes in coastal Mediterranean rivers: The case of the Tet River (Southern France). Applied Geochemistry, 22(1): 230-248.

Garnier, J., Leporcq, B., Sanchez, N. and Philippon, X., 1999. Biogeochemical mass-balances (C, N, P, Si) in three large reservoirs of the Seine Basin (France). Biogeochemistry, 47(2): 119-146.

Garrels, R.M. and Mackenzie, F.T., 1971. Evolution of Sedimentary Rocks. W.W. Norton, New York.

Goolsby, D.A., Battaglin, W.A., Lawrence, G.B., Artz, R.S., Aulenbach, B.T., Hooper, R.P., Keeney, D.R. and Stensland, G.J., 1999. Flux and sources of nutrients in the Mississippi-Atchafalaya River basin. Topic 3 Rept. of the Integrated Assessment on Hypoxia in the Gulf of Mexico. NOAA Coastal Ocean Program Deicision Analysis Ser. No. 17. NOAA Coastal Ocean Program, Silver Spring, MD.

Goto, N., Iwata, T., Akatsuka, T., Ishikawa, M., Kihira, M., Azumi, H., Anbutsu, K. and Mitamura, O., 2007. Environmental factors which influence the sink of silica in the limnetic system of the large monomictic Lake Biwa and its watershed in Japan. Biogeochemistry, 84(3): 285-295.

Government of Alberta - Environment, River Network Station Water Quality Data, http://www.environment.gov.ab.ca/, accessed 2009-Apr-01.

Granskog, M.A., Macdonald, R.W., Mundy, C.J. and Barber, D.G., 2007. Distribution, characteristics and potential impacts of chromophoric dissolved organic matter (CDOM) in Hudson Strait and Hudson Bay, Canada. Continental Shelf Research, 27(15): 2032-2050.

Guéguen, C., Guo, L., Wang, D., Tanaka, N. and Hung, C.-C., 2006. Chemical Characteristics and Origin of Dissolved Organic Matter in the Yukon River. Biogeochemistry, 77(2): 139-155.

Harrison, J.A., Caraco, N. and Seitzinger, S.P., 2005a. Global patterns and sources of dissolved organic matter export to the coastal zone: Results from a spatially explicit, global model. Global Biogeochemical Cycles, 19(4).

Harrison, J.A., Seitzinger, S.P., Bouwman, A.F., Caraco, N.F., Beusen, A.H.W. and Vörösmarty, C.J., 2005b. Dissolved inorganic phosphorus export to the coastal zone: Results from a spatially explicit, global model. Global Biogeochemical Cycles, 19(4).

Hartmann, J., 2009. Bicarbonate-fluxes and CO2-consumption by chemical weathering on the Japanese Archipelago - Application of a multi-lithological model framework. Chemical Geology, 265(3-4): 237-271.

Hartmann, J., Jansen, N., Dürr, H.H., Kempe, S. and Köhler, P., 2009. Global CO2-consumption by chemical weathering: What is the contribution of highly active weathering regions? Global and Planetary Change, 69(4): 185-194.

Hartmann, J., Jansen, N., Dürr, H.H., Harashima, A., Okubo, K. and Kempe, S., 2010a. Predicting riverine dissolved silica fluxes to coastal zones from a hyperactive region and analysis of their first-order controls. International Journal of Earth Sciences, 99(1): 207-230.

Hartmann, J., Levy, J. and Kempe, S., 2010b. Increasing dissolved silica trends in the Rhine River: an effect of recovery from high P loads? Limnology: 1-11.

Henry, W., 1803. Experiments on the Quantity of Gases Absorbed by Water, at Different Temperatures, and under Different Pressures. Philosophical Transactions of the Royal Society of London, 93: 29-276.

Herman, J.S. and Lorah, M.M., 1987. CO2 outgassing and calcite precipitation in Falling Spring Creek, Virginia, U.S.A. Chemical Geology, 62(3-4): 251-262.

Hijmans, R.J., Cameron, S.E., Parra, J.L., Jones, P.G. and Jarvis, A., 2005. Very high resolution interpolated climate surfaces for global land areas. International Journal of Climatology, 25(15): 1965-1978.
Hoffer-French, K.J. and Herman, J.S., 1989. Evaluation of Hydrological and Biological Influences on CO_2 Fluxes from a Karst Stream. Journal of Hydrology, 108(1-4): 189-212.
Hofmann, A., Roussy, D. and Filella, M., 2002. Dissolved silica budget in the North basin of Lake Lugano. Chemical Geology, 182(1): 35-55.
Holland, H.D., 1978. The Chemsitry of the Atmosphere and Oceans. John Wiley & Sons, New York, Chichester, Brisbane, and Toronto.
Homann, P.S., Kapchinske, J.S. and Boyce, A., 2007. Relations of mineral-soil C and N to climate and texture: regional differences within the conterminous USA. Biogeochemistry, 85(3): 303-316.
Hornberger, G.M., Scanlon, T.M. and Raffensperger, J.P., 2001. Modelling transport of dissolved silica in a forested headwater catchment: the effect of hydrological and chemical time scales on hysteresis in the concentration-discharge relationship. Hydrological Processes, 15(10): 2029-2038.
Hruška, J., Laudon, H., Johnson, C.E., Köhler, S. and Bishop, K., 2001. Acid/base character of organic acids in a boreal stream during snowmelt. Water Resources Research, 37(4): 1043-1056.
Hruška, J., Köhler, S., Laudon, H. and Bishop, K., 2003. Is a universal model of organic acidity possible: Comparison of the acid/base properties of dissolved organic carbon in the boreal and temperate zones. Environmental Science and Technology, 37(9): 1726-1730.
Hudon, C., Morin, R., Bunch, J. and Harland, R., 1996. Carbon and nutrient output from the Great Whale River (Hudson Bay) and a comparison with other rivers around Quebec. Canadian Journal of Fisheries and Aquatic Sciences, 53(7): 1513-1525.
Humborg, C., Ittekkot, V., Cociasu, A. and VonBodungen, B., 1997. Effect of Danube River dam on Black Sea biogeochemistry and ecosystem structure. Nature, 386(6623): 385-388.
Humborg, C., Smedberg, E., Blomqvist, S., Mörth, C.M., Brink, J., Rahm, L., Danielsson, A. and Sahlberg, J., 2004. Nutrient variations in boreal and subarctic Swedish rivers: Landscape control of land-sea fluxes. Limnology and Oceanography, 49(5): 1871-1883.
Humborg, C., Pastuszak, M., Aigars, J., Siegmund, H., Mörth, C.M. and Ittekkot, V., 2006. Decreased silica land-sea fluxes through damming in the Baltic Sea catchment - significance of particle trapping and hydrological alterations. Biogeochemistry, 77(2): 265-281.
Humborg, C., Smedberg, E., Medina, M.R. and Mörth, C.M., 2008. Changes in dissolved silicate loads to the Baltic Sea - The effects of lakes and reservoirs. Journal of Marine Systems, 73(3-4): 223-235.
Humborg, C., Morth, C.M., Sundbom, M., Borg, H., Blenckner, T., Giesler, R. and Ittekkot, V., 2010. CO2 supersaturation along the aquatic conduit in Swedish watersheds as constrained by terrestrial respiration, aquatic respiration and weathering. Global Change Biology, 16(7): 1966-1978.
IPCC, 2007. Climate Change 2007: The Physical Science Basis; Contribution of Working Group I. Fourth Assessment Report of the Intergovernmental Panel on Climate Change. Cambridge University Press, Cambridge, 987 pp.
Jansen, N., Hartmann, J., Lauerwald, R., Dürr, H.H., Kempe, S., Loos, S. and Middelkoop, H., 2010. Dissolved Silica mobilization in the conterminous USA. Chemical Geology.
Jarvie, H.P., Neal, C.O., Smart, R., Owen, R., Fraser, D., Forbes, I. and Wade, A., 2001. Use of continuous water quality records for hydrograph separation and to assess short-term variability and extremes in acidity and dissolved carbon dioxide for the River Dee, Scotland. Science of the Total Environment, 265(1-3): 85-98.
Jenerette, G.D. and Lal, R., 2005. Hydrologic sources of carbon cycling uncertainty throughout the terrestrial-aquatic continuum. Global Change Biology, 11(11): 1873-1882.
Johnson, M.S., Lehmann, J., Riha, S.J., Krusche, A.V., Richey, J.E., Ometto, J. and Couto, E.G., 2008. CO(2) efflux from Amazonian headwater streams represents a significant fate for deep soil respiration. Geophysical Research Letters, 35(17).
Johnson, T.C. and Eisenreich, S.J., 1979. Silica in Lake Superior: mass balance considerations and a model for dynamic response to eutrophication. Geochimica et Cosmochimica Acta, 43: 77–91.
Johnston, C.A., Shmagin, B.A., Frost, P.C., Cherrier, C., Larson, J.H., Lambert, G.A. and Bridgham, S.D., 2008. Wetland types and wetland maps differ in ability to predict dissolved organic carbon concentrations in streams. Science of the Total Environment, 404(2-3): 326-334.
Jones, J.B. and Mulholland, P.J., 1998a. Carbon dioxide variation in a hardwood forest stream: An integrative measure of whole catchment soil respiration. Ecosystems, 1(2): 183-196.
Jones, J.B.J. and Mulholland, P.J., 1998b. Influence of drainage basin topography and elevation on carbon dioxide and methane supersaturation of stream water. Biogeochemistry, 40(1): 57-72.

Jones, J.B.J., Stanley, E.H. and Mulholland, P.J., 2003. Long-term decline in carbon dioxide supersaturation in rivers across the contiguous United States. Geophysical Research Letters, 30(10): 2-1.

Jonsson, A., Algesten, G., Bergstrom, A.K., Bishop, K., Sobek, S., Tranvik, L.J. and Jansson, M., 2007. Integrating aquatic carbon fluxes in a boreal catchment carbon budget. Journal of Hydrology, 334(1-2): 141-150.

Kelly, V.J., 2001. Influence of reservoirs on solute transport: a regional-scale approach. Hydrological Processes, 15(7): 1227-1249.

Kempe, S., 1979. Carbon in the freshwater cycle. In: B. Bolin, E.T. Degens, S. Kempe and P. Ketner (Editors), The Global Carbon Cycle. SCOPE Report 13. Wiley & Sons, Chichester, pp. 317-342.

Kempe, S., 1982. Long-term Records of CO2 Pressure Fluctuations in Fresh Waters. Mitt. Geol-Paläont. Inst. Univ. Hamburg. SCOPE/UNEP Sonderband, 52: 91-332.

Kempe, S., 1984. Sinks of the Anthropogenically Enhance Carbon-Cycle in Surface Fresh Waters. Journal of Geophysical Research-Atmospheres, 89(ND3): 4657-4676.

Kempe, S., 1985. Carbonate Chemistry and the Formation of Plitvice Lakes. In: E.T. Degens and S. Kempe (Editors), Transport of Carbon and Minerals in Major World Rivers, Pt. 3. Mitt. Geol-Paläont. Inst. Univ. Hamburg. SCOPE/UNEP Sonderband 58, Hamburg, pp. 351-383.

Kim, J.H., Ludwig, W., Schouten, S., Kerherve, P., Herfort, L., Bonnin, J. and Damste, J.S.S., 2007. Impact of flood events on the transport of terrestrial organic matter to the ocean: A study of the Tet River (SW France) using the BIT index. Organic Geochemistry, 38(10): 1593-1606.

Koch, R.W., Guelda, D.L. and Bukaveckas, P.A., 2004. Phytoplankton growth in the Ohio, Cumberland and Tennessee Rivers, USA: inter-site differences in light and nutrient limitation. Aquatic Ecology, 38(1): 17-26.

Köhler, S.J., Löfgren, S., Wilander, A. and Bishop, K., 2001. Validating a simple equation to predict and analyze organic anion charge in Swedish low ionic strength surface waters. Water, Air, and Soil Pollution, 130(1-4 II): 799-804.

Köhler, S.J., Hruška, J., Jönsson, J., Lövgren, L. and Lofts, S., 2002. Evaluation of different approaches to quantify strong organic acidity and acid-base buffering of organic-rich surface waters in Sweden. Water Research, 36(18): 4487-4496.

Ladouche, B., Probst, A., Viville, D., Idir, S., Baque, D., Loubet, M., Probst, J.L. and Bariac, T., 2001. Hydrograph separation using isotopic, chemical and hydrological approaches (Strengbach catchment, France). Journal of Hydrology, 242(3-4): 255-274.

Laruelle, G.G., Roubeix, V., Sferratore, A., Brodherr, B., Ciuffa, D., Conley, D.J., Dürr, H.H., Garnier, J., Lancelot, C., Phuong, Q.L.T., Meunier, J.D., Meybeck, M., Michalopoulos, P., Moriceau, B., Longphuirt, S.N., Loucaides, S., Papush, L., Presti, M., Ragueneau, O., Regnier, P., Saccone, L., Slomp, C.P., Spiteri, C. and Van Cappellen, P., 2009. Anthropogenic perturbations of the silicon cycle at the global scale: Key role of the land-ocean transition. Global Biogeochemical Cycles, 23.

Le Thi Phuong, Q., Billen, G., Garnier, J., Thery, S., Ruelland, D., Nghiem, X.A. and Chau, V.M., 2010. Nutrient (N, P, Si) transfers in the subtropical Red River system (China and Vietnam): Modelling and budget of nutrient sources and sinks. Journal of Asian Earth Sciences, 37(3): 259-274.

Lehner, B. and Döll, P., 2004. Development and validation of a global database of lakes, reservoirs and wetlands. Journal of Hydrology, 296(1-4): 1-22.

Lehner, B., Verdin, K. and Jarvis, A., 2008. New global hydrography derived from spaceborne elevation data. Eos, Transactions, AGU, 89(10): 93-94.

Lerman, A., Wu, L. and Mackenzie, F.T., 2007. CO2 and H2SO4 consumption in weathering and material transport to the ocean, and their role in the global carbon balance. Marine Chemistry, 106(1-2): 326-350.

Li, S.L., Calmels, D., Han, G., Gaillardet, J. and Liu, C.Q., 2008. Sulfuric acid as an agent of carbonate weathering constrained by delta C-13(DIC): Examples from Southwest China. Earth and Planetary Science Letters, 270(3-4): 189-199.

Livingston, D.A., 1963. Chemical composition of rivers and lakes. Geological Survey Professional Paper 440-G, Washington.

Ludwig, W., Amiotte-Suchet, P. and Probst, J.L., 1996a. River discharges of carbon to the world's oceans: Determining local inputs of alkalinity and of dissolved and particulate organic carbon. Comptes Rendus De L Academie Des Sciences Serie Ii Fascicule a-Sciences De La Terre Et Des Planetes, 323(12): 1007-1014.

Ludwig, W., Probst, J.L. and Kempe, S., 1996b. Predicting the oceanic input of organic carbon by continental erosion. Global Biogeochemical Cycles, 10(1): 23-41.

Ludwig, W., Amiotte-Suchet, P., Munhoven, G. and Probst, J.L., 1998. Atmospheric CO2 consumption by continental erosion: present-day controls and implications for the last glacial maximum. Global and Planetary Change, 17: 107-120.
Lynch, J.K., Beatty, C.M., Seidel, M.P., Jungst, L.J. and Degrandpre, M.D., 2010. Controls of riverine CO2 over an annual cycle determined using direct, high temporal resolution pCO2 measurements. Journal of Geophysical Research G: Biogeosciences, 115(3).
Macpherson, G.L., 2009. CO(2) distribution in groundwater and the impact of groundwater extraction on the global C cycle. Chemical Geology, 264(1-4): 328-336.
Mattsson, T., Kortelainen, P., Laubel, A., Evans, D., Pujo-Pay, M., Raike, A. and Conan, P., 2009. Export of dissolved organic matter in relation to land use along a European climatic gradient. Science of the Total Environment, 407(6): 1967-1976.
Mayorga, E., Seitzinger, S.P., Harrison, J.A., Dumont, E., Beusen, A.H.W., Bouwman, A.F., Fekete, B.M., Kroeze, C. and Van Drecht, G., 2010. Global Nutrient Export from WaterSheds 2 (NEWS 2): Model development and implementation. Environmental Modelling & Software, 25(7): 837-853.
Melzer, S.E., Knapp, A.K., Kirkman, K.P., Smith, M.D., Blair, J.M. and Kelly, E.F., 2010. Fire and grazing impacts on silica production and storage in grass dominated ecosystems. Biogeochemistry, 97(2-3): 263-278.
Meybeck, M., 1979. Concentrations des eaux fluviales en elements majeurs et apports en solution aux oceans. Revue de géologie dynamique et de géographie physique, 21(3): 191-246.
Meybeck, M., 1993. Riverine Transport of Atmospheric Carbon - Sources, Global Typology and Budget. Water Air and Soil Pollution, 70(1-4): 443-463.
Meybeck, M. and Ragu, A., 1995. GEMS/Water Contribution to the Global Register of River Inputs (GLORI), Provisional Final Report, UNEP/WHO/UNESCO, Geneva.
Meybeck, M., Dürr, H.H., Roussennac, S. and Ludwig, W., 2007. Regional seas and their interception of riverine fluxes to oceans. Marine Chemistry, 106(1-2): 301-325.
Millot, R., Gaillardet, J., Dupre, B. and Allegre, C.J., 2003. Northern latitude chemical weathering rates: Clues from the Mackenzie River Basin, Canada. Geochimica Et Cosmochimica Acta, 67(7): 1305-1329.
Miotke, F.-D., 1974. Carbon dioxide and the soil atmosphere. Abh. Karst- und Höhlenkunde : Reihe A, 9: 1-49.
Moore, T.R., Pare, D. and Boutin, R., 2008. Production of dissolved organic carbon in Canadian forest soils. Ecosystems, 11(5): 740-751.
Moosdorf, N., Hartmann, J. and Lauerwald, R., 2011a. Changes in dissolved silica mobilization into river systems draining North America until the period 2081-2100. Journal of Geochemical Exploration, 110(1): 31-39.
Moosdorf, N., Hartmann, J. and Lauerwald, R., 2011b. Compatibility of space and time for modeling fluvial HCO3 - fluxes - A comparison. Applied Geochemistry, 26(SUPPL.): S295-S297.
Moosdorf, N., Hartmann, J., Lauerwald, R., Hagedorn, B. and Kempe, S., 2011c. Bicarbonate fluxes and CO2 consumption by chemical weathering in North America. Submitted to Geochimica et Cosmochimica Acta. , 75: 7829-7854.
Mulholland, P.J., 1997. Dissolved organic matter concentration and flux in streams. Journal of the North American Benthological Society, 16(1): 131-141.
Mundy, C.J., Gosselin, M., Starr, M. and Michel, C., 2010. Riverine export and the effects of circulation on dissolved organic carbon in the Hudson Bay system, Canada. Limnology and Oceanography, 55(1): 315-323.
NASA/NGA, 2003. SRTM Water Body Data Product Specific Guidance, Version 2.0.
Officer, C.B. and Ryther, J.H., 1980. The Possible Importance of Silicon in Marine Eutrophication. Marine Ecology-Progress Series, 3(1): 83-91.
Oh, N.H. and Raymond, P.A., 2006. Contribution of agricultural liming to riverine bicarbonate export and CO2 sequestration in the Ohio River basin. Global Biogeochemical Cycles, 20(3).
Oliver, B.G., Thurman, E.M. and Malcolm, R.L., 1983. The contribution of humic substances to the acidity of colored natural waters. Geochimica Et Cosmochimica Acta, 47(11): 2031-2035.
Ontario - Ministry of the Environment, Provincial Stream Water Quality Monitoring Network (PWQMN). http://www.ene.gov.on.ca/en/publications/dataproducts/#PWQMN, accessed on 2009-03-31.
Park, P.K., Gordon, L.I., Hager, S.W. and Cissell, M.C., 1969. Carbon dioxide partial pressure in the Columbia River. Science, 166(3907): 867-868.
Parker, J.I., Conway, H.L. and Yaguchi, E.M., 1977. Dissolution of diatom frustules and recycling of amorphous silicon in Lake Michigan. Journal of the Fisheries Research Board of Canada, 34: 545–551.

Parkhurst, D.L. and Appelo, C.A.J., 1999. User's Guide to PHREEQC (v2) - A Computer Program for Speciation, Batch-reaction, One-dimensional Transport, and Inverse Geochemical Calculations. In: USGS (Editor), Water-Resour. Invest. Rep. 99-4259.

Pinol, J. and Avila, A., 1992. Streamwater pH, Alkalinity, pCO_2 and Discharge Relationships in Some Forested Mediterranean Catchments. Journal of Hydrology, 131(1-4): 205-225.

Preiner, S., Drozdowski, I., Schagerl, M., Schiemer, F. and Hein, T., 2008. The significance of side-arm connectivity for carbon dynamics of the River Danube, Austria. Freshwater Biology, 53(2): 238-252.

Ragueneau, O., Schultes, S., Bidle, K., Claquin, P. and La Moriceau, B., 2006. Si and C interactions in the world ocean: Importance of ecological processes and implications for the role of diatoms in the biological pump. Global Biogeochemical Cycles, 20(4).

Rasera, M., Ballester, M.V.R., Krusche, A.V., Salimon, C., Montebelo, L.A., Alin, S.R., Victoria, R.L. and Richey, J.E., 2008. Small rivers in the southwestern Amazon and their role in CO2 outgassing. Earth Interactions, 12.

Raymond, P.A. and Cole, J.J., 2001. Gas exchange in rivers and estuaries: Choosing a gas transfer velocity. Estuaries, 24(2): 312-317.

Raymond, P.A. and Oh, N.H., 2007. An empirical study of climatic controls on riverine C export from three major U.S. watersheds. Global Biogeochemical Cycles, 21(2).

Raymond, P.A., Oh, N.H., Turner, R.E. and Broussard, W., 2008. Anthropogenically enhanced fluxes of water and carbon from the Mississippi River. Nature, 451(7177): 449-452.

Roila, T., Kortelainen, P., David, M.B. and Makinen, I., 1994. Effect of Organic-Anions on Acid Neutralizing Capacity in Surface Waters. Environment International, 20(3): 369-372.

Royer, T.V. and David, M.B., 2005. Export of dissolved organic carbon from agricultural streams in Illinois, USA. Aquatic Sciences, 67(4): 465-471.

Schelske, C.L. and Stoermer, E.F., 1971. Eutrophication, Silica depletion, and predicted changes in algal quality in Lake Michigan. Science, 173(3995): 423-&.

Schelske, C.L., 1985. Biogeochemical Silica Mass Balances in Lake Michigan and Lake Superior. Biogeochemistry, 1(3): 197-218.

Scott, D.T., Baisden, W.T., Davies-Colley, R., Gomez, B., Hicks, D.M., Page, M.J., Preston, N.J., Trustrum, N.A., Tate, K.R. and Woods, R.A., 2006. Localized erosion affects national carbon budget. Geophysical Research Letters, 33(1).

Sferratore, A., Billen, G., Garnier, J. and Thery, S., 2005. Modeling nutrient (N, P, Si) budget in the Seine watershed: Application of the Riverstrahler model using data from local to global scale resolution. Global Biogeochemical Cycles, 19(4): -.

Sferratore, A., Garnier, J., Billen, G., Conley, D.J. and Pinault, S., 2006. Diffuse and point sources of silica in the seine river watershed. Environmental Science & Technology, 40(21): 6630-6635.

Sferratore, A., Billen, G., Garnier, J., Smedberg, E., Humborg, C. and Rahm, L., 2008. Modelling nutrient fluxes from sub-arctic basins: Comparison of pristine vs. dammed rivers. Journal of Marine Systems, 73(3-4): 236-249.

Shapiro, J. and Swain, E.B., 1983. Lessons From the Silica Decline in Lake-Michigan. Science, 221(4609): 457-459.

Smis, A., Van Damme, S., Struyf, E., Clymans, W., Van Wesemael, B., Frot, E., Vandevenne, F., Van Hoestenberghe, T., Govers, G. and Meire, P., 2010. A trade-off between dissolved and amorphous silica transport during peak flow events (Scheldt river basin, Belgium): impacts of precipitation intensity on terrestrial Si dynamics in strongly cultivated catchments. Biogeochemistry: 1-13.

Sobek, S., Tranvik, L.J. and Cole, J.J., 2005. Temperature independence of carbon dioxide supersaturation in global lakes. Global Biogeochemical Cycles, 19(2).

Sobek, S., Tranvik, L.J., Prairie, Y.T., Kortelainen, P. and Cole, J.J., 2007. Patterns and regulation of dissolved organic carbon: An analysis of 7,500 widely distributed lakes. Limnology and Oceanography, 52(3): 1208-1219.

Stelzer, R.S. and Likens, G.E., 2006. Effects of sampling frequency on estimates of dissolved silica export by streams: The role of hydrological variability and concentration-discharge relationships. Water Resources Research, 42(7): -.

Street-Perrott, F.A. and Barker, P.A., 2008. Biogenic silica: a neglected component of the coupled global continental biogeochemical cycles of carbon and silicon. Earth Surface Processes and Landforms, 33(9): 1436-1457.

Striegl, R.G., Dornblaser, M.M., Aiken, G.R., Wickland, K.P. and Raymond, P.A., 2007. Carbon export and cycling by the Yukon, Tanana, and Porcupine rivers, Alaska, 2001-2005. Water Resources Research, 43(2).

Struyf, E., Mörth, C.-M., Humborg, C. and Conley, D.J., 2010a. An enormous amorphous silica stock in boreal wetlands. J. Geophys. Res., 115(G4): G04008.
Struyf, E., Smis, A., Van Damme, S., Garnier, J., Govers, G., Van Wesemael, B., Conley, D.J., Batelaan, O., Frot, E., Clymans, W., Vandevenne, F., Lancelot, C., Goos, P. and Meire, P., 2010b. Historical land use change has lowered terrestrial silica mobilization. Nat Commun, 1(8): 129.
Stumm, W. and Morgan, J.J., 1981. Aquatic Chemistry. An Introduction Emphasizing Chemical Equilibria in Natural Waters. John Wiley & Sons, New York.
Syvitski, J.P.M., Vörösmarty, C.J., Kettner, A.J. and Green, P., 2005. Impact of humans on the flux of terrestrial sediment to the global coastal ocean. Science, 308(5720): 376-380.
Szramek, K. and Walter, L.M., 2004. Impact of carbonate precipitation on riverine inorganic carbon mass transport from a mid-continent, forested watershed. Aquatic Geochemistry, 10(1-2): 99-137.
Tans, P., 2011. NOAA/ESRL, www.esrl.noaa.gov/gmd/ccgg/trends/, accesessed on 2011-05-21.
Telmer, K. and Veizer, J., 1999. Carbon fluxes, pCO2 and substrate weathering in a large northern river basin, Canada: Carbon isotope perspectives. Chemical Geology, 159(1-4): 61-86.
Teodoru, C.R., Del Giorgio, P.A., Prairie, Y.T. and Camire, M., 2009. Patterns in pCO2 in boreal streams and rivers of northern Quebec, Canada. Global Biogeochemical Cycles, 23(2).
Tipping, E., Marker, A.F.H., Butterwick, C., Collett, G.D., Cranwell, P.A., Ingram, J.K.G., Leach, D.V., Lishman, J.P., Pinder, A.C., Rigg, E. and Simon, B.M., 1997. Organic carbon in the Humber rivers. Science of the Total Environment, 194: 345-355.
Tobias, C. and Böhlke, J.K., 2011. Biological and geochemical controls on diel dissolved inorganic carbon cycling in a low-order agricultural stream: Implications for reach scales and beyond. Chemical Geology.
Treguer, P., Nelson, D.M., Vanbennekom, A.J., Demaster, D.J., Leynaert, A. and Queguiner, B., 1995. The Silica Balance in the World Ocean - A Reestimate. Science, 268(5209): 375-379.
Triplett, L.D., Engstrom, D.R., Conley, D.J. and Schellhaass, S.M., 2008. Silica fluxes and trapping in two contrasting natural impoundments of the upper Mississippi River. Biogeochemistry, 87(3): 217-230.
Turner, R.E., Rabalais, N.N., Justic, D. and Dortch, Q., 2003. Global patterns of dissolved N, P and Si in large rivers. Biogeochemistry, 64(3): 297-317.
USGS, National Water Information System (NWIS), http://waterdata.usgs.gov/nwis, accessed on 2009-06-24.
Van Bennekom, A.J. and Salomons, W., 1981. Pathways of nutrients and organic matter from land to ocean through rivers. In: J.M. Martin, J.D. Burton and D. Eisma (Editors), River Inputs to Ocean Systems. UNEP/UNESCO, Rome, pp. 33-51.
Van Dokkum, H.P., Hulskotte, J.H.J., Kramer, K.J.M. and Wilmot, J., 2004. Emission, fate and effects of soluble silicates (waterglass) in the aquatic environment. Environmental Science & Technology, 38(2): 515-521.
Vörösmarty, C.J., Meybeck, M., Fekete, B., Sharma, K., Green, P. and Syvitski, J.P.M., 2003. Anthropogenic sediment retention: major global impact from registered river impoundments. Global and Planetary Change, 39(1-2): 169-190.
Wang, F.S., Wang, Y., Zhang, J., Xu, H. and Wei, X., 2007. Human impact on the historical change of CO2 degassing flux in River Changjiang. Geochemical Transactions, 8.
Wetzel, R.G., 2001. Limnology. Lake and River Ecosystems. 3rd edition. Academic Press, San Diego & London.
Williams, M., Hopkinson, C., Rastetter, E., Vallino, J. and Claessens, L., 2005. Relationships of land use and stream solute concentrations in the Ipswich River basin, northeastern Massachusetts. Water Air and Soil Pollution, 161(1-4): 55-74.
Worrall, F., Harriman, R., Evans, C.D., Watts, C.D., Adamson, J., Neal, C., Tipping, E., Burt, T., Grieve, I., Monteith, D., Naden, P.S., Nisbet, T., Reynolds, B. and Stevens, P., 2004. Trends in dissolved organic carbon in UK rivers and lakes. Biogeochemistry, 70(3): 369-402.
Worrall, F. and Burt, T., 2005. Reconstructing long-term records of dissolved CO2. Hydrological Processes, 19(9): 1791-1806.
Worrall, F. and Burt, T., 2007. Flux of dissolved organic carbon from UK rivers. Global Biogeochemical Cycles, 21(1).
Worrall, F., Guilbert, T. and Besien, T., 2007. The flux of carbon from rivers: the case for flux from England and Wales. Biogeochemistry, 86(1): 63-75.
Xu, Z.F. and Liu, C.Q., 2010. Water geochemistry of the Xijiang basin rivers, South China: Chemical weathering and CO2 consumption. Applied Geochemistry, 25(10): 1603-1614.

Yang, C., Telmer, K. and Veizer, J., 1996. Chemical dynamics of the ''St Lawrence'' riverine system: delta D-H2O, delta O-18(H2O), delta C-13(DIC), delta S-34(sulfate), and dissolved Sr-87/Sr-86. Geochimica Et Cosmochimica Acta, 60(5): 851-866.
Zeng, F.W. and Masiello, C.A., 2010. Sources of CO2 evasion from two subtropical rivers in North America. Biogeochemistry, 100(1): 211-225.

7 Acknowledgements

First of all, I want to thank my supervisor Jens Hartmann for all his support. He always found the time to help me with any question or problem. I thank Nils Moosdorf for all the good times we had in our office. He was a constant partner in discussion. I greatly benefited from his IT skills. Stephan Kempe, my second supervisor, is thanked for sharing his long-standing experience and knowledge.

Tom Jäppinen, Thorben Amann, and Andreas Weiss are acknowledged for being pleasant-natured colleagues and, of course, for all their helpful advices. Hans Dürr and his colleagues at Utrecht University are thanked for their hospitality during my stay as guest scientist in winter 2008/2009.

StatSoft is thanked for providing a student license for Statistica®, one of the main software packages I used for the analyses in this thesis. The DFG is thanked for funding my position. This really meant a lot to me. KlimaCampus and SiCCS are thanked for their financial support and for providing a platform for scientific exchange and social networking.

8 Appendix

A Maps of selected geo-spatial data sets used for analyses

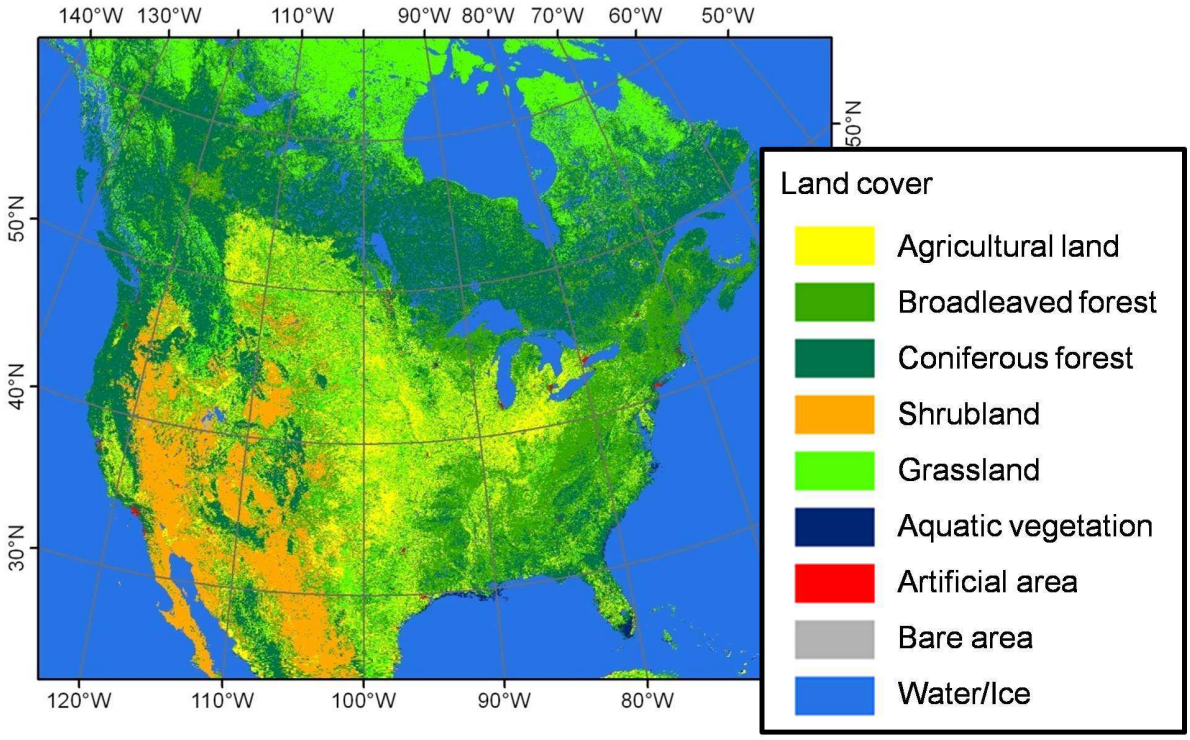

Fig. A.1: Land cover after Globcover (Arino et al., 2007).

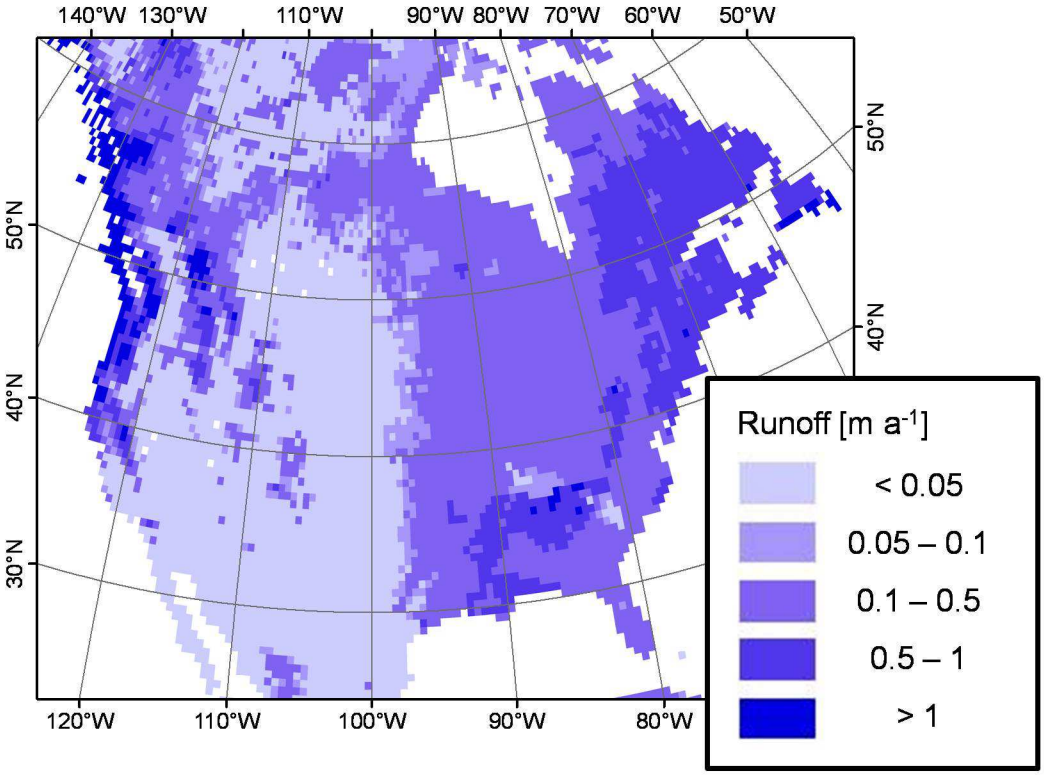

Fig. A.2: UNH/GRDC runoff (Fekete et al., 2002).

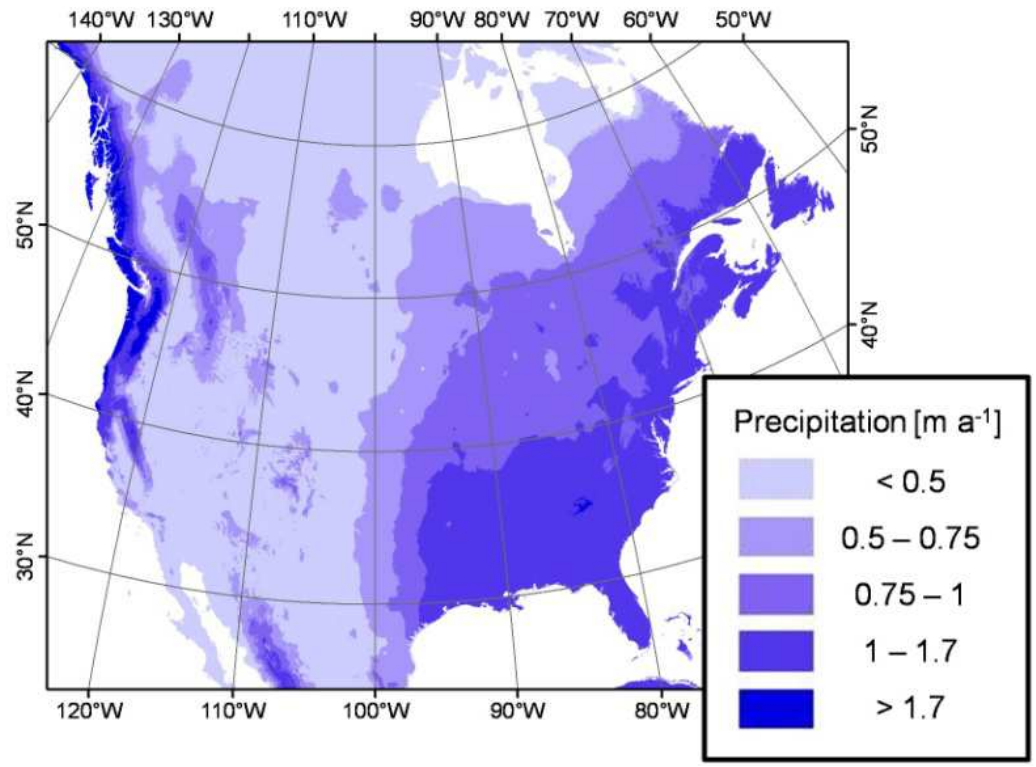

Fig. A.3: Mean annual precipitation after Worldclim (Hijmans et al., 2005).

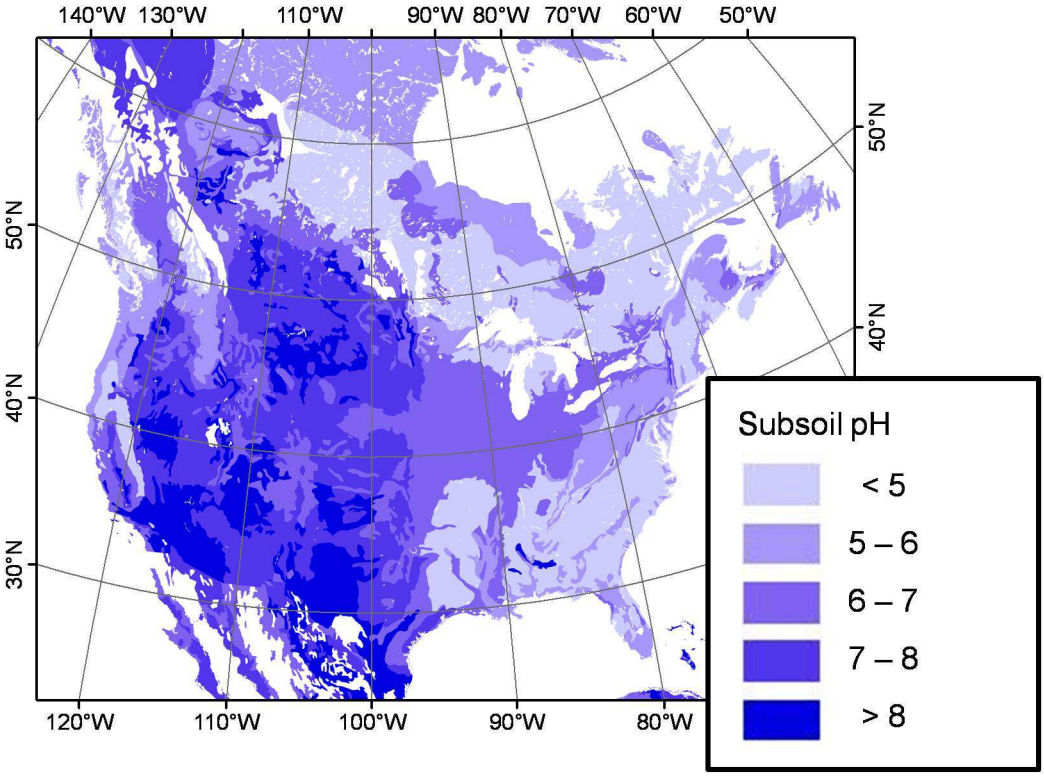

Fig. A.4: Subsoil pH after HSWD (FAO/IIASA/ISRIC/ISS-CAS/JRC, 2009).

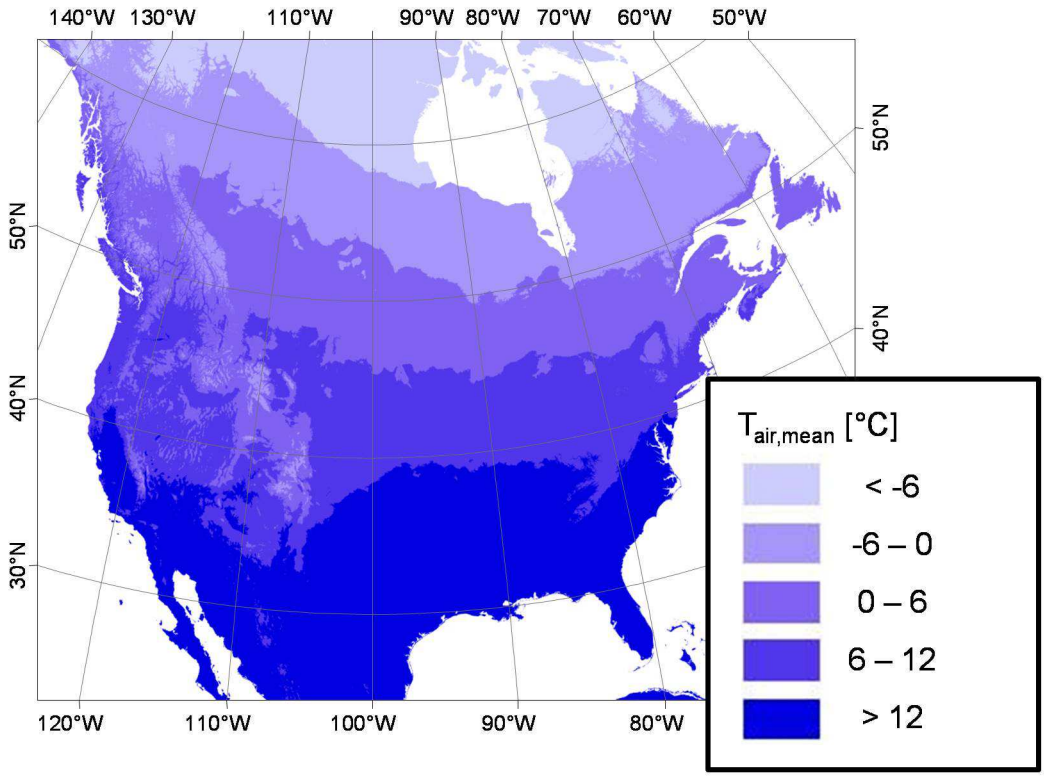

Fig. A.5: Mean air temperature after Worldclim (Hijmans et al., 2005).

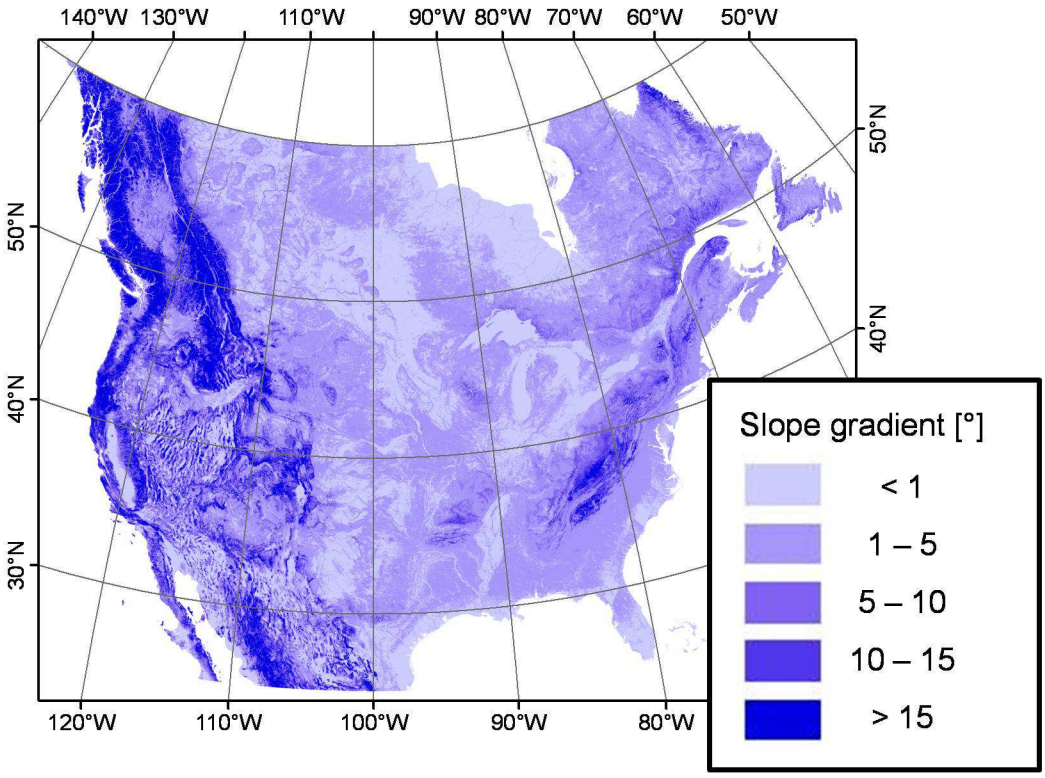

Fig. A.6: Slope gradient derived from SRTM DEM 3'' (Jarvis et al., 2006).

B Properties of catchments used for the spatially explicit assessment of DSi retention

Table B.1: Average physiographic properties derived from different geodata sets, averages of DSi concentrations, calculated DSi fluxes, and estimated DSi mobilization. For the monitored area, statistics of estimated DSi mobilization, runoff, and air temperature refer to the raster data sets.

Subset of catchments (c.)	N	Mean	Min	Max	10th Perc.	90th Perc.	Std.Dev.
			Catchment size [km²]				
Training c.	140	3,963	8.45	37,891	113	11,335	7,583
Non-training c.	484	54,003	0.34	2,914,988	110	100,737	201,079
			Areal proportion of lakes				
Training c.	140	0.002	0	0.03	0	0.004	0.004
Non-training c.	484	0.012	0	0.439	0	0.023	0.035
Monitored area		0.048					
			Runoff [mm a^{-1}]				
Training c.	140	340	0	2308	41	626	301
Non-training c.	484	308	0	1793	12	657	267
Monitored area		217	0	2681	0	545	261
			Mean DSi concentration [µmol L^{-1}]				
Training c.	140	159	24	781	70	244	108
Non-training c.	484	162	8	761	77	305	107
Monitored area		109[a]					
			$f_{DSi,calc}$ [t SiO_2 $km^{-2}a^{-1}$]				
Training c.	140	2.61	0	19.98	0.49	4.35	2.64
Non-training c.	484	2.5	0	26.98	0.11	5.41	2.82
Monitored area		1.42[b]					
			$f_{DSi,mob}$ [t SiO_2 $km^{-2}a^{-1}$]				
Training c.	140	2.57	0	19.03	0.48	4.01	2.6
Non-training c.	484	2.47	0	48.87	0.13	4.39	3.42
Monitored area		1.63	0	82.27	0	3.812	2.96
			Mean air temperature [℃]				
Training c.	140	9.4	-2.3	20.5	2.0	18.1	5.5
Non-training c.	484	10.2	-0.9	22.4	4.5	17.2	4.7
Monitored area		10.0	-7.9	23.4	3.8	17.4	5.2

[a]was derived as flux weighted average of DSi concentration of the 161 non-overlapping catchments
[b]was derived as catchment area weighted average of $f_{DSi,calc}$ of the 161 non-overlapping catchments

Table B.2: Average lithologic and land cover composition of different sets of catchments.

Subset of catchments (c.)	Training catchments		Non-training catchments		Monitored area
N	140		484		
	Mean	Std.	Mean	Std.	Mean
	Lithology				
Unconsolidated sediments	0.21	0.34	0.21	0.29	0.24
Siliciclastic sedimentary rocks	0.34	0.35	0.31	0.29	0.33
Mixed sedimentary rocks	0.08	0.17	0.07	0.13	0.08
Carbonate rocks	0.19	0.29	0.16	0.26	0.13
Metamorphic rocks	0.08	0.19	0.11	0.22	0.06
Basic and intermediate plutonics	0.00	0.02	0.01	0.03	0.01
Acid plutonics	0.05	0.16	0.05	0.12	0.04
Basic volcanics and pyroclastic rocks	0.04	0.12	0.04	0.11	0.04
Acid and intermediate volcanics	0.02	0.09	0.03	0.09	0.03
	Land cover				
Agricultural land	0.18	0.21	0.18	0.18	0.20
Broadleaved forest	0.35	0.28	0.34	0.24	0.31
Coniferous forest	0.26	0.3	0.23	0.25	0.16
Shrubland	0.03	0.08	0.07	0.13	0.10
Grassland	0.17	0.15	0.16	0.12	0.18
Urban area	0.00	0.00	0.01	0.04	0.00
Other land cover than listed above	0.00	0.01	0.02	0.04	0.05

Table B.3: Correlation matrix of catchment parameters. Correlations which are significant to the p=0.05-level are highlighted in bold. Non-significant correlations are in italic. Refers to set of all 624 catchments considered in this study.

	Catchment size	$\log_{10}$(Catchment size)	Mean air temp. ($T_{air,mean}$)	Acricultural land (A_{AL})	Broad-leaved forest (A_{BF})	Coniferous forest (A_{CF})	Shrub-land (A_{SL})	Grass-land (A_{HV})	Artificial areas (A_{AA})	Lake area proportion	Runoff (q)	Avg. DSi conc.	$f_{DSi,calc}$	$f_{DSi,mob}$	r_{DSi}
Catchment size	*1.00*	**0.44**	*-0.08*	*0.06*	*-0.06*	**-0.09**	**0.13**	**0.08**	*-0.05*	**0.16**	**-0.15**	*-0.02*	**-0.13**	**-0.10**	*0.02*
$\log_{10}$(Catchment size)		*1.00*	**-0.09**	**0.10**	**-0.10**	**-0.15**	**0.30**	**0.12**	**-0.22**	**0.21**	**-0.36**	**0.13**	**-0.25**	**-0.26**	*-0.07*
Mean air temp. ($T_{air,mean}$)			*1.00*	**0.11**	**0.19**	**-0.25**	**-0.21**	**0.17**	**0.16**	**-0.14**	*-0.01*	**-0.13**	*-0.06*	*-0.03*	**0.15**
Acricultural land (A_{AL})				*1.00*	**-0.39**	**-0.57**	**-0.14**	**0.67**	**-0.11**	**-0.10**	**-0.33**	*0.06*	**-0.26**	**-0.24**	*0.01*
Broadleaved forest (A_{BF})					*1.00*	**-0.38**	**-0.30**	**-0.25**	**-0.14**	*-0.03*	**0.24**	**-0.34**	*-0.06*	*0.01*	**0.19**
Coniferous forest (A_{CF})						*1.00*	*0.03*	**-0.60**	**0.08**	*0.07*	**0.36**	**0.12**	**0.50**	**0.41**	**-0.14**
Shrubland (A_{SL})							*1.00*	**-0.19**	*-0.07*	*-0.06*	**-0.38**	**0.34**	**-0.20**	**-0.24**	**-0.15**
Grassland (A_{HV})								*1.00*	*-0.03*	**-0.12**	**-0.41**	*0.07*	**-0.35**	**-0.32**	*0.01*
Artificial area (A_{AA})									*1.00*	*-0.02*	*0.04*	*-0.08*	*0.00*	*0.04*	**0.09**
Lake area proportion										*1.00*	*0.02*	*-0.08*	*0.00*	*0.01*	*0.04*
Runoff (q)											*1.00*	**-0.30**	**0.75**	**0.75**	*0.06*
Avg. DSi conc.												*1.00*	**0.14**	*-0.08*	**-0.68**
$f_{DSi,calc}$													*1.00*	**0.83**	**-0.27**
$f_{DSi,mob}$														*1.00*	**0.08**
r_{DSi}															*1.00*

C Properties of catchments used for the spatially explicit assessment of in-river DOC loss

Table C.1: Statistical distribution of parameters within the small and the large catchments, and the spatially explicit extrapolation raster.

Parameter	Set	Mean	Median	Min	Max	10th Perc.	90th Perc.	Std.
q [mma^{-1}]	small c.	536	496	0	2,543	78	1,071	387
	large c.	297	268	0	1,035	24	642	228
	raster	306		0	4,738			391
s [°]	small c.	5.17	2.66	0.49	26.61	1.10	15.55	5.61
	large c.	6.63	6.41	0.68	22.63	1.12	12.50	4.79
	raster	4.21		0.00	61.82			5.96
A_{BF} [1]	small c.	0.34	0.28	0.00	0.97	0.02	0.75	0.28
	large c.	0.28	0.19	0.03	0.88	0.08	0.67	0.22
	raster	0.25		0.00	1.00			0.33
A_{CF} [1]	small c.	0.32	0.19	0.00	1.00	0.00	0.85	0.33
	large c.	0.30	0.23	0.00	0.92	0.01	0.69	0.26
	raster	0.31		0.00	1.00			0.41
A_{HV} [1]	small c.	0.14	0.11	0.00	0.47	0.00	0.32	0.13
	large c.	0.17	0.14	0.00	0.49	0.04	0.33	0.12
	raster	0.15		0.00	1.00			0.26
A_{WL} [1]	small c.	0.09	0.00	0.00	0.53	0.00	0.38	0.15
	large c.	0.08	0.03	0.00	0.39	0.00	0.33	0.12
	raster	0.15		0.00	1.00			0.25
DOC conc. [mg C L^{-1}]	small c.	4.53	3.83	0.60	17.59	1.32	9.03	3.20
	large c.	4.59	3.90	0.58	18.11	1.65	7.87	3.11
$f_{DOC,calc}$ [t C km^{-2}a^{-1}]	small c.	2.24	1.42	0.00	13.38	0.24	5.07	2.15
	large c.	1.09	0.83	0.00	4.87	0.14	2.35	0.92
$f_{DOC,mod}$[S] [t C km^{-2}a^{-1}]	small c.	2.29	2.03	0.00	5.44	0.56	4.34	1.40
	large c.	1.35	1.24	0.02	3.96	0.38	2.42	0.82
	raster	1.82		0.00	17.61			1.61
$f_{DOC,mod}$[L] [t C km^{-2}a^{-1}]	small c.	1.88	1.70	0.01	5.51	0.45	3.38	1.11
	large c.	1.12	1.13	0.02	3.08	0.31	1.99	0.68
	raster	1.40		0.00	15.24			1.61

D Properties of catchments used for the spatially explicit assessment of the carbonate system of North American rivers

Table D.1: Correlation matrix of main predictors, parameters of the carbonate system and DOC concentration vs. catchment properties. n=1,120, with the exception of correlations with subsoil pH (n=1,119) and correlations with DOC (n=717). Pearson correlation coefficients which are statistically significant (p<0.05) are highlighted in red. Substantial correlations of r>0.3 are further high-lighted in bold letters and with yellow background.

	SC	P	$T_{air,mean}$	ln(s [°])	A_{AL}	S_pH	PCO_2	$pPCO_2$	Alkalinity	pH	DOC
log_{10}(catchment size)	-0.07	**-0.40**	-0.04	0.02	0.12	0.21	-0.12	0.09	0.19	**0.33**	0.11
Metamorphic rocks (MT)	-0.17	0.15	-0.02	0.17	-0.29	**-0.30**	0.03	-0.02	**-0.32**	-0.23	-0.07
Acid plutonics (PA)	-0.21	-0.05	-0.23	0.19	-0.25	-0.14	-0.07	0.09	-0.20	-0.17	0.03
Basic plutonics (PB)	-0.09	0.07	-0.08	0.00	-0.13	-0.12	-0.02	0.02	-0.14	-0.10	-0.01
Intermediate plutonics (PI)	-0.10	-0.05	-0.19	0.07	-0.15	-0.11	-0.07	0.09	-0.06	0.02	0.05
Pyroclastics (PY)	-0.07	-0.10	-0.14	0.18	-0.08	0.07	-0.10	0.15	-0.01	0.09	-0.01
Carbonate rocks (SC)	1.00	0.05	0.18	-0.24	**0.36**	0.10	0.01	-0.08	**0.32**	0.26	-0.10
Mixed sedimentary rocks (SM)	-0.03	0.06	-0.25	-0.07	0.03	-0.06	-0.04	-0.00	0.01	-0.09	-0.03
Siliciclastic sedimentary rocks (SS)	-0.20	-0.08	-0.12	0.16	0.02	0.06	-0.15	0.12	0.08	0.17	-0.07
Unconsolidated sediments (SU)	-0.23	-0.01	**0.48**	**-0.34**	0.15	0.15	**0.36**	**-0.31**	0.04	-0.15	**0.32**
Acid volcanics (VA)	-0.09	-0.22	-0.12	0.13	-0.03	0.18	-0.11	0.16	0.04	0.13	-0.03
Basic volcanics (VB)	-0.16	-0.05	-0.20	0.17	-0.14	0.07	-0.17	0.22	-0.04	0.10	-0.09
Lake area proportion	-0.11	0.04	-0.17	-0.10	-0.14	-0.21	-0.05	0.04	-0.13	-0.12	0.07
Runoff (q)	-0.10	**0.75**	-0.17	0.24	**-0.38**	**-0.58**	-0.04	0.06	**-0.58**	**-0.48**	-0.26
Precipitation (P)	0.05	1.00	**0.33**	-0.10	-0.22	**-0.68**	0.27	**-0.30**	**-0.61**	**-0.65**	-0.11
Mean air temperature ($T_{air,mean}$)	0.18	**0.33**	1.00	**-0.48**	0.21	-0.07	**0.46**	**-0.53**	-0.04	-0.24	0.24
Slope gradient (S) [°]	-0.19	-0.05	**-0.47**	**0.91**	**-0.44**	0.00	**-0.38**	**0.52**	-0.20	0.18	**-0.49**
ln(s [°])	-0.24	-0.10	**-0.48**	1.00	**-0.54**	-0.04	**-0.43**	**0.56**	-0.22	0.17	**-0.55**
Agricultural land (A_{AL})	**0.36**	-0.22	0.21	**-0.54**	1.00	**0.42**	0.07	-0.15	**0.55**	**0.34**	0.20
Broadleafed forest (A_{BF})	0.00	**0.33**	0.22	-0.14	-0.28	**-0.44**	0.16	-0.24	-0.27	**-0.32**	0.02
Coniferous forest (A_{CF})	-0.29	0.16	**-0.33**	**0.56**	**-0.59**	-0.21	-0.14	0.26	**-0.40**	-0.18	-0.24
Shrub lands (A_{SL})	-0.16	**-0.52**	-0.10	0.21	-0.08	**0.45**	-0.20	0.26	0.24	**0.32**	0.02
Grass lands (A_{HV})	**0.32**	-0.23	0.14	**-0.40**	**0.61**	**0.40**	0.09	-0.15	**0.47**	0.28	0.15
Artificial areas (A_{AA})	0.05	0.07	0.10	-0.10	-0.08	0.00	0.06	-0.07	-0.02	-0.03	0.09
Wetlands (A_{WL})	-0.13	0.14	-0.02	**-0.35**	-0.10	-0.25	0.26	-0.26	-0.14	-0.29	**0.38**
Population density (1990)	0.03	0.11	0.13	-0.13	-0.10	-0.07	0.09	-0.11	-0.05	-0.06	0.06
Topsoil C org.	-0.08	0.17	-0.29	-0.02	-0.22	-0.22	-0.03	-0.00	-0.21	-0.24	0.14
Topsoil $CaCO_3$	-0.11	**-0.56**	0.01	0.07	0.15	**0.69**	-0.16	0.18	**0.47**	**0.40**	0.03
Subsoil $CaCO_3$	-0.13	**-0.65**	0.00	0.04	0.19	**0.79**	-0.17	0.18	**0.55**	**0.47**	0.07
Topsoil pH	0.11	**-0.67**	-0.02	-0.03	**0.42**	**0.98**	-0.18	0.18	**0.70**	**0.61**	0.03
Subsoil pH (S_pH)	0.10	**-0.68**	-0.07	-0.04	**0.42**	1.00	-0.21	0.20	**0.71**	**0.60**	0.04
DOC	-0.10	-0.11	0.24	**-0.55**	0.20	0.04	**0.40**	**-0.45**	**0.15**	-0.15	1.00

Table D.2: Correlation matrix of main predictors, parameters of the carbonate system and DOC concentration vs. catchment properties for P < 1.7 m a^{-1} (see text). n=1,102, with the exception of correlations with subsoil pH (n=1,101) and correlations with DOC (n=707). Pearson correlation coefficients which are statistically significant (p<0.05) are highlighted in red. Substantial correlations of r>0.3 are further highlighted in bold letters and with yellow background.

	SC	P	$T_{air,mean}$	ln(s [°])	A_{AL}	S_pH	PCO_2	$pPCO_2$	Alkalinity	pH	DOC
log_{10}(catchment size)	-0.08	**-0.39**	-0.05	0.04	0.11	0.20	-0.13	0.11	0.18	**0.33**	0.10
Metamorphic rocks (MT)	-0.18	0.20	-0.03	0.19	-0.30	**-0.31**	0.03	-0.01	**-0.33**	-0.23	-0.08
Acid plutonics (PA)	-0.21	-0.04	-0.24	0.20	-0.26	-0.14	-0.07	0.09	-0.21	-0.17	0.02
Basic plutonics (PB)	-0.09	0.08	-0.08	0.01	-0.14	-0.12	-0.02	0.02	-0.14	-0.10	-0.01
Intermediate plutonics (PI)	-0.10	-0.06	-0.19	0.08	-0.15	-0.11	-0.06	0.09	-0.06	0.02	0.06
Pyroclastics (PY)	-0.07	-0.10	-0.14	0.19	-0.08	0.07	-0.10	0.15	-0.01	0.08	-0.01
Carbonate rocks (SC)	1.00	0.09	0.17	-0.23	**0.36**	0.09	0.00	-0.08	**0.32**	0.25	-0.10
Mixed sedimentary rocks (SM)	-0.03	0.09	-0.25	-0.05	0.02	-0.06	-0.05	0.01	0.00	-0.09	-0.04
Siliciclastic sedimentary rocks (SS)	-0.20	-0.11	-0.12	0.16	0.02	0.07	-0.15	0.12	0.09	0.17	-0.07
Unconsolidated sediments (SU)	-0.23	0.00	**0.48**	**-0.34**	0.15	0.15	**0.36**	**-0.31**	0.03	-0.15	**0.32**
Acid volcanics (VA)	-0.09	-0.23	-0.12	0.14	-0.03	0.18	-0.11	0.16	0.03	0.13	-0.03
Basic volcanics (VB)	-0.16	-0.21	-0.21	0.13	-0.12	0.10	-0.16	0.21	0.00	0.13	-0.05
Lake area proportion	-0.11	0.06	-0.17	-0.10	-0.15	-0.21	-0.05	0.05	-0.14	-0.12	0.07
Runoff (q)	-0.08	**0.70**	-0.17	0.18	**-0.38**	**-0.63**	-0.01	0.02	**-0.60**	**-0.53**	-0.24
Precipitation (P)	0.09	1.00	**0.39**	-0.21	-0.20	**-0.73**	**0.34**	**-0.39**	**-0.62**	**-0.71**	-0.07
Mean air temperature ($T_{air,mean}$)	0.17	**0.39**	1.00	**-0.48**	0.21	-0.07	**0.46**	**-0.53**	-0.05	-0.24	0.23
Slope gradient (s) [°]	-0.18	-0.20	**-0.48**	**0.91**	**-0.43**	0.01	**-0.38**	**0.52**	-0.17	0.20	**-0.48**
ln(s [°])	-0.23	-0.21	**-0.48**	1.00	**-0.53**	-0.03	**-0.43**	**0.56**	-0.21	0.19	**-0.54**
Agricultural land (A_{AL})	**0.36**	-0.20	0.21	**-0.53**	1.00	**0.42**	0.06	-0.14	**0.55**	**0.33**	0.20
Broadleafed forest (A_{BF})	-0.01	**0.45**	0.22	-0.11	**-0.30**	**-0.46**	0.15	-0.23	-0.30	**-0.33**	0.00
Coniferous forest (A_{CF})	-0.29	0.03	**-0.33**	**0.54**	**-0.59**	-0.20	-0.12	0.24	**-0.38**	-0.18	-0.22
Shrub lands (A_{SL})	-0.17	**-0.56**	-0.10	0.23	-0.08	**0.45**	-0.21	0.27	0.23	**0.32**	0.01
Grass lands (A_{HV})	**0.31**	-0.19	0.14	**-0.38**	**0.60**	**0.40**	0.08	-0.14	**0.46**	0.28	0.13
Artificial areas (A_{AA})	0.05	0.09	0.10	-0.10	-0.08	0.00	0.06	-0.07	-0.02	-0.03	0.08
Wetlands (A_{WL})	-0.13	0.18	-0.02	**-0.35**	-0.11	-0.26	0.25	-0.26	-0.15	-0.29	**0.37**
Population density (1990)	0.03	0.14	0.13	-0.13	-0.10	-0.07	0.08	-0.11	-0.05	-0.06	0.06
Topsoil C org.	-0.07	0.14	-0.29	-0.05	-0.21	-0.22	-0.03	-0.01	-0.20	-0.24	0.15
Topsoil $CaCO_3$	-0.12	**-0.60**	0.01	0.08	0.15	**0.69**	-0.17	0.19	**0.46**	**0.40**	0.02
Subsoil $CaCO_3$	-0.13	**-0.69**	0.00	0.06	0.19	**0.79**	-0.18	0.19	**0.55**	**0.46**	0.06
Topsoil pH	0.11	**-0.72**	-0.02	-0.03	**0.42**	**0.98**	-0.19	0.19	**0.70**	**0.61**	0.02
Subsoil pH (S_pH)	0.09	**-0.73**	-0.07	-0.03	**0.42**	1.00	-0.22	0.21	**0.71**	**0.60**	0.03
DOC	-0.10	-0.07	0.23	**-0.54**	0.20	0.03	**0.40**	**-0.44**	0.14	-0.16	1.00

Table D.3: Statistical distribution of parameters within the subsets of small, medium, and large training catchments.

	small catchments					medium catchments					large catchments				
	N	**Mean**	**10th perc.**	**90th perc.**	**Std.**	**N**	**Mean**	**10th perc.**	**90th perc.**	**Std.**	**N**	**Mean**	**10th perc.**	**90th perc.**	**Std.**
catch. size [10^3 km^2]	356	0.31	0.04	0.77	0.27	353	4.21	1.35	8.45	2.59	393	133	12.0	219	397
s [‰]	356	5.5	1.0	16.1	6.0	353	5.7	1.1	12.8	5.2	393	5.3	1.2	11.4	4.3
P[m a^{-1}]	356	1.0	0.6	1.4	0.3	353	0.9	0.4	1.4	0.3	393	0.7	0.4	1.2	0.3
q [m a^{-1}]	356	0.5	0.0	1.0	0.4	353	0.4	0.0	0.7	0.3	393	0.2	0.0	0.6	0.2
$T_{air,mean}$ [°C]	356	9.3	3.2	17.6	5.4	353	9.4	2.8	17.8	5.5	393	8.7	2.5	16.3	5.2
SC	356	16%	0%	79%	31%	353	15%	0%	60%	26%	393	11%	0%	31%	17%
SM	356	13%	0%	56%	29%	353	9%	0%	28%	16%	393	10%	0%	29%	15%
A_{AL}	356	13%	0%	45%	19%	353	15%	0%	46%	19%	393	18%	0%	41%	16%
S_pH [a]	355	5.7	4.8	7.1	1.0	353	5.8	4.8	7.0	0.9	393	6.2	4.9	7.5	1.0
PCO_2 [ppmv]	356	2482	732	5309	2399	353	2008	705	3842	1339	393	1860	695	3361	1314
Alkalinity [µeq L^{-1}]	356	1792	92	4400	1836	353	2102	307	4290	1673	393	2515	640	4346	1404
pH	356	6.6	6.3	8.1	-	353	7.1	6.7	8.2	-	393	7.5	7.1	8.2	-
DOC	254	390	116	696	275	229	447	131	939	328	224	447	158	777	249

[a] Note that mean and standard deviation have been calculated directly from the values of subsoil pH, neglecting the logarithmic character of this variable. This is here considered reasonable, as this catchment property is used as a predictor for alkalinity with a linear effect.

Table D.4: Suggested functions describing constraints on expectable value ranges of alkalinity, pH, and $pPCO_2$ depending on catchment characteristics.

Valid value range of independent variable	Function for constraint (on minimum or maximum expectable value)	Valid cases[a]	Reference population[b]	Valid prop.[c]
P<1.7 m a^{-1}	Alk_{max} = 11,500 – 6,000 * P	1101	1102	99.9%
all	Alk_{max} = -3,500 + 1,650 * S_pH	1116	1119	99.7%
all	Alk_{min} = 1,000 * SC	1120	1120	100.0%
P<1.7 m a^{-1}	pH_{min}= 7.9 - 0.7*P-1.4*P^2	1102	1102	100.0%
P<1.7 m a^{-1}	pH_{min}= 7.9-0.1*P-1.3*P^2	1080	1102	98.0%
P<1.7 m a^{-1}	pH_{max}= 8.7-0.3*P^2	1101	1102	99.9%
all	pH_{max}= 8.1+0.065*S_pH	1116	1119	99.7%
all	pH_{min}= -7.9+3.8*S_pH-0.235*S_pH^2	1114	1119	99.6%
all	$pPCO_{2\ max}$= 2.3 - 0.028*$T_{air,mean}$	1113	1120	99.4%
all	$pPCO_{2\ min}$ = 3.6 - 0.021*$T_{air,mean}$	1117	1120	99.7%
all	$pPCO_{2\ max}$= 1.7+0.28*ln(s)	1117	1120	99.7%
all	$pPCO_{2\ min}$ = 3.2+0.14*ln(s)	1117	1120	99.7%
P< 1.7 m a^{-1}	$pPCO_{2\ max}$ = 2.6-0.7*P	1100	1102	99.8%
P< 1.7 m a^{-1}	$pPCO_{2\ min}$ = 3.5-0.16*P	1096	1102	99.5%

[a] Number of cases for which the suggested constraint is valid
[b] Number of cases for which the value range of the independent variable is valid
[c] Proportion that [a] takes on [b]

Alk: alkalinity [µeq L^{-1}]
SC: areal proportion of carbonate rocks per catchment [1]
P: mean annual precipitation per catchment [m a^{-1}]
S_pH: average subsoil pH per catchment
$T_{air,mean}$: mean annual air temperature [℃]

E List of important acronyms

A_{AA}	areal proportions of artificial areas (=urban + industrial areas)
A_{AL}	areal proportion of agricultural land
A_{BF}	areal proportion of broadleaved forests
A_{CF}	areal proportion of coniferous forests
A_{HV}	areal proportion of herbaceous vegetation (=grasslands)
A_{SL}	areal proportion of shrublands
A_{other}	areal proportion of land cover other than forests and grasslands
A_{WL}	areal proportion of wetlands
BSi	biogenic, amorphous silica
DIC	dissolved inorganic carbon
DOC	dissolved organic carbon
DSi	dissolved silica
f_{DOC}	specific fluvial DOC flux
$f_{DOC,calc}$	f_{DOC} calculated from hydrochemical data
$f_{DOC,mod}[L]$	f_{DOC} estimated spatially explicitly by regression equation fitted for catchments > 2,000 km² (‘large catchments’)
$f_{DOC,mod}[S]$	f_{DOC} estimated spatially explicitly by regression equation fitted for catchments < 2,000 km² (‘small catchments’)
f_{DSi}	specific fluvial DSi flux
$f_{DSi,calc}$	f_{DSi} calculated from hydrochemical monitoring data
$f_{DSi,mob}$	spatially explicit estimates of DSi mobilization after Moosdorf et al. (2011)
P	mean annual precipitation
PCO_2	partial pressure of CO_2
$pPCO_2$	negative decadic logarithm of PCO_2
q	mean annual runoff
r_{DSi}	DSi retention rate
s	slope gradient
$SI_{calcite}$	saturation index of calcite
SC	areal proportions of carbonate rocks
SM	areal proportions of mixed sedimentary rocks
S_pH	average subsoil pH
$T_{air,mean}$	mean air temperature

F Curriculum vitae

Ronny Lauerwald was born in Mühlhausen on 7th of September 1979

Working experience

April 2009 – ongoing	Research assistant, Institute for Biogeochemistry and Marine Chemistry, University of Hamburg
May 2008 – March 2009	Research assistant, Institute of Applied Geosciences, TU Darmstadt

Academic education

April 2009 – ongoing	Doctoral student at the University of Hamburg, School of integrated Climate System Sciences
October 2008 – March 2009	Doctoral student at the TU Darmstadt
8th of November 2007	Diplom Geographie at FSU Jena, Thesis title: “Die potentielle Verbreitung von Böden im Stadtgebiet von Jena”
May 2000 – September 2007	Studying geography with focus on geo-information science and physical geography

G Individual contributions to the list of publications, submitted manuscripts, and manuscripts in preparation

Submitted manuscripts and manuscripts in preparation

Lauerwald, R., Hartmann, J., Moosdorf, and Kempe, S., in prep., Controls of spatial patterns in the carbonate system of North American rivers.	**Research Idea:** R. Lauerwald, J. Hartmann **Analysis Framework:** R. Lauerwald, J. Hartmann **Data preparation:** R. Lauerwald, N. Moosdorf **Analysis & Results:** R. Lauerwald **Discussion:** R. Lauerwald, J. Hartmann, N. Moosdorf, S. Kempe
Lauerwald, R., Hartmann, J., Moosdorf, N., Dürr, H. H., and Kempe, S., in prep., Retention of dissolved silica within the fluvial systems of the conterminous USA.	**Research Idea:** R. Lauerwald, J. Hartmann **Analysis Framework:** J. Hartmann, R. Lauerwald **Data preparation:** R. Lauerwald, N. Moosdorf **Analysis & Results:** R. Lauerwald **Discussion:** R. Lauerwald, J. Hartmann, N. Moosdorf, S. Kempe
Lauerwald, R., Hartmann, J., Ludwig, W., Moosdorf, N., submitted, Loss of DOC within the fluvial system of North America. Submitted to Journal of Geophysical Research - Biogeochemistry.	**Research Idea:** R. Lauerwald, J. Hartmann, W. Ludwig **Analysis Framework:** R. Lauerwald, J. Hartmann, W. Ludwig **Data preparation:** R. Lauerwald, N. Moosdorf **Analysis & Results:** R. Lauerwald **Discussion:** R. Lauerwald, J. Hartmann, W. Ludwig
Moosdorf, N., Hartmann, J., **Lauerwald, R.**, Hagedorn, B. and Kempe, S., in revision. Bicarbonate fluxes and CO2 consumption by chemical weathering in North America. Submitted to Geochimica et Cosmochimica Acta.	**Research Idea:** N. Moosdorf, J. Hartmann **Analysis Framework:** N. Moosdorf, J. Hartmann **Data preparation:** N. Moosdorf, R. Lauerwald **Analysis & Results:** N. Moosdorf **Discussion:** N. Moosdorf, J. Hartmann, R. Lauerwald, B. Hagedorn, S. Kempe

Published articles

Moosdorf, N., Hartmann, J. and **Lauerwald, R.**, 2011. Compatibility of space and time for modeling fluvial HCO3 - fluxes - A comparison. Applied Geochemistry, 26 (SUPPL.): S295-S297. [extended abstract]	**Research Idea:** N. Moosdorf, J. Hartmann **Analysis Framework:** N. Moosdorf, J. Hartmann **Data preparation:** N. Moosdorf, R. Lauerwald **Analysis & Results:** N. Moosdorf **Discussion:** N. Moosdorf, J. Hartmann, R. Lauerwald
Moosdorf, N., Hartmann, J. and **Lauerwald, R.**, 2011. Changes in dissolved silica mobilization into river systems draining North America until the period 2081-2100. Journal of Geochemical Exploration, 110(1): 31-39.	**Research Idea:** N. Moosdorf, J. Hartmann **Analysis Framework:** N. Moosdorf, J. Hartmann **Data preparation:** N. Moosdorf, R. Lauerwald **Analysis & Results:** N. Moosdorf **Discussion:** N. Moosdorf, J. Hartmann, R. Lauerwald
Jansen, N., Hartmann, J., **Lauerwald, R.**, Dürr, H.H., Kempe, S., Loos, S. and Middelkoop, H., 2010. Dissolved silica mobilization in the conterminous USA. Chemical Geology, 270(1-4): 90-109.	**Research Idea:** N. Moosdorf (née Jansen), J. Hartmann **Analysis Framework:** N. Moosdorf (née Jansen), J. Hartmann **Data preparation:** N. Moosdorf (née Jansen), R. Lauerwald **Analysis & Results:** N. Moosdorf (née Jansen) **Discussion:** N. Moosdorf (née Jansen), J. Hartmann, R. Lauerwald, H.H. Dürr, S. Kempe, S. Loos, H. Middelkoop